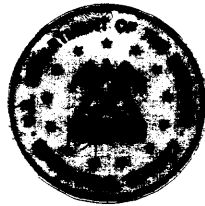


U.S. DEPARTMENT OF THE INTERIOR
GEOLOGICAL SURVEY



ANALYSIS OF TRACE METALS IN BOTTOM SEDIMENTS IN SUPPORT OF
DEEPWATER BIOLOGICAL PROCESSES STUDIES ON
THE U.S. MID-ATLANTIC CONTINENTAL SLOPE AND RISE

By

M. H. Bothner¹, E. Y. Campbell², G. P. DiLisio¹,
C. M. Parmenter¹, R. R. Rendigs¹, J. R. Gillison²,
W. Dangelo², and J. A. Commeau¹

Open-File Report 88-3

Final Report submitted to the
U.S. Minerals Management Service under
Interagency Agreement No. 14-12-0001-30197

¹Woods Hole, MA
²Reston, VA

ANALYSIS OF TRACE METALS IN BOTTOM SEDIMENTS IN SUPPORT OF
DEEPWATER BIOLOGICAL PROCESSES STUDIES ON
THE U.S. MID-ATLANTIC CONTINENTAL SLOPE AND RISE

By

M. H. Bothner¹, E. Y. Campbell², G. P. DiLisio¹,
C. M. Parmenter¹, R. R. Rendigs¹, J. R. Gillison²,
W. Dangelo² and J. A. Commeau¹

U.S. Geological Survey

Final Report prepared in cooperation with the
U.S. Minerals Management Service under
Interagency Agreement No. 14-12-0001-30197

This report is preliminary and has not been reviewed for conformity with U.S. Geological Survey editorial standards. Any use of trade names is for descriptive purposes only and does not imply endorsement by the USGS or MMS.

¹Woods Hole, MA
²Reston, VA

1987

CONTENTS

	Page
Abstract.....	1
Introduction.....	3
Field sampling and sample preparation.....	6
Trace-metal analysis procedures.....	8
Preparation of stock solution A.....	8
Preparation of stock solution B.....	10
Barium.....	10
Aluminum, iron, chromium, nickel, and vanadium.....	11
Lead, copper, and cadmium.....	11
Manganese and zinc.....	11
Mercury.....	12
Textural analyses procedures.....	12
Analytical accuracy and precision.....	13
Results and discussion.....	21
Within-station variability.....	21
Distribution of metals in surface sediments.....	29
Changes in metal concentration as a result of drilling.....	35
Trace-metal variations with depth in sediments.....	36
Lead inventories.....	53
Ba concentration in sediment trap samples.....	56
Physical and chemical concentration of barite particles.....	59
Trace-metals in sediments from recolonization trays.....	62
Trace-metals in different size fractions of sediments.....	62
Sediment texture.....	64
Summary of important findings.....	68
References.....	71
Appendix tables: Navigation data for samples analyzed for trace metals...	75

ANALYSIS OF TRACE METALS IN BOTTOM SEDIMENTS IN SUPPORT OF
DEEPWATER BIOLOGICAL PROCESSES STUDIES ON
THE U.S. MID-ATLANTIC CONTINENTAL SLOPE AND RISE

FINAL REPORT

M. H. Bothner, E. Y. Campbell, G. P. DiLisio,
C. M. Parmenter, R. R. Rendigs, J. R. Gillison,
W. Dangelo and J. A. Commeau

ABSTRACT

This study is part of a multidisciplinary program conducted on the continental slope and rise off the North, Middle, and South Atlantic states to characterize the biology, chemistry, and geology of the sea floor. The specific objectives are to measure and evaluate the extent of environmental changes which relate to exploratory drilling activities. In this report we use trace-metal concentrations to assess both the depositional pattern and fate of discharged drilling mud.

Sediment samples collected during six cruises to the continental slope and rise off the Mid-Atlantic states have been analyzed for 12 metals [aluminum (Al), barium (Ba), cadmium (Cd), chromium (Cr), copper (Cu), iron (Fe), lead (Pb), manganese (Mn), mercury (Hg), nickel (Ni), vanadium (V), and zinc (Zn)]. We found that Ba was the only metal that showed an increase as a result of drilling, and the magnitude of the Ba increase was small (<32%). In one core collected during Cruise 3 at Station 1, adjacent to the drilling site

in Block 372, the Ba concentration in the surface sediment was 13 percent higher than measured deeper in the core. Concentrations of Ba in one of the three replicate surface sediments from Cruise 6, Station 1, were 20 percent higher than concentrations in deeper sediments. Neither samples from other replicate box cores from Cruise 3 or from Cruise 6, Station 1, nor replicate sub-cores from the same box core, show the same increase, indicating a patchy distribution of drilling-related Ba. There is no consistent trend of increasing Ba concentration in blended surface sediment from Station 1, Cruises 1 to 6. The average concentrations of Ba at Station 1 are similar to concentrations at stations away from drilling rigs and in sediments having similar grain size.

At stations 13 and 14, located within 1.4 km of the drilling in Block 93, no significant changes in the average Ba concentration of bottom sediments were measured between predrilling and postdrilling samples.

The barium increases are probably not harmful to benthic organisms on the basis of the low enrichments, the patchy distribution, and the low toxicity of $BaSO_4$ (based on its use in medicine).

The strongest Ba signal from drilling mud was measured in sediments collected in sediment traps positioned in the upper 850 m of the water column at a mooring located 2.4 km southwest of the drilling rig in Block 372. Discrete particles of barite were identified in the sample using a scanning electron microscope equipped with an energy dispersive X-ray detector. The larger particles have dimensions of 60 x 90 μm . Their transport from the drilling rig to the sediment trap mooring is predictable given a calculated settling velocity and the measured currents.

For samples collected from the study area during Cruise 1, the distribution of metals in surface sediments appears to vary with the changes in the concentrations of fine sediment and organic carbon. The concentrations of the metals analyzed in these sediments are the same or lower than they are in average shales from around the world, and are characteristic of uncontaminated sediments. The highest concentration (555 ppm) of Ba measured in sediments at Station 1 is less than the concentration in average shales (580 ppm).

Pb concentrations are consistently higher in the upper 5-10 cm of sediment than in deeper sections of sediment cores, but the average values in surface sediments do not exceed those measured in average shales. Pb enrichment in surface sediments has been observed at other locations off the U.S. East Coast and is thought to be related to the onshore burning of gasoline containing Pb additives. The inventories of anthropogenic lead in the sediments of this study area are higher than are predicted from long-term atmospheric fluxes. This suggests enhanced deposition of lead in these sediments.

INTRODUCTION

This U.S. Geological Survey (USGS) study was designed to establish the concentrations of trace metals in sediments prior to petroleum exploration drilling on the continental slope and rise off the U.S. Middle Atlantic States, and to quantify changes in trace-metal concentrations that are related to exploration activities. Some of the specific questions addressed during this three-year sampling and analysis program are: (1) Where do discharged drilling muds accumulate on the continental slope and rise? and (2) How much do trace metals increase as a result of accumulating drilling mud?

This study is part of a cooperative, multidisciplinary program that is managed and funded by the U.S. Minerals Management Service. The overall goal is to evaluate potential adverse effects of drilling effluents on bottom-dwelling organisms. Other major components of the program include studies of infaunal and epifaunal communities, hydrocarbon concentrations in sediments and organisms, trace-metal concentrations in organisms, sediment texture, and hydrography. These studies will be accomplished under separate contracts awarded to Battelle New England Marine Research Laboratory, Woods Hole Oceanographic Institution (WHOI), and Lamont-Doherty Geological Observatory. Study areas on the continental slope and rise off both the South and North Atlantic states are included in the overall program.

Fourteen station locations were selected on the Mid-Atlantic continental slope and rise (Fig. 1). This station array was established on the premise that drilling mud will be transported by currents over long distances before being deposited. The mean current flow on the continental slope (about 5 cm/s to the southwest) and currents generated by winds and Gulf Stream rings are generally parallel to isobaths (Beardsley and others, 1985; Butman, 1985) and can be in the direction opposite to the mean flow. Tidal currents induce periodic flows across isobaths. In response to this current regime, ten of the stations are arranged along the 2,100-m isobath centered around the drilling site at Station 1. Stations 11, 1, and 12 represent a transect across the slope. Station 13 is located 1.3 km southwest of the drill site in Block 93. Station 14 was located on the drilling site in Block 93 and was not sampled during cruises 2 and 3 while the drill rig was on location.

These stations were sampled three times per year for a two-year period. The first cruise was conducted in March 1984 (Leg 1) and May 1984 (Leg 2). Other cruises were conducted in August 1984, November 1984, May 1985, August 1985 and November 1985.

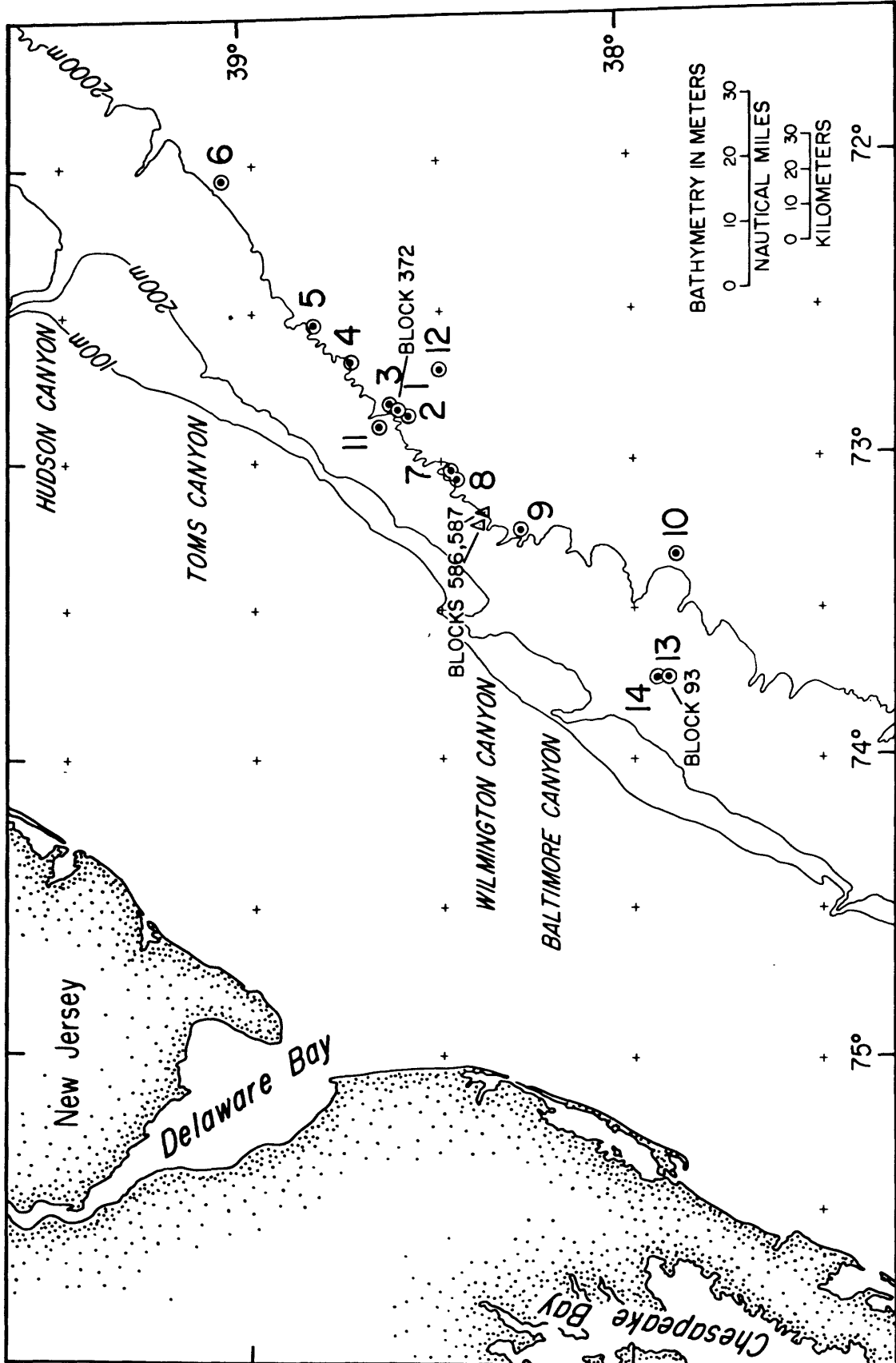


Figure 1. Station locations on the continental slope and rise off the Middle Atlantic states.

Cruise 1 predated the drilling activity in Lease Blocks 372 and 93. However, exploratory drilling had already taken place in this general area at the time of Cruise 1. Two wells had been completed approximately 60 km southwest of Station 1 (Blocks 586 and 587), and 28 wells were drilled on the continental shelf off the Mid-Atlantic states between April 1978 and October 1981.

FIELD SAMPLING AND SAMPLE PREPARATION

Positioning of the ship at each sampling location was based on time delays within the Loran-C navigation network read by a Northstar 6000 receiver (Digital Marine Equipment Corp., Bedford, Mass.). Latitude and longitude values listed in Appendix Table 1 were calculated using updated additional secondary factor corrections (McCullough and others, 1982, 1983). The accuracy of collecting a sample at a given location is more dependent upon wind and current conditions than on the navigation system. Replicate samples collected at a given station typically fall within a circle having a diameter of 400 m.

A 0.25-m² box core, manufactured by Ocean Instruments, Inc., San Diego, Calif., was used to collect sediment samples for this study. The box was divided into 25 subcores of 0.01 m² each. Three box cores were collected at each station. Two and occasionally three of the subcores from each box core were allocated for trace-metal studies. Surfaces of the aluminum subcores were precoated with teflon as a precaution against metal contamination. At sea, an acid-cleaned round plastic tube, 8.2 cm internal diameter (ID), was pushed into the center of the sediments collected in the teflon subcores, thereby sampling material not in contact with the coring apparatus. These tubes were capped at both ends and frozen. The length of the core samples averaged 24 cm and typically ranged from 19 to 32 cm.

Surficial sediment was sampled by partially extruding the frozen sediment from the core barrel and cutting off the top 2 cm of the sediment with a plastic utensil. To generate a blend from a single station, the material from the upper 2 cm of each of three replicates was thawed, homogenized by stirring and shaking in a closed container, and then subsampled with a syringe constructed of glass and teflon.

On selected samples, sand and coarser material were removed by washing the wet sample through a 60- μ m nylon sieve using filtered distilled water. The resultant slurry was dried at <70°C in an oven having teflon-coated surfaces and a filtered nitrogen atmosphere.

Cores from selected stations were subsampled in sequential 2-cm depth intervals so that the concentration profile of metals could be measured over increasing sediment depth. The frozen cores were extruded into a holding tray, thawed overnight, and cut into 2-cm depth intervals using plastic utensils. These samples, from which some of the interstitial water had drained while thawing, were subsequently oven dried. On the basis of trace metal concentrations in interstitial water reported by Lyons and Fitzgerald (1983), less than 0.05 percent of the metal in bulk sediment is lost with the drained interstitial water.

All samples prepared for trace-metal analysis were ground using an agate grinding mill.

The field numbers (for example, C10123 and C21300) that identify samples in each data table have the following code: The first two characters define the cruise as occurring in the Mid-Atlantic region; the second two characters are the station number; the fifth character is the replicate box core number; and the sixth character is the core number within the box core. The use of "00" for the fifth and sixth characters indicates that the sample is a

homogenized mixture of subsamples from each of three replicate box cores. Digits in the seventh and eighth space indicate the bottom of a 2-cm-thick depth interval; where these are missing, the 0 to 2-cm interval is implied. The letter "X" at the end of the field number indicates that the fraction of sediment coarser than 60 μm has been removed from the sample.

The USGS prepared thirteen sediment traps for deployment by Science Applications International Corporation (SAIC) near the drilling site in Block 372. Two sizes of traps were used. Ten of the traps were constructed from clear polybuterate tubing 6.6 cm ID and 60 cm length. The other traps were constructed from molded fiberglass. They were cone shaped, and had a mouth diameter of 50 cm, tapering to a 2-cm-ID sample collection tube. All the trap openings were fitted with baffles to prevent occupation by fish and other large organisms and to reduce turbulence in the traps. The baffles, which had a cell diameter of 1 cm and a length of 7.5 cm, were constructed of an aramid fiber/phenolic resin (HEXCELL). Details of the trap design and relative collection efficiencies are described in Bothner and others, 1987.

TRACE-METAL ANALYSES PROCEDURES

The analyses of trace metals in these marine sediments were carried out by the U.S. Geological Survey laboratories in Reston, Va. Concentrations of the following elements were determined: Al, Ba, Cd, Cr, Cu, Fe, Hg, Mn, Ni, Pb, V, and Zn. The various procedures employed in each of the analyses are detailed below and summarized in Table 1.

Preparation of stock solution A

Exactly 0.5 g of ground bulk sediment or 0.2 g of the fine fraction was added to a covered teflon beaker and digested overnight in 5 mL of HClO_4 , 5 mL

Table 1. Summary of analytical conditions.

Element	Instrument	Instrument conditions	Extraction procedure	Procedure determination limit in sample, ug/g	Average blanks, as measured in ug/g in solution
Al	ICP (argon)	308.2 nm FP (Forward power)=1.1 kw Fixed cross flow nebulizer Spectral band width 0.036 nm Observation height 16 mm.	None	50	0.02
Ba	ICP (argon)	455.4 nm FP=1.1 kw Fixed cross flow nebulizer Spectral band width 0.036 nm Observation height 16 mm.	None	20	.01
Cd	Graphite furnace AA.	110°C dry temperature 250°C char temperature 2100°C atom temperature Regular graphite tube Interrupt gas flow W.l.=228.8 nm Slit=0.7 nm.	Butyl acetate and DDTC.	0.02	.0002
Cr	Graphite furnace AA.	110°C dry temperature 850°C char temperature 2700°C atom temperature Pyrolytic tube Normal gas flow (low) W.l.=357.9 nm Slit=0.7 nm.	None	2	.003
Cu	Graphite furnace AA.	110°C dry temperature 850°C char temperature 2700°C atom temperature Regular graphite tube Interrupt gas flow W.l.=324.7 nm Slit=0.7 nm.	Butyl acetate and DDTC.	1	.005
Fe	ICP (argon)	259.9 nm FP=1.1 kw Fixed cross flow nebulizer Spectral band width 0.036 nm Observation height 16 mm.	None	50	.02
Hg	Induction furnace AA.	Wavelength=254 nm Cold vapor AA.	None	.005	.005
Mn	ICP (argon)	257.6 nm FP=1.1 kw Fixed cross flow nebulizer Spectral band width 0.036 nm Observation height 16 mm.	Butyl acetate (removal of iron).	10	.006
Ni	Graphite furnace AA.	110°C dry temperature 900°C char temperature 2700°C atom temperature Pyrolytic tube Normal gas flow (low) W.l.=232.0 nm Slit=0.2 nm.	None	2	.02
Pb	Graphite furnace AA.	110°C dry temperature 500°C char temperature 2700°C atom temperature Regular graphite tube Interrupt gas flow W.l.=283.3 Slit=0.7 nm.	Butyl acetate and DDTC.	1	.02
V	Graphite furnace AA.	110°C dry temperature 1000°C char temperature 2800°C atom temperature Pyrolytic curtained tube Normal gas flow (high) W.l.=318.4 nm Slit=0.7 nm.	None	2	.002
Zn	Flame AA.	Oxidizing; air-acetylene flame W.l.=213.9 Slit=0.7 nm.	Butyl acetate	1	.01

of HNO_3 , and 13 mL of HF at approximately 140°C . The covers were removed and the temperature was increased to between 180° and 190°C , first producing fumes of HClO_4 and then evaporating the solution to dryness. The residue was dissolved and diluted to exactly 25 mL using 8 N HCl. This solution is referred to as stock solution A.

Two blanks containing all reagents were analyzed along with samples. All reagents were analyzed for contaminants prior to use, as is always necessary. The Canadian reference sediment standard MESS-1 was analyzed in each set of samples. A series of solutions was prepared that approximated the concentration levels expected in the samples; this series was used as the standard in calibrating the inductively coupled plasma (ICP) spectrometer and atomic absorption (AA) spectrophotometer.

Preparation of stock solution B

Stock solution B was made by adding 10 mL of butyl acetate (distilled to remove impurities such as copper) to 15 mL of stock solution A in a 60-mL separatory funnel. This solution was vigorously agitated by an automatic shaker for six minutes to extract iron. The layers were separated, and the extraction step was repeated with an additional 10 mL of butyl acetate. The aqueous layer was evaporated to dryness at 150°C in a 50-mL beaker. The residue was dissolved and diluted to 25 mL by adding 1 N HCl.

Barium

The measurements for Ba were made by ICP spectrometry using 2 mL of stock solution A diluted with distilled H_2O to 4 mL.

Aluminum, iron, chromium, nickel, and vanadium

Concentrations of Al and Fe were determined by ICP spectrometry by using 1 mL of stock solution A diluted to 10 mL with distilled H₂O. The measurements for Cr, Ni, and V were made by injecting 20 µL of diluted (1:10) stock solution A into a graphite-furnace AA spectrophotometer.

Lead, copper, and cadmium

Fifteen mL of 0.5-percent (weight:volume) diethyldithiocarbamic acid diethylammonium salt (DDTC) in chloroform were added to 10 mL of solution B in a 60-mL separatory funnel and mixed for 10 minutes by an automatic shaker. The chloroform layer was drained into a 30-mL beaker and the aqueous layer washed with 10 mL of chloroform. The second chloroform layer was combined with the first, and the total volume of chloroform was evaporated to dryness at 90°C. The organic matter was destroyed by adding 0.1 mL of concentrated HNO₃ and the solution was evaporated to dryness. This residue then was dissolved in 2 mL of warm 1 N HCl. The beaker was rinsed four times with 2 mL portions of distilled H₂O, and the solution was transferred to a small polyethylene container. The measurements for Pb, Cu, and Cd were made by injecting 20 µL of the final solution into a graphite-furnace AA spectrophotometer.

Manganese and zinc

The measurements for Mn were made by ICP spectrometry with a solution made by diluting 2 mL of stock solution B to 4 mL by adding distilled H₂O. Zinc was measured by flame AA directly from stock solution B.

Mercury

Mercury concentration was determined on a separate portion of the sample. Two hundred milligrams of sediment were decomposed in a 1-oz teflon screw-top vial using 2 mL of concentrated HNO_3 (J. T. Baker Chemical Co.) and 2 mL of HClO_4 (G. Frederick Smith Chemical Co. -- double distilled from Vycor, a pure silica glass). The mixture was heated in a capped vial until the solution reached 200°C . The solution was then heated with the cap off for about 45 minutes, after which the samples were removed from the heat source. Immediately, 1 mL of concentrated HNO_3 was added; the vial was filled with distilled H_2O and capped tightly until used. This sample solution was added to a flask containing 125 mL of H_2O and 4 mL of 10 percent (weight:volume) SnCl_2 in 20 percent HCl . Nitrogen was passed through the solution to remove elemental Hg, which was collected on gold foil located in the center of the coils of an induction furnace. Activation of the furnace released the Hg, which was measured by a cold-vapor AA technique. Blanks, standard rocks, and internal sediment standards were analyzed for each set of samples. A series of solutions was prepared that had the same Hg concentration range expected in the samples.

TEXTURAL ANALYSIS PROCEDURES

Sediment samples selected from different depth horizons within the box cores were analyzed for texture by the standard pipette method (Folk, 1974). The specific procedures were essentially identical to those used by other contractors within this program (Maciolek and others, 1987). The textural results are reported in phi units ($-\log_2 D$) where D is the grain diameter in millimeters.

ANALYTICAL ACCURACY AND PRECISION

Analytical accuracy was determined by analyzing rock standard MESS-1. The metals are within one or, at most, two standard deviations of the "best value" determined for this sediment standard (Table 2A). A new fine-grained sediment standard, established for the Georges Bank Monitoring Program by Bothner and others (1983), also has been used during this program (B series, Table 2A).

In our second interim report we discussed a systematic increase in the Cr data generated on standards and samples after a pyrolytically coated graphite tube was installed in the graphite furnace. Chromium values for the standard MESS using the original non-coated graphite tube averaged 47.7 ± 0.5 ppm; values obtained with the pyrolytically coated tube averaged 63.1 ± 4.3 ppm. The latter value is within the published acceptable range for Cr (71 ± 11 ppm).

Using a new graphics display, we were able to observe the Cr peak shapes of sediment standards and liquid standards. With the graphite tube, which is more porous than the pyrolytically coated tube, sediment standards had a broader peak than pure liquid standards. The interpretation is that some of the analyzed solution evaporated within the fabric of the graphite tube and that the residual salts slightly retarded the release of Cr during the heating cycle. The liquid standards having less salt were not affected. Both liquid and sediment standards give the same shape with the pyrolytically coated tube, which is glazed and nonporous.

We corrected the Cr data generated using the graphite-tube furnace by basing the Cr signal on the sediment standards that were run with each batch of samples rather than on the liquid standards. To confirm the calculation, we reanalyzed 11 samples using a furnace equipped with the pyrolytically coated tube. In all but one sample, the calculated correction agreed with the new data at the 99 percent level of confidence (t test).

Table 2A. Analysis of sediment standard.

Sediment Standard	Al (%)	Ba (ppm)	Cd (ppm)	Cr (ppm)	Cu (ppm)	Fe (%)	Hg (ppm)	Mn (ppm)	Ni (ppm)	Pb (ppm)	V (ppm)	Zn (ppm)
MESS-1-----	5.30	280	0.46	64 ¹	27	2.9	-	470	35	28	70	170
	5.70	260	.43	65 ¹	21	2.9	-	470	31	31	71	180
	5.40	260	.45	65 ¹	23	2.8	-	480	37	29	73	200
	5.30	280	.46	64 ¹	27	2.9	-	470	35	28	70	170
	5.70	260	.43	65 ¹	21	2.9	-	470	31	31	71	180
	5.40	260	.45	65 ¹	23	2.8	-	480	37	29	73	200
	5.41	258	.48	65	23	2.78	-	469	35	31	85	174
	4.89	259	.42	61	25	2.80	-	483	31	25	80	178
	5.06	259	.41	61	28	2.85	-	489	34	27	74	186
	5.38	257	.50	59	25	2.81	-	481	31	32	85	187
	5.21	256	.40	62	24	2.79	-	476	34	32	85	184
	5.61	277	.46	66	22	2.97	-	485	32	31	80	200
	5.27	278	.40	65	23	2.86	-	476	34	33	80	173
	4.83	259	.39	73	23	2.84	.14	458	35	26	74	178
	5.41	258	.44	69	25	2.86	.20	474	34	26	76	179
	5.65	263	.43	57	25	2.87	.20	469	37	23	73	176
	5.73	265	.44	57	24	2.87	.20	480	38	27	70	174
	5.28	259	.44	62	24	2.87	.20	471	36	26	85	174
	5.05	263	.43	62	24	2.84	-	472	37	25	88	174
	4.94	276	.45	62	23	2.83	-	476	37	25	86	176
	5.43	264	.44	65	24	2.86	-	494	40	27	88	173
\bar{x} ----	5.32	263	.44	63.1	24.2	2.85	.19	475	35	27.8	77.7	180
σ -----	.27	7	.03	4.3	1.8	.04	.03	8	2.6	2.7	6.9	9
CV(%) ² -	5.1	2.8	5.9	6.8	7.6	1.4	14	1.7	7.4	9.6	8.9	4.8
Best value ³	5.8	270	.59	71	25	3.0	-	513	30	34	72	191
σ -----	.2	-	.1	11	4	.2	-	25	3	6	5	17
B-10 ⁴	3.4	280	.066	43 ¹	6.3	1.6	.015	290	12	17	40	40
B-12	3.5	270	.063	44 ¹	6.0	1.6	-	290	20	15	38	40
B-11	3.7	270	.060	46 ¹	5.8	1.7	.015	300	10	15	38	42
	3.4	269	.066	50	6.1	1.65	.015	289	11	17	41	44
	3.11	268	.071	46	6.0	1.60	.015	281	10	17	43	37
	3.11	260	.088	47	5.0	1.62	.015	286	12	14	40	38
	3.62	269	.073	42	6.1	1.64	.015	282	14	14	44	35
	3.22	264	.083	47	5.5	1.62	.015	278	11	13	46	40
	3.12	270	.075	43	6.6	1.60	.015	287	14	13	41	43
	3.46	260	.058	40	6.0	1.65	.015	299	14	13	46	40
\bar{x} ----	3.39	268	.071	45	5.9	1.63	.015	289	13.4	14.2	41.6	39.8
σ -----	.22	7	.011	3.5	.5	.03	0	8	3.1	1.4	3.3	2.4
CV(%) ² -	6.6	2.4	15	7.7	8.3	2.1	0	2.6	23	9.7	7.9	6.1

1 Corrected Cr values

2 Coefficient of variation

3 Values reported by the Marine Analytical Chemistry Program, National Research Council, Canada.

4 A fine-grained sediment standard collected from station 13 of the Georges Bank Monitoring Program (Bothner and others, 1983).

Table 2B. Analysis of replicate sediment samples.

Sample Replicate	Al (%)	Ba (ppm)	Cd (ppm)	Cr (ppm)	Cu (ppm)	Fe (%)	Hg (ppm)	Mn (ppm)	Ni (ppm)	Pb (ppm)	V (ppm)	Zn (ppm)
C11311	5.7	420	.095	83 ¹	27	3.2	-	810	50	24	87	76
W-228624	5.7	430	.075	79	27	3.2	-	800	50	22	87	76
	5.7	420	.083	83	26	3.2	-	800	48	22	90	76
	5.7	410	.095	82	26	3.2	-	780	49	22	90	76
	5.7	420	.091	84	27	3.2	-	790	49	22	87	78
\bar{x} ---	5.7	420	.09	82.2	26.6	3.2	-	796	49.2	22.4	88.2	76.4
σ ----	0	7	.01	1.9	.5	0	-	11	.8	.9	1.6	.9
CV(%) ² --	0	1.7	11.1	2.3	7.9	0	-	1.2	1.6	4.0	1.8	1.2

Sample Replicate	Al (%)	Ba (ppm)	Cd (ppm)	Cr (ppm)	Cu (ppm)	Fe (%)	Hg (ppm)	Mn (ppm)	Ni (ppm)	Pb (ppm)	V (ppm)	Zn (ppm)
C1142202	5.98	414	.066	73	24	3.25	.070	576	53	15	95	83
W-233733	5.99	413	.063	72	23	3.25	.070	575	53	14	98	83
	5.96	413	.063	73	23	3.23	.070	574	53	14	85	83
	6.00	418	.063	72	24	3.24	.060	576	50	14	85	83
	5.96	426	.063	73	24	3.21	.070	578	53	15	85	83
\bar{x} ---	5.98	417	.064	72.6	23.6	3.24	.068	576	52.4	14.4	89.6	83
σ ----	.02	5	.001	.5	.5	.02	.004	1	1.3	.5	6.4	0
CV(%) ²	.3	1.3	2.1	.8	2.3	.5	6.6	.3	2.6	3.8	7.1	0

Sample Replicate	Al (%)	Ba (ppm)	Cd (ppm)	Cr (ppm)	Cu (ppm)	Fe (%)	Hg (ppm)	Mn (ppm)	Ni (ppm)	Pb (ppm)	V (ppm)	Zn (ppm)
C20131	5.0	390	.042	68 ¹	16	3.0	-	670	40	14	90	75
W-228517	4.9	390	.048	68	16	2.9	-	670	42	12	83	73
	5.0	380	.048	69	16	3.0	-	640	42	12	90	73
	5.0	380	.050	68	16	3.0	-	610	40	12	83	73
	5.0	410	.042	68	16	3.0	-	650	41	13	87	75
\bar{x} ---	4.98	390	.046	68.2	16	2.98	-	648	41	12.6	86.6	73.8
σ ----	.05	12	.004	.4	0	.05	-	25	1	.9	3.5	1.1
CV(%) ²	1.0	3.1	8.7	.6	0	1.7	-	3.9	2.4	7.1	4.0	1.5

¹ Corrected Cr values

² Coefficient of variation

Table 2B. Analysis of replicate sediment samples.- Continued

Sample Replicate	Al (%)	Ba (ppm)	Cd (ppm)	Cr (ppm)	Cu (ppm)	Fe (%)	Hg (ppm)	Mn (ppm)	Ni (ppm)	Pb (ppm)	V (ppm)	Zn (ppm)
C21300	6.3	430	.075	79 ¹	24	3.4	-	790	34	18	120	91
W-228542	6.3	420	.075	82	23	3.4	-	780	36	16	120	90
	6.4	420	.071	82	24	3.4	-	800	38	16	110	90
	6.4	430	.063	82	23	3.4	-	810	36	16	120	90
	6.3	430	.066	82	23	3.3	-	790	34	16	120	90
\bar{x} ---	6.34	426	.07	81.4	23.4	3.4	-	794	35.6	16.4	116	90.4
σ	.06	5	.01	1.3	.5	0	-	11	1.7	.9	5.5	.5
CV(%) ² -	.9	1.2	14.3	1.6	2.1	0	-	1.4	4.8	5.5	4.7	.5

Sample Replicate	Al (%)	Ba (ppm)	Cd (ppm)	Cr (ppm)	Cu (ppm)	Fe (%)	Hg (ppm)	Mn (ppm)	Ni (ppm)	Pb (ppm)	V (ppm)	Zn (ppm)
C-3011114	5.70	461	.058	82 ¹	22	3.25	.04	360	48	8.7	102	90
W-229793	5.71	442	.073	83	23	3.26	.035	353	48	9.8	98	90
	5.69	444	.065	80	20	3.24	.036	352	44	8.7	98	88
	5.67	450	.065	80	24	3.23	.035	349	44	9.8	98	90
	5.73	452	.065	84	24	3.25	.035	353	46	10	102	89
\bar{x} ---	5.7	450	.065	81.8	22.6	3.25	.036	353	46	9.4	99.6	89.4
σ ----	.02	7	.005	1.8	1.7	.01	.002	4	2	.6	2.2	.9
CV(%) ² -	.4	1.7	8.1	2.2	7.4	.4	6	1.1	4.3	6.8	2.2	1

Sample Replicate	Al (%)	Ba (ppm)	Cd (ppm)	Cr (ppm)	Cu (ppm)	Fe (%)	Hg (ppm)	Mn (ppm)	Ni (ppm)	Pb (ppm)	V (ppm)	Zn (ppm)
C3020002X	5.40	418	.041	86 ¹	22	3.03	.030	686	50	12	94	76
W-229825	5.43	418	.050	83	22	3.06	.030	686	50	12	98	76
	5.41	420	.041	82	23	3.04	.027	712	45	13	90	76
	5.50	416	.050	82	22	3.10	.030	702	45	12	98	76
	5.43	413	.058	86	23	3.05	.030	704	50	12	98	75
\bar{x} ---	5.43	417	.048	83.8	22.4	3.06	.029	698	47.4	12.4	95.6	75.8
σ ----	.04	3	.007	2	.5	.03	.001	12	2.5	.5	3.6	.4
CV(%) ²	.7	.6	15	2.4	2.4	.9	4.6	1.7	5.3	4.4	3.7	.6

- 1 Corrected Cr values
2 Coefficient of variation

Table 2B. Analysis of replicate sediment samples.- Continued

Sample Replicate	Al (%)	Ba (ppm)	Cd (ppm)	Cr (ppm)	Cu (ppm)	Fe (%)	Hg (ppm)	Mn (ppm)	Ni (ppm)	Pb (ppm)	V (ppm)	Zn (ppm)
C4012122	5.52	423	.071	80	23	3.03	.040	360	36	9.6	109	75
W-232029	5.41	420	.080	82	23	3.00	.040	360	36	10	104	75
	5.39	418	.071	80	22	2.98	.040	354	36	10	109	75
	5.39	416	.080	80	23	2.99	.040	362	39	9.6	104	76
	5.42	416	.075	80	23	3.00	.040	361	39	9.6	109	75
\bar{x} ---	5.43	419	.075	80.4	22.8	3.00	.04	359	37.2	9.8	107	75.2
σ ----	.05	3	.004	.9	.4	.02	0	3	1.6	.2	3	.4
CV(%) ²	1	.7	6	1.1	2	.6	0	.9	4.4	2.2	2.6	.6
<hr/>												
Sample Replicate	Al (%)	Ba (ppm)	Cd (ppm)	Cr (ppm)	Cu (ppm)	Fe (%)	Hg (ppm)	Mn (ppm)	Ni (ppm)	Pb (ppm)	V (ppm)	Zn (ppm)
C5141112	5.99	418	.083	84	23	3.29	.015	357	51	6.8	96	85
W-233040	5.96	426	.083	84	23	3.27	.015	358	52	6.8	103	88
	5.96	409	.091	86	23	3.26	.015	356	53	7.3	94	85
	5.97	421	.091	84	23	3.27	.015	354	51	6.8	101	88
	5.96	416	.091	85	23	3.27	.015	362	52	7.3	94	88
\bar{x} ---	5.97	418	.088	84.6	23	3.27	.015	357	51.8	7	97.6	86.8
σ ----	.01	6	.004	.9	0	.01	0	3	.8	.3	4.2	1.6
CV(%) ²	.2	1.5	5	1.1	0	.3	0	.8	1.6	3.9	4.3	1.9
<hr/>												
Sample Replicate	Al (%)	Ba (ppm)	Cd (ppm)	Cr (ppm)	Cu (ppm)	Fe (%)	Hg (ppm)	Mn (ppm)	Ni (ppm)	Pb (ppm)	V (ppm)	Zn (ppm)
C6020002X	5.42	429	.042	67	21	3.02	.030	626	45	10	98	73
W-234543	5.49	427	.042	67	21	3.07	.020	625	45	9.0	96	73
	5.46	432	.050	65	20	3.06	.020	625	46	8.3	102	71
	5.48	427	.050	66	21	3.04	.020	622	45	10	98	71
	5.49	431	.050	67	20	3.05	.030	632	45	10	98	73
\bar{x} ---	5.47	429	.047	66.4	20.6	3.05	.024	626	45.2	9.5	98.4	72.2
σ ----	.03	2	.004	.9	.5	.02	.005	4	.4	.8	2.2	1.1
CV(%) ²	.5	.5	9.4	1.3	2.7	.6	23	.6	1	8.2	2.2	1.5

² Coefficient of variation

Table 2C. - Chemical analysis of blind duplicates.

Field no.	Top (cm)	Btm (cm)	Lab no.	Al (%)	Ba (ppm)	Cd (ppm)	Cr (ppm)	Cu (ppm)	Fe (%)	Hg (ppm)	Mn (ppm)	Ni (ppm)	Pb (ppm)	V (ppm)	Zn (ppm)	
C11411	0	2	W-233730	5.79	408	.055	70	23	3.16	.002L	592	50	15.0	85	81	
C11411	0	2	W-233736	5.79	418	.091	73	23	3.09	.070	593	53	14.0	90	83	BLIND #
C40121	2	4	W-232024	5.37	412	.050	80	20	2.98	.040	603	36	10.0	94	61	
C40121	2	4	W-232039	5.39	418	.058	80	23	2.97	.040	599	37	12.0	109	70	BLIND #
C51411	16	18	W-233041	5.94	423	.120	84	22	3.22	.020	352	52	19.0	99	90	
C51411	16	18	W-233043	5.91	420	.120	82	22	3.20	.025	347	53	11.0	99	85	BLIND #
C60112	0	2	W-234525	4.58	343	.033	59	14	2.83	.010	490	30	14.0	72	55	
C60112	0	2	W-234547	4.54	367	.033	57	15	2.70	.020	498	36	18.0	74	57	BLIND #
C40100S0	0	2	W-235344	5.23	404	.082	57	22.0	2.95	.040	358	39	15.0	100	73	
C40100S0	0	2	W-235358	5.43	403	.077	68	23.0	3.16	.090	664	44	22.0	100	81	BLIND #

The concentration of V in the sediment standard MESS (Table 2A) showed a slight increase corresponding to the change in procedure, but there was no consistent change in results on samples reanalyzed using the pyrolytically coated tube and so no correction to V results was applied.

The concentrations of Pb in the last three batches of samples analyzed were systematically lower than values measured at comparable stations collected earlier in the program. Reanalysis of these three sets of samples were consistent with earlier results and the new data are reported in the data tables (lab numbers W-233008 - W-233043; W-234511 - W-234587).

Analytical precision was determined by periodically analyzing replicate aliquots taken from a single sample. Coefficients of variation shown in Table 2B indicate that the standard deviations are typically less than 10 percent of the mean value, except for concentrations at or near the detection limit of the method. Analytical precision for Ba averages 1.4 percent (range 0.5 - 3.1 percent) for five replicates from each of nine samples.

An additional precision check was conducted by submitting unidentified (blind) duplicates to all stages in the analytical procedure. The agreement between duplicates was generally excellent (Table 2C).

During the early phases of this program, we evaluated the metal concentrations in surface sediment that had been in contact with different materials used in the box of the box corer. Mr. George Hampson, WHOI, suggested this experiment and provided the carefully collected samples.

To assess contamination effects from the box core sampler, we compared the metal concentrations in sediments from the center of a teflon-coated subcore (i.e., material that had not been in contact with the sampler) with sediments in direct contact with either the teflon-coated or the uncoated aluminum corer (Table 3). Bulk sediments and the fraction $<60 \mu\text{m}$ were

Table 3. - Chemical analyses of replicate samples collected from different areas of a single box core.

[Samples A, B, and C from center of a teflon-coated subcore (assumed to be the least contaminated); D, E, and F in contact with the side of teflon-coated subcore; G, H, and I in contact with the side of aluminum subcore. Field no. ending in X means size fraction finer than 60 μ m analyzed.]

Field no.	Lab no.	Al (%)	Ba (ppm)	Cd (ppm)	Cr (ppm)	Cu (ppm)	Fe (%)	Hg (ppm)	Mn (ppm)	Ni (ppm)	Pb (ppm)	V (ppm)	Zn (ppm)
SA21A	W-226341	1.8	120	0.068	26	8.4	1.1	0.02	120	11	5	12	30
SA21B	W-226342	1.8	130	.140	26	8.6	1.0	.02	120	11	5	17	32
SA21C	W-226343	1.9	130	.180	28	12	1.1	--	120	13	6	16	32
\bar{x}		1.83	127	.13	26.7	9.7	1.07	.02	120	11.7	5.3	15	31
σ		.06	5.8	.06	1.2	2.0	.06	0	0	1.2	.6	2.6	1.2
CV(%) ¹		3.2	4.6	44	4.3	21	5.4	0	0	9.9	10.8	17.6	3.7
SA21D	W-226344	1.9	130	.150	26	10	1.1	.02	130	12	7	20	33
SA21E	W-226345	1.9	130	.130	26	8.6	1.1	.02	130	11	5	21	32
SA21F	W-226346	1.9	130	.088	29	7.8	1.1	.02	150	12	6	23	32
\bar{x}		1.9	130	.12	27.0	8.8	1.1	.02	137	11.7	6.0	21	32
σ		0	0	.03	1.7	1.1	0	0	12	.6	1.0	1.5	.6
CV(%) ¹		0	0	26	6.4	13	0	0	8.4	4.9	16.7	7.2	1.8
SA21G	W-226347	1.8	120	.083	26	10	1.1	.02	160	11	6	10	30
SA21H	W-226348	1.8	130	.110	25	7.5	1.0	.02	130	11	5	12	30
SA21I	W-226349	1.8	130	.130	26	8.0	1.0	.02	120	11	4	10	30
\bar{x}		1.80	127	.11	25.7	8.5	1.03	.02	137	11	5.0	11	30
σ		0	5.8	.02	.6	1.3	.06	0	21	0	1.0	1.2	0
CV(%) ¹		0	4.6	22	2.2	16	5.6	0	15	0	20	10.8	0
SA21AX	W-226350	2.8	160	.085	35	13	1.28	.04	149.5	20	8	36	48.0
SA21BX	W-226351	2.8	158	.105	35	14	1.26	.04	147.5	20	7	33	44.2
SA21CX	W-226352	2.7	158	.148	35	14	1.27	--	147.7	20	6	33	44.3
\bar{x}		2.79	159	.11	35	14	1.27	.04	149	20	7.0	34	45.3
σ		.05	1.2	.03	0	.6	.01	0	1.2	0	1.0	1.7	2.3
CV(%) ¹		1.8	0.7	28	0	4.2	.8	0	.8	0	14.3	5.1	5.1
SA21DX	W-226353	2.8	161	.098	35	9.8	1.29	.05	150.3	19	11	33	48.3
SA21EX	W-226354	2.8	160	.097	35	13	1.28	.04	192.5	20	10	37	48.1
\bar{x}		2.78	160	.10	35	11	1.28	.04	172	19.5	10.5	35	48.2
σ		.01	.7	0	0	2.3	.01	.01	30	.7	.7	2.8	.1
CV(%) ¹		.2	.4	.7	0	20	.6	16	18	3.6	6.7	8.1	.2

¹Coefficient of variation.

compared. We found that the concentrations of Ba and Cr, the metals most likely to indicate the presence of drilling mud in sediments, were not contaminated by contact with the walls of the box corer. In the bulk sediments, vanadium appeared to be slightly higher in the samples collected from the edge of the teflon-coated subcore compared to the other samples. In the fine fraction, the lead values from the edges of the subcores are about 40 percent higher than in the sediment not in contact with the box-core material.

The material that was in contact with the walls of the subcore probably represent the worst case of contamination from the material used to construct the box-core sample chamber. The sediment that is routinely removed from the subcore for trace-metal analysis, however, excludes the material in contact with the wall of the subcore. We therefore conclude that contamination from the walls of the box core is insignificant. Although this test does not rule out the possibility that metal contamination could occur from flakes of material falling onto the sediment surface from the coring apparatus above the sample box, such contamination would be random and severe and should be obvious from the chemical analyses. Within this program we have observed less than five spurious values that might be explained by contamination from field or laboratory operations.

RESULTS AND DISCUSSION

Within-station variability

We determined the variability of metal concentrations within an individual box core and between replicate box cores taken at the same station (Table 4A-G). In samples unaffected by drilling muds, the within-box core variability for Ba is typically less than 2 percent, and the within-station

Table 4A. - Comparison of within-station variability to within box core variability at Station 1, Cruise 1.

Field no.	Top (cm)	Btm (cm)	Lab no.	Al (%)	Ba (ppm)	Cd (ppm)	Cr (ppm)	Cu (ppm)	Fe (%)	Hg (ppm)	Mn (ppm)	Ni (ppm)	Pb (ppm)	V (ppm)	Zn (ppm)
C10111	0	2	W-228607	5.2	400	0.110	54	27	2.9	0.03	750	39	12	78	63
C10121	0	2	W-228608	5.5	430	.096	56	26	3.0	.02	770	47	12	78	70
C10131	0	2	W-228611	5.4	420	.071	56	25	2.9	.02	720	41	15	80	70
\bar{x}				5.37	416	.092	55.3	26	2.93	.02	747	42.3	13	79	68
σ				.15	15	.020	1.1	1	.06	0	25	4.2	1.7	1.1	4.0
CV% ¹				2.8	3.7	21	2.1	3.8	2.0	6.4	3.4	9.8	13	1.5	6.0
C10121	0	2	W-228608	5.5	430	.096	56	26	3.0	.02	770	47	12	78	70
C10122	0	2	W-228609	5.5	430	.046	58	28	3.0	.02	800	45	14	84	71
C10123	0	2	W-228610	5.5	430	.063	58	28	3.0	.02	860	46	16	90	73
\bar{x}				5.5	430	.068	57.3	27.3	3.0	.02	810	46.0	14	84	71
σ				0	0	.025	1.0	1.0	0	0	46	1.0	2	6	1.5
CV%				0	0	37	1.8	3.7	0	0	5.7	2.2	14	7.1	2.1

Table 4B. - Comparison of within station variability to within box core variability at Station 1, Cruise 2.

Field no.	Top (cm)	Btm (cm)	Lab no.	Al (%)	Ba (ppm)	Cd (ppm)	Cr (ppm)	Cu (ppm)	Fe (%)	Hg (ppm)	Mn (ppm)	Ni (ppm)	Pb (ppm)	V (ppm)	Zn (ppm)
C20111	0	2	W-228513	5.2	420	0.055	52	14	2.9	0.03	710	50	12	90	83
C20121	0	2	W-228516	4.7	410	.042	48	15	2.7	.04	590	40	13	80	73
C20131	0	2	W-228517	5.0	390	.046	50	16	3.0	.04	650	41	13	86	74
\bar{x}				4.97	407	.048	50	15	2.87	.04	650	43.7	13	86	77
σ				.25	15	.006	2	1.0	.15	.01	60	5.5	.6	5.1	5.5
CV%				5.1	3.8	14	4	6.7	5.3	14	9.2	13	4.5	5.9	7.2
C20111	0	2	W-228513	5.2	420	.055	52	14	2.9	.03	710	50	12	90	83
C20112	0	2	W-228514	5.2	430	.048	54	17	3.0	.03	790	52	16	87	80
C20113	0	2	W-228515	5.2	430	.042	52	19	2.9	.05	750	46	14	90	80
\bar{x}				5.2	427	.048	52.7	16.7	2.93	.04	750	49.3	14	89	81
σ				0	5.8	.065	1.2	2.5	.06	.01	40	3.1	2	1.7	1.7
CV%				0	1.4	13	2.2	15	2.0	31	5.3	6.2	14	1.9	2.1

¹Coefficient of variation.

Table 4C. - Comparison of within station variability to within box core variability at Station 1, Cruise 3.

Field no.	Top (cm)	Btm (cm)	Lab no.	Al (%)	Ba (ppm)	Cd (ppm)	Cr (ppm)	Cu (ppm)	Fe (%)	Hg (ppm)	Mn (ppm)	Ni (ppm)	Pb (ppm)	V (ppm)	Zn (ppm)
C30111	0	2	W-229828	5.08	493	0.041	62	22	2.87	0.03	565	41	12	90	73
C30121	0	2	W-229831	5.27	427	.041	64	23	2.93	.03	652	44	12	94	75
C30131	0	2	W-229832	5.19	401	.075	62	22	2.87	.02	343	40	12	94	70
\bar{x}				5.18	440	.052	62.7	22.3	2.89	.03	520	41.7	12.0	92.7	72.7
σ				0.09	47.4	.020	1.2	.6	.03	.01	159	2.1	.0	2.3	2.5
CV% ¹				1.84	10.8	38	1.8	2.6	1.2	22	31	5.0	.0	2.6	3.5
C30111	0	2	W-229828	5.08	493	.041	62	22	2.87	.03	565	41	12	90	73
C30112	0	2	W-229829	5.17	412	.055	66	22	2.90	.02	507	42	10	84	75
C30113	0	2	W-229830	5.13	400	.041	75	22	2.88	.02	513	43	12	89	73
\bar{x}				5.13	435	.046	67.7	22.0	2.88	.02	528	42.0	10.7	87.8	73.7
σ				.04	50.6	.008	6.7	0.0	0.01	.01	31.9	1.0	1.2	3.2	1.2
CV% ¹				.88	12	18	9.8	0.0	0.53	25	6.0	2.4	11	3.7	1.6

Table 4D. - Comparison of within station variability to within box core variability at Station 14, Cruise 4.

Field no.	Top (cm)	Btm (cm)	Lab no.	Al (%)	Ba (ppm)	Cd (ppm)	Cr (ppm)	Cu (ppm)	Fe (%)	Hg (ppm)	Mn (ppm)	Ni (ppm)	Pb (ppm)	V (ppm)	Zn (ppm)
C41411	0	2	W-231772	5.60	389	0.071	81	21	3.10	0.04	689	36	20	87	86
C41421	0	2	W-231773	5.59	411	.055	79	21	3.15	.04	832	42	18	82	88
C41431	0	2	W-231774	5.62	386	.071	79	23	3.13	.04	710	39	26	105	85
\bar{x}				5.60	395	.066	79.7	21.7	3.13	.04	744	39.0	21.3	91.3	86.3
σ				.01	13.6	.009	1.2	1.3	.02	.00	77.2	3.0	4.2	12.1	1.5
CV% ¹				.27	3.5	14	1.5	5.3	.80	.00	10	7.7	20	13	1.8
C41411	0	2	W-231772	5.60	389	.071	81	21	3.10	.04	689	36	20	87	86
C41412	0	2	W-231775	5.60	397	.055	80	22	3.07	.04	593	36	18	87	88
C41413	0	2	W-231776	5.66	386	.038	85	21	3.11	.03	577	39	16	96	88
\bar{x}				5.62	391	.055	82.0	21.3	3.09	.04	620	37.0	18.0	40.0	87.3
σ				.03	5.7	.016	2.7	.6	.02	.01	60.6	1.7	2.0	5.2	1.2
CV% ¹				.62	1.5	30	3.2	2.7	.67	16	9.8	4.7	11	5.8	1.3

¹Coefficient of variation.

Table 4E. - Comparison of within - station variability to within box core variability at Station 14, Cruise 5.

Field no.	Top (cm)	Btm (cm)	Lab no.	Al (%)	Ba (ppm)	Cd (ppm)	Cr (ppm)	Cu (ppm)	Fe (%)	Hg (ppm)	Mn (ppm)	Ni (ppm)	Pb (ppm)	V (ppm)	Zn (ppm)
C51411	0	2	W-233019	5.2	381	.09	77	20	2.89	.04	641	44	19	78	85
C51421	0	2	W-233020	5.23	375	.075	73	18	2.90	.045	578	39	14	88	81
C51431	0	2	W-233021	5.46	383	.075	77	21	3.03	.05	633	41	23	92	83
\bar{x} ---				5.3	380	.08	75.7	19.7	2.94	.045	617	41.3	18.7	86	83
σ ---				.14	4	.009	2.3	1.5	.08	.005	34	2.5	4.5	7.2	2
CV(%) ¹ ---				2.7	1.1	11	3	7.8	2.7	11	5.6	6.1	24	8.4	2.4
C51411	0	2	W-233019	5.2	381	.09	77	20	2.89	.04	641	44	19	78	85
C51412	0	2	W-233022	5.0	355	.075	75	18	2.81	.04	635	41	21	78	76
C51413	0	2	W-233023	5.19	381	.088	79	20	2.89	.05	610	43	19	82	76
\bar{x} ---				5.13	372	.084	77	19.3	2.86	.043	629	42.7	20	79.3	79
σ ---				.11	15	.008	2	1.2	.05	.006	16	1.5	1.2	2.3	5.2
CV(%) ¹ ---				2.2	4	9.7	2.6	6	1.6	13	2.6	3.6	5.7	2.9	6.6

¹ Coefficient of variation

Table 4F. - Comparison of within - station variability to within box core variability at Station 1, Cruise 6.

Field no.	Top (cm)	Btm (cm)	Lab no.	Al (%)	Ba (ppm)	Cd (ppm)	Cr (ppm)	Cu (ppm)	Fe (%)	Hg (ppm)	Mn (ppm)	Ni (ppm)	Pb (ppm)	V (ppm)	Zn (ppm)
C60111	0	2	W-234524	5.04	362	.03	62	16	2.94	.02	421	37	21	88	63
C60121	0	2	W-234527	5.06	443	.02	67	18	2.89	.02	721	39	11	82	63
C60131	0	2	W-234528	5.07	555	.042	65	17	2.87	.02	613	42	12	82	70
\bar{x} ---				5.06	453	.031	64.7	17	2.9	.02	585	39.3	14.7	84	68
σ -----				.02	97	.011	2.5	1	.04	-	152	2.5	5	3.5	4.4
CV(%) ¹ ---				.3	21	36	3.9	5.9	1.2	-	26	6.4	37	4.1	6.4
C60111	0	2	W-234524	5.04	362	.03	62	16	2.94	.02	421	37	21	88	63
C60112	0	2	W-234525	4.58	343	.033	59	14	2.83	.01	490	30	14	72	55
C60113	0	2	W-234526	5.08	380	.03	60	16	3.04	.01	440	35	17	110	61
\bar{x} ---				4.9	362	.031	60.3	15.3	2.94	.013	450	34	17.3	90	59.7
σ -----				0.28	18	.002	1.5	1.2	.1	.006	36	3.6	3.5	19	4.2
CV(%) ¹ ---				5.7	5.1	5.6	2.5	7.5	3.6	43	7.9	11	20	21	7

Table 4G. - Within station variability for Cruise 1, Stations 5 and 13; Cruise 2, Stations 2, 4, 6 and 13; Cruise 3, Stations 6 and 13; Cruise 4, Stations 1 and 13 and Cruise 6, Stations 6, 13, and 14.

Field no.	Top (cm)	Btm (cm)	Lab no.	Al (%)	Ba (ppm)	Cd (ppm)	Cr (ppm)	Cu (ppm)	Fe (%)	Hg (ppm)	Mn (ppm)	Ni (ppm)	Pb (ppm)	V (ppm)	Zn (ppm)
C10511	0	2	W-228612	5.5	440	.066	58	28	3.0	.02	840	45	15	84	73
C10521	0	2	W-228613	5.5	430	.096	60	26	2.9	.02	830	49	15	87	70
C10531	0	2	W-228614	5.5	420	.075	60	29	3.0	.02	700	46	17	86	71
\bar{x}				5.5	430	.08	59.3	27.7	2.97	.02	790	46.7	16	86	71
σ				0	10	.02	1.2	1.5	.06	0	78	2.1	1.2	1.5	1.5
CV%				0	2.3	19	1.9	5.5	1.9	0	9.9	4.4	7.5	1.8	2.2
C11311	0	2	W-228624	5.7	420	.088	60	27	3.2	.03	800	49	22	88	76
C11321	0	2	W-228625	5.7	410	.090	58	22	3.1	.04	590	46	22	84	73
C11331	0	2	W-228626	5.9	440	.095	62	25	3.3	.03	410	50	24	94	78
\bar{x}				5.77	423	.09	60	24.7	3.20	.03	600	48.3	23	89	76
σ				.12	15	0	2.0	2.5	.10	.01	200	2.1	1.2	5.0	2.5
CV%				2.0	3.6	4.0	3.3	10	3.1	19	32	4.3	5.1	5.6	3.3
C20211	0	2	W-228615	5.0	370	0.075	50	18	2.7	0.01	500	34	8.3	74	58
C20221	0	2	W-228616	4.6	360	.058	44	19	2.5	.01	440	30	15	66	56
C20231	0	2	W-228617	4.8	380	.058	46	24	2.6	.02	610	34	15	74	60
\bar{x}				4.8	370	.06	46.7	20.3	2.6	.01	517	32.7	13	71	58
σ				.2	10	.01	3.1	3.2	.1	0	86	2.3	3.9	4.6	2.0
CV%				4.2	2.7	15	6.5	16	3.8	14	17	7.1	30	6.5	3.4
C20411	0	2	W-228618	4.9	380	.076	48	20	2.6	.01	490	33	13	74	60
C20421	0	2	W-228619	5.2	410	.063	52	23	2.8	.02	430	42	11	84	63
C20431	0	2	W-228620	4.6	370	.061	44	20	2.4	.01	420	32	12	70	51
\bar{x}				4.9	387	.07	48	21.0	2.6	.01	447	35.7	12	76	58.0
σ				.3	21	.01	4.0	1.7	.2	0	38	5.5	1.0	7.2	6.2
CV%				6.1	5.4	12	8.3	8.2	7.7	11	8.5	15	8.3	9.5	11
C20611	0	2	W-228621	5.1	420	.075	50	25	2.8	.02	840	40	14	80	65
C20621	0	2	W-228622	5.3	430	.091	56	24	2.9	.02	720	42	13	84	65
C20631	0	2	W-228623	5.2	400	.066	52	27	2.8	.02	810	44	16	87	61
\bar{x}				5.2	417	.077	52.7	25.3	2.83	.02	790	42	14	84	64
σ				.1	15	.013	3.1	1.5	.06	0	62	2.0	1.5	3.5	2.3
CV%				1.9	3.7	16	5.8	6.0	2.0	6.0	7.9	4.8	11	4.2	3.6
C21311	0	2	W-228510	5.8	430	0.063	58	22	3.4	0.05	900	54	21	100	100
C21321	0	2	W-228511	5.8	430	.066	59	22	3.3	.04	730	54	11	100	95
C21331	0	2	W-228512	5.5	410	.042	60	18	3.2	.06	720	54	22	95	93
\bar{x}				5.7	423	.06	59	20.7	3.30	.05	780	54	18	98	96
σ				.17	11	.01	1.0	2.3	.10	.01	100	0	6.1	2.9	3.6
CV%				3.0	2.7	23	1.7	11	3.0	20	13	0	34	2.9	3.8

¹Coefficient of variation.

Table 4G. - Within station variability for Cruise 1, Stations 5 and 13; Cruise 2, Stations 2, 4, 6 and 13; Cruise 3, Stations 6 and 13; Cruise 4, Stations 1 and 13 and Cruise 6, Stations 6, 13, and 14.- Continued.

Field no.	Top (cm)	Btm (cm)	Lab no.	Al (%)	Ba (ppm)	Cd (ppm)	Cr (ppm)	Cu (ppm)	Fe (%)	Hg (ppm)	Mn (ppm)	Ni (ppm)	Pb (ppm)	V (ppm)	Zn (ppm)
C30611	0	2	W-229833	4.74	368	.063	55	18	2.57	.02	537	33	10.0	84	66
C30621	0	2	W-229834	5.13	406	.050	64	23	2.82	.02	674	41	12.0	94	71
C30631	0	2	W-229835	5.24	409	.045	69	22	3.01	.02	1,202	47	13.0	94	73
\bar{x}				5.04	394	.053	62.7	21.0	2.80	.02	804	40.3	11.7	90.7	70.0
σ				.26	22.8	.009	7.1	2.6	.22	.00	351	7.02	1.5	5.8	3.6
CV% ¹				5.2	5.8	18	11	13	7.9	.00	44	17	13	6.4	5.2
C31311	0	2	W-229836	5.45	425	.066	69	24	3.10	.03	611	50	25.0	104	80
C31321	0	2	W-229837	5.55	428	.066	67	23	3.20	.03	665	50	18.0	95	85
C31331	0	2	W-229838	5.65	417	.075	68	23	3.29	.03	1,171	49	21.0	95	83
\bar{x}				5.55	423	.069	68.0	23.3	3.20	.03	816	49.7	21.3	98.0	82.7
σ				.10	5.7	.005	1.0	.6	.09	.00	309	.6	3.5	5.2	2.5
CV% ¹				1.8	1.3	7.5	1.5	2.5	3.0	.00	38	1.2	17	5.3	3.0
C40111	0	2	W-231766	5.32	424	.038	78	24	2.97	.03	717	34	14.0	87	80
C40121	0	2	W-231767	5.14	400	.055	74	21	2.81	.02	810	32	12.0	82	73
C40131	0	2	W-231768	5.31	418	.083	78	24	2.94	.02	704	34	13.0	87	85
\bar{x}				5.26	414	.059	76.7	23.0	2.91	.02	744	33.3	13.0	85.3	79.3
σ				.10	12.5	.023	2.3	1.7	.08	.01	57.8	1.2	1.0	2.9	6.0
CV% ¹				1.9	3.0	39	3.0	7.5	2.9	25	7.8	3.5	7.7	3.4	7.6
C41311	0	2	W-231769	5.63	412	.066	81	26	3.15	.03	783	40	20.0	92	100
C41321	0	2	W-231770	5.70	404	.075	83	26	3.30	.04	904	43	22.0	110	101
C41331	0	2	W-231771	5.72	399	.310(?)	83	24	3.24	.05	655	40	22.0	82	95
\bar{x}				5.68	405		82.3	25.3	3.23	.04	781	41.0	21.3	94.7	98.7
σ				.05	6.6		1.2	1.2	.07	.01	124	1.7	1.2	14.2	3.2
CV% ¹				.83	1.6		1.4	4.6	2.3	25	16	4.2	5.4	15	3.3

¹Coefficient of variation.

Table 4G. - Within station variability for Cruise 1, Stations 5 and 13; Cruise 2, Stations 2, 4, 6 and 13; Cruise 3, Stations 6 and 13; Cruise 4, Stations 1 and 13 and Cruise 6, Stations 6, 13, and 14.- Continued.

Field no.	Top (cm)	Btm (cm)	Lab no.	Al (%)	Ba (ppm)	Cd (ppm)	Cr (ppm)	Cu (ppm)	Fe (%)	Hg (ppm)	Mn (ppm)	Ni (ppm)	Pb (ppm)	V (ppm)	Zn (ppm)
C60611	0	2	W-234563	5.17	399	.03	72	18	2.81	.02	644	49	12	96	71
C60621	0	2	W-234529	5.05	409	.042	65	17	2.83	0.03	637	44	14	88	68
C60631	0	2	W-234530	4.83	397	.042	65	18	2.73	.03	889	44	17	82	65
\bar{x} ---				5.02	402	.038	67.3	17.7	2.79	.027	723	45.7	14.3	88.7	68
σ ---				.17	6	.007	4	.6	.05	.006	144	2.9	2.5	7	3
CV(%) ¹ ---				3.4	1.6	18	6	3.3	1.9	22	20	6.3	18	7.9	4.4
C61311	0	2	W-234571	5.48	447	.055	76	20	3.06	.03	802	55	30	115	81
C61321	0	2	W-234531	5.48	427	.055	71	20	3.07	.03	886	51	22	98	80
C61331	0	2	W-234532	5.36	420	.075	69	21	3.08	.05	849	49	26	88	80
\bar{x} ---				5.44	431	.062	72	20.3	3.07	.037	846	51.7	26	100	80.3
σ ---				.07	14	.012	3.6	.6	.01	.012	42	3	4	14	.6
CV(%) ¹ ---				3.2	19	5	2.8	.3	31	5	5.9	7.7	15	.7	
C61411	0	2	W-234579	5.37	414	.055	74	19	2.92	.04	706	50	26	110	75
C61421	0	2	W-234533	4.95	374	.042	62	15	2.82	.03	574	42	16	77	68
C61431	0	2	W-234534	5.28	372	.042	67	18	3.01	.03	581	42	17	88	73
\bar{x} ---				5.2	387	.046	67.7	17.3	2.92	.033	620	44.7	19.7	91.7	72
σ ---				.22	24	.008	6	2.1	.1	.006	74	4.6	5.5	17	3.6
CV(%) ¹ ---				4.3	6.1	16	8.9	12	3.3	17	12	10	28	18	5

¹ Coefficient of variation

variability is less than 6 percent. From this, we conclude that the distribution of Ba is fairly uniform within circular areas on the continental slope having a diameter of 400 m. This size circle in most cases contains all the replicate box cores at a given station. The samples from Station 1, Cruises 3 and 6, and from Station 13, Cruise 6, show a higher coefficient of variation than other stations because the replicates include one sample that has elevated Ba, presumably caused by the addition of drilling mud.

Distribution of metals in surface sediments

We have plotted the concentration of metals, organic carbon, and textural parameters for each station occupied during Cruise 1 in the order of their latitude from north to south (Fig. 2A, B, C, and D and Table 5). Organic carbon and textural data were provided by the Battelle-WHOI contractors for this program.

The concentrations of metals in these sediments are the same or lower than they are in average shales from various locations around the world (Krauskopf, 1967), a similarity which suggests that these predrilling sediments had not been contaminated prior to this program. The variation in metal concentrations is small, generally within a factor of 2 over the entire study area.

The variation in concentration of metals, organic carbon, and clay is very similar from station to station. The close correlation among these variables can be explained by the varying proportion of clay in the sediment, which is expected to contain the highest concentration of the metals analyzed. At Station 11, the clay fraction, organic carbon, and most of the metals are at higher concentrations than those at adjacent stations shown in Figure 2C and 2D. At Station 12, we observed the lowest concentrations of clay, organic carbon, and most of the metals.

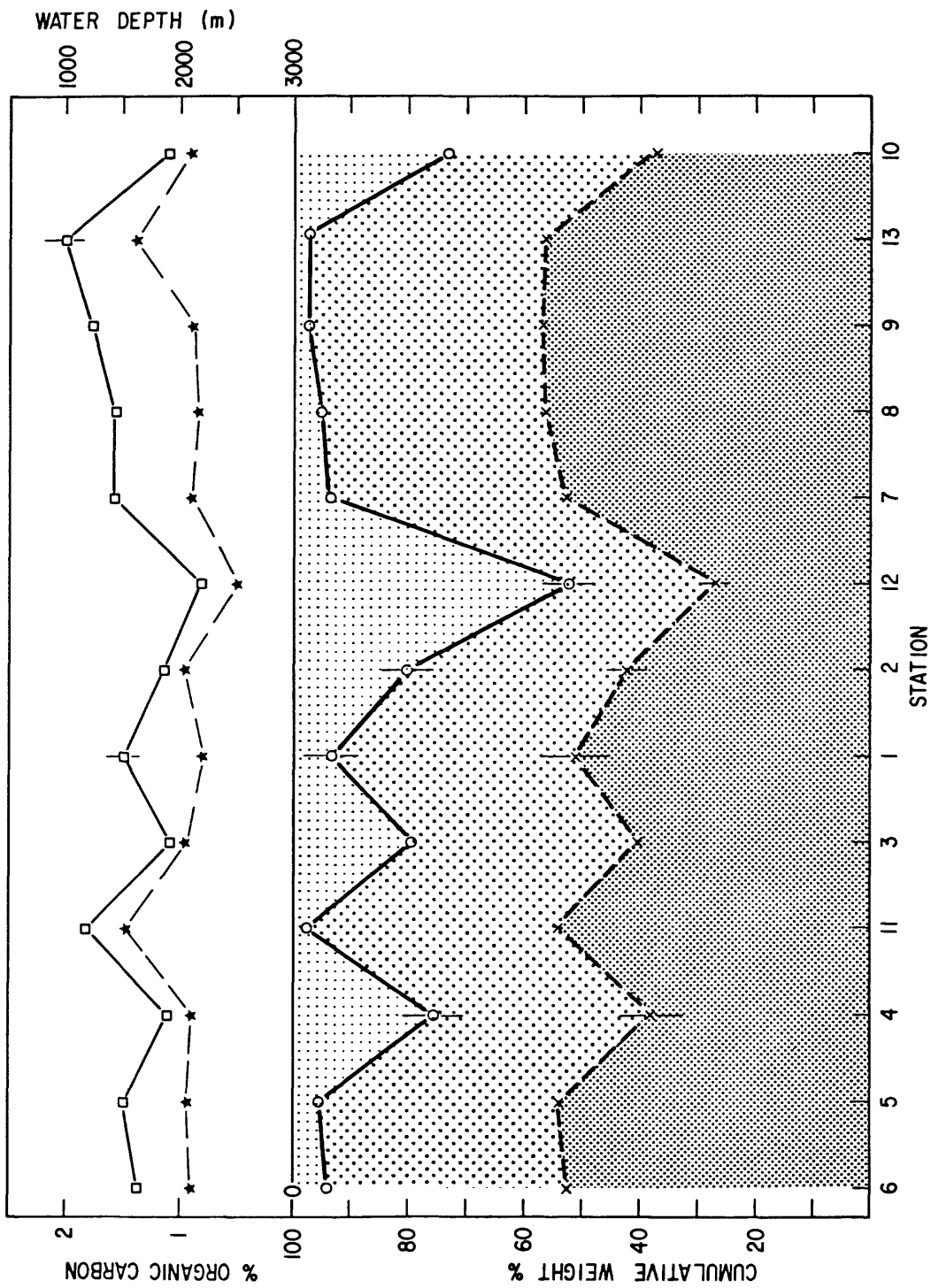


Figure 2A. Average concentration of organic carbon (□ in percent) and water depth (★ in meters) at stations from Cruise 1 listed from north to south. Error bars represent standard deviation among three replicates.

2B. Average concentrations of clay (▣), silt (▤), and sand (▥) in cumulative weight percent at stations from Cruise 1 listed from north to south. Error bars represent standard deviation among three replicates.

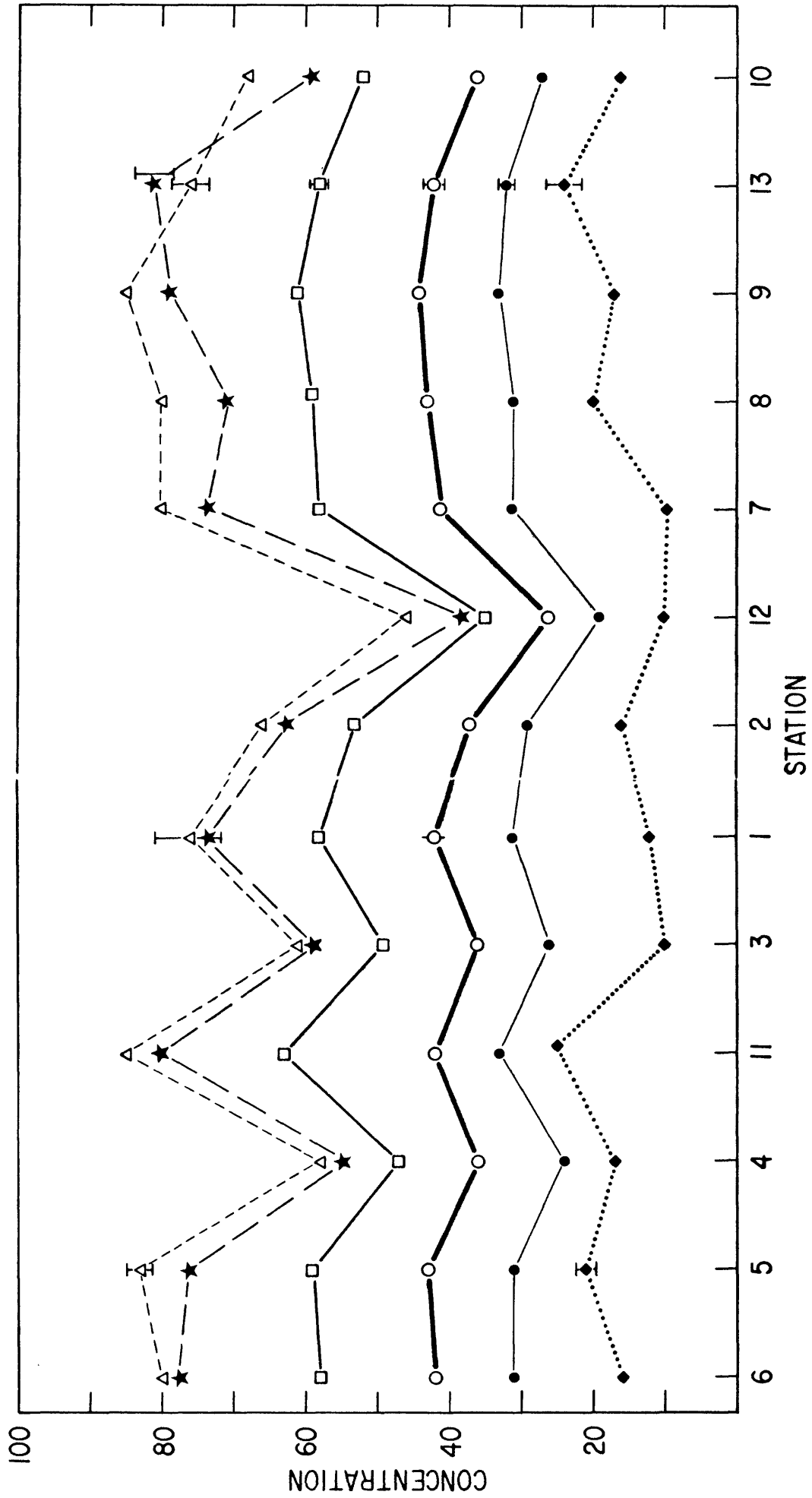


Figure 2C. Concentrations of metals in station blends from Cruise 1. Stations listed from north to south. (Al, \square % x 10; Ba, \square ppm x 10⁻¹; Cr, \star ppm; Cu, \diamond ppm; Fe, \bullet % x 10; Zn, Δ ppm.) Error bars represent standard deviation among three replicates at Stations 1, 5, and 13. Where error bars do not appear at these stations, error is within the area of the symbol.

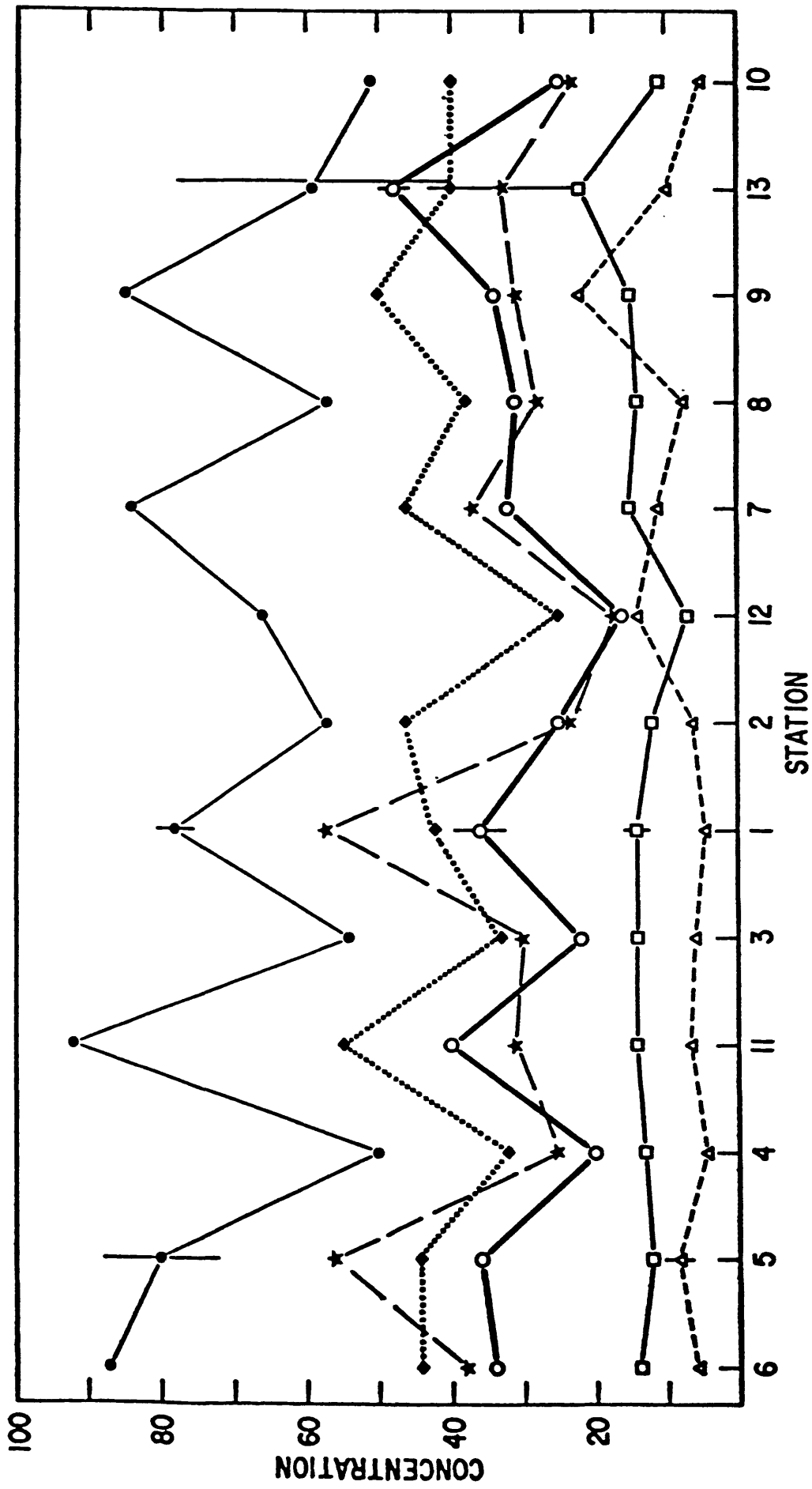


Figure 2D. Concentration of metals in station blends from Cruise 1. Stations listed from north to south. (Cd, Δ ppm x 10²; Hg, \star ppm x 10³; Mn, \bullet ppm x 10¹; Ni, \circ ppm; Pb, \square ppm; V, \blacklozenge ppm x 1/2.) Error bars represent standard deviation among three replicates at Stations 1, 5, and 13. Where error bars do not appear at these stations, error is within the area of the symbol.

Table 5. - Chemical analysis of station blends.

Field no.	Top (cm)	Btm (cm)	Lab no.	Al (%)	Ba (ppm)	Cd (ppm)	Cr (ppm)	Cu (ppm)	Fe (%)	Hg (ppm)	Mn (ppm)	Ni (ppm)	Pb (ppm)	V (ppm)	Zn (ppm)
C10100	0	2	W-228518	5.80	420	.045	73	12	3.10	.057	780	36	14.0	83	76
C20100	0	2	W-228530	5.50	440	.060	71	14	3.00	.028	670	30	12.0	91	75
C30100	0	2	W-229811	5.25	444	.041	75	18	2.97	.031	519	36	13.0	90	71
C40100	0	2	W-231781	5.30	415	.100	74	22	2.89	.023	750	36	12.0	87	73
C50100	0	2	W-233024	4.53	364	.033	69	16	2.57	.025	494	34	9.1	74	66
C60100	0	2	W-234511	4.98	451	.020L	67	17	2.90	.020	565	39	14.0	74	68
C10200	0	2	W-228519	5.30	370	.063	63	16	2.90	.023	570	25	12.0	91	66
C20200	0	2	W-228531	5.20	370	.050	60	15	2.70	.025	550	27	14.0	83	65
C30200	0	2	W-229812	4.82	386	.045	69	17	2.72	.027	607	30	11.0	84	63
C40200	0	2	W-231782	5.14	374	.055	78	19	2.77	.024	712	32	12.0	87	68
C50200	0	2	W-233025	4.28	323	.042	64	14	2.32	.005	502	30	13.0	70	60
C60200	0	2	W-234512	4.49	362	.050	59	15	2.54	.020	530	35	15.0	74	58
C10300	0	2	W-228520	4.90	360	.060	58	10	2.60	.030	540	22	14.0	66	61
C20300	0	2	W-228532	4.80	340	.045	52	13	2.40	.020	700	25	14.0	81	58
C30300	0	2	W-229813	4.20	335	.120	55	13	2.25	.024	439	24	10.0	76	50
C40300	0	2	W-231783	4.28	319	.028	62	16	2.24	.020	448	22	9.1	68	55
C50300	0	2	W-233026	4.26	333	.066	64	16	2.29	.010	476	35	9.1	78	63
C60300	0	2	W-234513	4.54	365	.030	59	15	2.54	.010	559	34	14.0	74	58
C10400	0	2	W-228521	4.70	360	.045	54	17	2.40	.025	500	20	13.0	63	58
C20400	0	2	W-228533	5.20	390	.071	60	17	2.60	.020	470	31	12.0	91	65
C30400	0	2	W-229814	4.49	365	.025	62	14	2.43	.023	594	30	10.0	94	56
C40400	0	2	W-231784	4.93	374	.042	72	18	2.65	.020	584	32	9.1	82	61
C50400	0	2	W-233027	4.43	354	.050	68	17	2.41	.025	585	36	11.0	74	63
C60400	0	2	W-234514	4.49	364	.058	59	16	2.51	.010	571	44	14.0	107	58
C10500	0	2	W-228522	5.90	430	.083	76	21	3.10	.056	800	36	12.0	87	83
C20500	0	2	W-228534	5.80	430	.060	73	13	3.10	.031	930	38	12.0	87	80
C30500	0	2	W-229815	5.33	438	.050	85	21	3.04	.035	775	44	14.0	98	76
C40500	0	2	W-231785	5.37	407	.091	78	24	2.97	.028	843	39	14.0	105	76
C50500	0	2	W-233028	4.93	380	.055	75	20	2.73	.030	723	41	11.0	94	75
C60500	0	2	W-234515	5.03	408	.066	66	20	2.86	.020	540	39	14.0	85	68
C10600	0	2	W-228523	5.80	420	.060	78	16	3.10	.038	870	34	14.0	87	80
C20600	0	2	W-228535	5.60	410	.150	68	10	2.90	.027	800	32	12.0	83	75
C30600	0	2	W-229816	5.10	406	.050	70	19	2.86	.030	777	35	13.0	87	68
C40600	0	2	W-231786	5.37	412	.050	85	24	2.94	.028	887	40	18.0	92	71
C50600	0	2	W-233029	4.96	382	.088	75	20	2.74	.020	570	43	13.0	84	71
C60600	0	2	W-234516	4.98	424	.042	64	20	2.84	.020	754	40	15.0	90	68
C10700	0	2	W-228524	5.80	410	.110	73	9.5	3.10	.037	840	32	15.0	91	80
C20700	0	2	W-228536	5.90	430	.055	73	20	3.00	.028	760	34	12.0	100	80
C30700	0	2	W-229817	5.48	443	.063	80	22	3.10	.030	710	39	11.0	98	76
C40700	0	2	W-231787	5.40	411	.055	78	21	2.95	.025	599	34	14.0	92	73
C50700	0	2	W-233030	5.12	399	.063	77	21	2.83	.030	468	43	9.9	88	75
C60700	0	2	W-234517	5.25	427	.038	70	20	3.00	.020	659	42	15.0	85	71

Table 5. - Chemical analysis of station blends. - Continued

Field no.	Top (cm)	Btm (cm)	Lab no.	Al (%)	Ba (ppm)	Cd (ppm)	Cr (ppm)	Cu (ppm)	Fe (%)	Hg (ppm)	Mn (ppm)	Ni (ppm)	Pb (ppm)	V (ppm)	Zn (ppm)
C10800	0	2	W-228525	5.90	430	.075	71	20	3.10	.028	570	31	14.0	75	80
C20800	0	2	W-228537	6.10	430	.083	79	21	3.10	.027	610	38	12.0	110	81
C30800	0	2	W-229818	5.63	441	.058	82	22	3.18	.030	510	45	14.0	102	80
C10900	0	2	W-228526	6.10	440	.220	79	17	3.30	.031	850	34	15.0	100	85
C20900	0	2	W-228538	6.30	440	.091	79	22	3.30	.033	800	37	13.0	100	81
C30900	0	2	W-229819	5.64	451	.066	82	23	3.25	.023	723	47	13.0	106	80
C40900	0	2	W-231788	5.72	429	.063	83	24	3.16	.025	587	45	12.0	110	85
C50900	0	2	W-233031	5.55	426	.063	82	21	3.11	.025	891	47	13.0	86	85
C60900	0	2	W-234518	5.15	430	.058	69	21	2.97	.020	513	44	15.0	96	70
C11000	0	2	W-228527	5.20	360	.050	63	16	2.70	.023	510	25	11.0	79	68
C21000	0	2	W-228539	5.00	350	.055	60	16	2.60	.030	520	24	7.5	87	65
C31000	0	2	W-229820	4.64	363	.033	66	15	2.61	.020	554	30	10.0	84	61
C41000	0	2	W-231789	4.75	345	.033	70	17	2.60	.028	594	36	9.1	82	68
C51000	0	2	W-233032	4.63	341	.042	68	15	2.56	.020	582	35	13.0	78	66
C61000	0	2	W-234519	4.39	371	.033	57	16	2.46	.010	525	33	12.0	80	58
C11100	0	2	W-228528	6.30	420	.066	80	25	3.30	.031	920	40	14.0	110	85
C21100	0	2	W-228540	6.10	410	.075	76	20	3.20	.033	660	32	14.0	96	83
C31100	0	2	W-229821	5.35	409	.058	76	20	3.05	.030	669	43	13.0	84	75
C41100	0	2	W-231790	5.52	392	.033	79	21	3.08	.028	699	43	14.0	94	83
C51100	0	2	W-233033	5.27	374	.066	77	18	2.99	.030	654	44	16.0	78	76
C61100	0	2	W-234520 ¹	4.40	295	.030	129	15	6.96	.010	398	36	12.0	158	66
C11200	0	2	W-228529	3.50	260	.140	38	10	1.90	.017	660	16	7.0	50	46
C21200	0	2	W-228541	3.80	270	.220	44	10	2.00	.017	660	19	5.8	69	50
C31200	0	2	W-229822	3.21	258	.050	46	11	1.82	.020	590	19	6.3	54	43
C41200	0	2	W-231791	3.20	246	.028	46	11	1.73	.016	626	17	6.3	45	43
C51200	0	2	W-233034	3.14	248	.038	49	11	1.73	.020	593	23	7.5	52	45
C61200	0	2	W-234521	3.06	241	.042	43	9.6	1.78	.010	611	20	4.6	42	38
C11300	0	2	W-228627	5.80	420	.100	83	24	3.20	.033	590	48	22.0	80	76
C21300	0	2	W-228542	6.30	430	.070	82	23	3.40	.038	790	36	16.0	116	90
C31300	0	2	W-229823	5.12	404	.058	76	20	2.94	.037	695	44	16.0	87	78
C41300	0	2	W-231792	5.70	407	.075	81	28	3.21	.044	776	46	23.0	98	88
C51300	0	2	W-233035	5.28	400	.075	82	22	3.02	.050	804	48	20.0	94	88
C61300	0	2	W-234522	5.40	434	.050	71	20	3.11	.030	841	47	18.0	98	78
C41400	0	2	W-231793	5.57	393	.055	78	22	3.08	.044	764	40	22.0	96	88
C51400	0	2	W-233036	5.10	386	.083	78	20	2.85	.045	610	45	24.0	86	85
C61400	0	2	W-234523	5.33	410	.050	69	18	3.02	.030	652	45	10.0	88	75

¹ Possibly contaminated with metal fragment.

According to some preliminary microscopic analyses of the sand fraction by Mr. Brian Dade, WHOI, the very high (50%) sand fraction at Station 12 is composed primarily of foraminifera tests. Because the metal concentration of calcite making up the foram tests is much lower than concentrations found in the clay minerals, the sand fraction in these samples essentially dilutes the metal concentrations with little influence on their relative proportions. Similar covariation in metals, organic carbon, and clay content was observed among the stations of the Georges Bank Monitoring Program (Bothner and others, 1982). On Georges Bank, however, the sand fraction was composed primarily of quartz and feldspar.

Changes in metal concentration as a result of drilling

Ba was the only metal found to increase in concentration as a result of drilling. The concentration increases were found only at one station adjacent to the drilling rig in Block 372. The magnitude of increases were small. We found that one core collected at Station 1 on Cruises 3 and 6 (Table 4C and 4F) had Ba concentrations 13 percent and 32 percent higher, respectively, than the predrilling mean value of 422 ± 15 ppm. The Ba profile with depth in the core from Cruise 3 (see next section) confirms that the surface material is enriched.

The fact that only one of three subcores from the same box core shows the increase in Ba above background suggests that the distribution of Ba resulting from drilling is patchy on a very small scale. The patchy increase in Ba may be due to the random addition of relatively large particles of barite. We have identified large particles of barite ($60 \times 90 \mu\text{m}$) in sediment trap samples (discussed in a following section).

At Station 13, 1.4 km southwest of the drill site in Block 92, and at Station 14, 0.6 km from the drill site, no indication of increased Ba was observed during analyses of replicates (Table 4) and station blends (Table 5).

In an attempt to concentrate any drilling mud, we separated the size fraction finer than 60 μm . Based on the textural analyses of standard barite by the American Petroleum Institute, approximately 96 percent of the barite is finer than 60 μm . By removing the natural sediment fraction coarser than 60 μm , the chemical signal of drilling mud in the remaining fine fraction can be significantly enhanced. This technique proved to be valuable on Georges Bank where the coarse fraction represented more than 98 percent of the sample (Bothner and others, 1985). On the slope and rise off the Middle Atlantic states, and due in part to the lower sand content (<20%) at most stations (Fig. 2B), the drilling-mud signal in the fine fraction at the drill sites (Table 6) was no more obvious than in the total sample.

Trace-metal variations with depth in sediments

Samples from four stations have been subsampled as a function of sediment depth to determine the depth profiles of metal concentrations. The metal concentrations are shown in Table 7.

In the core collected at Station 1 before drilling began, the concentration of Ba and the Ba to Al ratio were essentially constant for the entire length of the core (Fig. 3). The Ba to Al ratio is plotted because it partially normalizes the Ba data for inhomogeneity in clay, calcium carbonate, and/or salt content of the sediments.

In the core collected during Cruises 2 and 3, the Ba concentration and the Ba to Al ratio were higher in surface sediments than in subsurface sediments. In postdrilling cores, the Ba maximum concentration and Ba to Al

Table 6. Chemical analyses of the fine fraction (less than 60 μm) from station blends.

Field no.	Top (cm)	Btm (cm)	Lab no.	Al %	Ba (ppm)	Cd (ppm)	Cr (ppm)	Cu (ppm)	Fe %	Hg (ppm)	Mn (ppm)	Ni (ppm)	Pb (ppm)	V (ppm)	Zn (ppm)
C10100X	0	2	W-228543	6.10	430	.091	79	24	3.20	.039	780	36	14.0	120	85
C20100X	0	2	W-228547	6.10	460	.190	79	14	3.20	.033	670	32	13.0	120	80
C30100X	0	2	W-229824	5.47	445	.045	80	21	3.08	.031	532	47	12.0	87	78
C40100X	0	2	W-231777	5.56	440	.050	81	23	3.08	.028	773	37	13.0	105	85
C50100X	0	2	W-233012	5.06	409	.055	73	21	2.77	.025	556	38	16.0	78	71
C60100X	0	2	W-234542	5.69	480	.050	70	21	3.20	.040	624	48	16.0	90	76
C10200X	0	2	W-228544	6.30	430	.050	79	21	3.30	.043	610	32	15.0	120	81
C20200X	0	2	W-228548	6.10	420	.060	79	22	3.10	.025	600	36	14.0	100	75
C30200X	0	2	W-229825	5.43	417	.048	83	22	3.06	.029	698	47	12.0	96	76
C60200X	0	2	W-234543	5.47	429	.047	66	21	3.05	.030	626	45	16.0	98	72
C10300X	0	2	W-228545	5.90	410	.083	76	16	3.10	.033	590	30	15.0	110	76
C20300X	0	2	W-228549	5.90	420	.180	76	22	3.00	.029	500	32	11.0	100	76
C10400X	0	2	W-228546	5.80	400	.046	76	19	2.90	.037	560	32	14.0	100	73
C20400X	0	2	W-228550	5.80	390	.066	73	22	3.00	.025	810	31	15.0	100	73
C30400X	0	2	W-229826	5.22	402	.045	81	22	2.87	.024	702	47	12.0	96	70
C40400X	0	2	W-231778	5.43	420	.055	81	27	2.97	.044	662	39	12.0	101	76
C60400X	0	2	W-234544	5.23	414	.042	62	21	2.89	.040	639	46	14.0	90	68
C50600X	0	2	W-233013	5.31	419	.075	80	22	2.98	.025	603	43	17.0	82	76
C11300X	0	2	W-228628	6.00	430	.083	89	26	3.30	.033	590	49	22.0	90	76
C21300X	0	2	W-228551	6.30	420	.078	83	23	3.30	.056	690	38	21.0	120	90
C31300X	0	2	W-229827	5.74	434	.066	86	23	3.33	.042	743	54	17.0	94	86
C41300X	0	2	W-231779	5.79	415	.073	85	25	3.28	.058	781	46	22.0	110	90
C51300X	0	2	W-233014	5.35	398	.080	78	25	3.08	.060	779	45	20.0	82	81
C61300X	0	2	W-234545	5.68	452	.063	70	22	3.28	.040	859	54	22.0	102	81
C41400X	0	2	W-231780	5.70	398	.063	81	22	3.17	.044	776	42	22.0	110	78
C51400X	0	2	W-233015	5.37	391	.075	80	25	3.02	.050	633	51	22.0	82	85
C61400X	0	2	W-234546	5.66	448	.050	71	21	3.22	.030	675	49	20.0	128	77

Table 7. - Chemical analyses of core samples subsectioned in 2 cm intervals.

Field no.	Top (cm)	Dep (cm)	Bot (cm)	Lab no.	Al (%)	Ba (ppm)	Cd (ppm)	Cr (ppm)	Cu (ppm)	Fe (%)	Hg (ppm)	Mn (ppm)	Ni (ppm)	Pb (ppm)	V (ppm)	Zn (ppm)
C10111	0	2		W-228480	5.00	410	0.030	65	16	2.90	0.060	830	39	15.0	90	63
C10111	2	4		W-228481	5.00	410	.048	69	12	2.90	.040	960	40	13.0	90	753
C10111	4	6		W-228482	5.00	410	.048	65	13	2.90	.037	950	39	15.0	83	73
C10111	8	10		W-228483	5.00	410	.055	68	21	2.80	.023	490	39	14.0	89	76
C10111	12	14		W-228484	5.00	410	.083	71	17	2.80	.030	410	39	12.0	87	76
C10111	16	18		W-228485	5.00	410	.091	69	12	2.80	.030	320	36	12.0	100	75
C10111	22	24		W-228486	5.00	410	.080	67	15	2.70	.030	320	39	11.0	90	70
C10111	28	30		W-228487	4.90	400	.110	67	14	2.70	.028	320	40	12.0	87	73
C20131	0	2		W-228488	4.90	430	.075	76	15	2.90	.026	680	40	16.0	85	81
C20131	2	4		W-228489	5.00	400	.055	71	18	3.00	.036	660	41	14.0	85	76
C20131	4	6		W-228490	4.90	410	.048	65	14	2.90	.026	450	40	15.0	90	70
C20131	8	10		W-228491	4.90	400	.066	68	15	2.80	.027	340	40	13.0	87	75
C20131	12	14		W-228492	5.10	420	.063	69	22	2.90	.027	350	40	12.0	87	73
C20131	16	18		W-228493	5.10	400	.075	72	29	2.90	.021	330	44	11.0	85	73
C20131	22	24		W-228494	5.00	390	.063	72	17	2.90	.027	330	44	11.0	93	75
C20131	28	30		W-228495	5.10	390	.083	71	23	2.90	.023	330	42	11.0	89	75
C30111	0	2		W-229828	5.08	493	.041	74	22	2.87	.027	565	41	12.0	90	73
C30111	2	4		W-229790	5.62	509	.057	80	23	3.12	.024	542	40	9.8	102	89
C30111	4	6		W-229791	5.47	441	.066	84	21	2.90	.021	317	48	7.3	95	87
C30111	8	10		W-229792	5.64	451	.065	87	22	3.16	.021	341	50	8.7	102	90
C30111	12	14		W-229793	5.70	450	.065	82	23	3.25	.035	353	46	9.4	100	89
C30111	16	18		W-229794	5.77	453	.066	84	23	3.05	.020	354	46	7.3	98	89
C30111	22	24		W-229795	5.78	445	.075	82	24	3.13	.020	357	42	7.9	95	90
C30111	24	26		W-229796	5.66	449	.077	82	30	3.17	.016	360	44	7.9	95	90
C40121	0	2		W-232023	5.08	404	.037	79	19	2.81	.040	819	36	9.1	87	61
C40121	2	4		W-232024	5.37	412	.050	80	20	2.98	.040	603	36	10.0	94	61
C40121	4	6		W-232025	5.39	423	.050	80	22	2.98	.040	391	36	10.0	104	65
C40121	6	8		W-232026	5.38	423	.058	80	22	2.94	.040	355	39	7.5	100	70
C40121	8	10		W-232027	5.33	423	.240	81	23	2.92	.040	355	39	7.5	90	70
C40121	14	16		W-232028	5.54	415	.071	84	23	2.99	.040	346	36	9.6	102	75
C40121	20	22		W-232029	5.43	419	.075	80	23	3.00	.040	359	37	9.8	107	75
C40121	24	26		W-232030	5.45	414	.055	83	22	3.00	.040	362	36	9.1	102	61
C50111	0	2		W-233016	4.72	382	.055	70	15	2.59	.030	516	32	12.0	74	68
C50111	2	4		W-233769	5.40	408	.050	70	20	2.89	.050	595	45	7.8	117	75
C50111	4	6		W-233770	5.28	417	.058	71	21	2.82	.050	372	43	8.6	119	71
C50111	6	8		W-233771	5.47	418	.083	70	22	2.89	.050	326	46	9.3	123	68
C50111	8	10		W-233772	5.40	407	.071	70	22	2.86	.050	323	45	9.3	119	68
C50111	14	16		W-233773	5.39	417	.083	70	22	2.86	.050	327	48	8.6	123	68
C50111	20	22		W-233774	5.49	404	.075	71	21	2.95	.030	328	44	7.0	107	71
C50111	26	28		W-233775	5.51	412	.071	70	22	2.97	.040	338	50	7.0	109	66
C60100	0	2		W-234511	4.98	451	.020L	67	17	2.90	.020	565	39	14.0	74	68
C60121	2	4		W-234535	5.68	452	.025	72	22	3.23	.030	798	48	16.0	98	77
C60121	4	6		W-234536	5.90	458	.046	71	22	3.33	.030	778	53	15.0	77	78
C60121	6	8		W-234537	5.82	455	.050	72	21	3.22	.030	388	51	14.0	104	78
C60121	8	10		W-234538	5.86	466	.083	71	22	3.17	.020	365	51	16.0	104	76
C60121	14	16		W-234539	5.59	475	.091	72	20	2.96	.020	360	51	15.0	137	76
C60121	20	22		W-234540	5.62	448	.100	73	21	3.10	.030	356	55	12.0	90	77
C60121	28	30		W-234541	5.65	463	.091	69	22	3.19	.020	360	49	12.0	112	75
C10611	0	2		W-228496	5.10	430	.090	71	19	2.80	.029	740	45	17.0	75	78
C10611	2	4		W-228497	5.30	440	.075	73	17	3.00	.027	680	51	14.0	90	81
C10611	4	6		W-228498	5.30	450	.120	76	18	2.90	.021	370	47	13.0	97	80
C10611	8	10		W-228499	5.30	440	.130	72	27	2.80	.025	330	47	14.0	87	80
C10611	12	14		W-228500	5.30	450	.075	72	16	2.90	.034	330	47	14.0	90	80
C10611	16	18		W-228501	5.30	460	.110	76	15	2.90	.013	340	51	13.0	91	80
C10611	22	24		W-228502	5.20	420	.110	75	17	2.90	.036	340	49	11.0	100	81
C20611	0	2		W-228503	4.80	420	.063	69	17	2.70	.034	880	45	15.0	100	71
C20611	2	4		W-228504	5.00	410	.120	69	16	2.80	.027	820	45	14.0	89	75
C20611	4	6		W-228505	5.10	420	.075	71	17	2.70	.032	350	42	13.0	100	80
C20611	8	10		W-228506	5.30	410	.091	71	18	2.90	.034	330	48	13.0	85	76
C20611	12	14		W-228507	5.20	400	.190	71	21	2.90	.031	330	48	15.0	100	80
C20611	16	18		W-228508	5.20	410	.091	69	21	2.90	.020	330	44	13.0	100	80
C20611	20	22		W-228509	5.20	420	.100	73	20	3.00	.057	340	47	13.0	100	80

Table 7. - Chemical analyses of core samples subsectioned in 2 cm intervals. - Continued

Field no.	Top Dep (cm)	Bot Dep (cm)	Lab no.	Al (%)	Ba (ppm)	Cd (ppm)	Cr (ppm)	Cu (ppm)	Fe (%)	Hg (ppm)	Mn (ppm)	Ni (ppm)	Pb (ppm)	V (ppm)	Zn (ppm)
C30631	0	2	W-229835	5.24	409	.045	82	22	3.01	.022	1202	47	13.0	94	73
C30631	2	4	W-229797	5.76	458	.054	84	25	3.24	.021	801	48	12.0	102	90
C30631	4	6	W-229798	5.64	455	.077	82	24	3.09	.020	409	42	11.0	98	90
C30631	8	10	W-229799	5.49	456	.100	79	24	3.02	.020	331	46	13.0	98	87
C30631	12	14	W-229800	5.62	445	.100	76	24	3.11	.020	338	42	13.0	98	85
C30631	16	18	W-229801	5.74	457	.110	82	24	3.23	.020	341	46	10.0	102	87
C30631	20	22	W-229802	5.74	457	.066	60	22	3.22	.020	341	43	7.7	110	87
C30631	24	26	W-229803	5.83	457	.066	88	24	3.27	.016	346	50	7.3	98	90
C40600	0	2	W-231786	5.37	412	.050	85	24	2.94	.028	887	40	18.0	92	71
C40611	2	4	W-232031	5.60	429	.045	84	23	3.15	.044	1187	40	11.0	104	70
C40611	4	6	W-232032	5.57	435	.055	84	23	3.12	.044	637	40	10.0	104	68
C40611	6	8	W-232033	5.58	446	.091	84	24	3.04	.040	357	40	11.0	120	68
C40611	8	10	W-232034	5.63	446	.083	83	25	3.06	.040	345	39	11.0	104	75
C40611	10	12	W-232035	5.58	446	.063	82	26	3.00	.040	340	39	10.0	120	75
C40611	16	18	W-232036	5.52	431	.083	84	28	2.98	.040	345	39	8.8	110	61
C40611	22	24	W-232037	5.52	438	.110	82	23	3.06	.040	356	42	9.1	102	76
C40611	28	30	W-232038	5.56	432	.083	83	22	3.08	.040	358	42	9.1	120	70
C50611	0	2	W-233017	5.13	416	.063	75	18	2.85	.040	618	39	9.9	82	73
C50611	2	4	W-233762	5.61	424	.080	77	24	3.02	.040	587	52	8.6	111	71
C50611	4	6	W-233763	5.64	423	.100	76	24	2.99	.050	413	48	8.0	127	75
C50611	6	8	W-233764	5.75	415	.110	73	23	3.01	.050	326	50	8.0	123	76
C50611	8	10	W-233765	5.79	426	.096	74	22	3.04	.050	316	52	8.0	111	71
C50611	14	16	W-233766	5.70	419	.096	74	23	3.00	.050	317	50	7.0	131	76
C50611	22	24	W-233767	5.75	413	.080	75	24	3.09	.040	334	52	7.1	127	75
C50611	30	32	W-233768	5.66	412	.091	75	22	3.07	.030	347	52	6.6	127	70
C60611	0	2	W-234563	5.17	399	.030	72	18	2.81	.020	644	49	12.0	96	71
C60611	2	4	W-234564	5.42	423	.083	80	21	2.88	.020	376	52	15.0	113	76
C60611	4	6	W-234565	5.50	426	.083	80	23	2.88	.020	324	52	17.0	118	76
C60611	6	8	W-234566	5.63	427	.083	78	23	2.91	.020	322	52	15.0	113	75
C60611	8	10	W-234567	5.44	425	.055	76	23	2.96	.020	325	55	15.0	120	76
C60611	16	18	W-234568	5.51	422	.071	80	24	2.97	.020	338	55	14.0	125	73
C60611	22	24	W-234569	5.50	427	.083	76	20	3.00	.005L	339	50	9.0	120	71
C60611	28	30	W-234570	5.60	432	.083	80	20	3.03	.005L	353	55	11.0	115	73
C11311	0	2	W-228600	6.00	430	.110	83	28	3.40	.035	800	45	27.0	86	81
C11311	2	4	W-228601	6.00	430	.100	86	30	3.40	.031	700	45	19.0	84	81
C11311	4	6	W-228602	6.10	440	.083	89	29	3.40	.023	350	45	17.0	100	76
C11311	8	10	W-228603	6.20	460	.230	88	28	3.20	.017	320	47	12.0	110	80
C11311	12	14	W-228604	6.10	440	.180	86	25	3.10	.020	320	47	15.0	86	78
C11311	16	18	W-228605	6.10	440	.180	86	29	3.20	.017	330	44	13.0	92	76
C11311	24	26	W-228606	6.20	440	.200	92	24	3.30	.017	320	50	9.1	100	76
C21311	0	2	W-228593	6.00	430	.096	81	29	3.40	.060	880	48	24.0	84	80
C21311	2	4	W-228594	6.10	440	.075	81	25	3.50	.034	440	45	16.0	80	76
C21311	4	6	W-228595	6.20	450	.160	86	28	3.40	.025	340	47	14.0	86	78
C21311	8	10	W-228596	6.00	430	.190	95	25	3.20	.023	310	47	13.0	84	75
C21311	12	14	W-228597	6.20	440	.170	83	28	3.30	.023	320	47	11.0	84	78
C21311	16	18	W-228598	6.10	430	.200	83	25	3.30	.023	330	47	13.0	89	75
C21311	24	26	W-228599	5.90	420	.220	83	26	3.30	.018	330	47	11.0	90	76
C31311	0	2	W-229836	5.45	425	.066	82	24	3.10	.032	611	50	25.0	104	80
C30631	2	4	W-229804	5.96	461	.058	95	25	3.43	.033	723	50	18.0	107	100
C31311	4	6	W-229805	5.99	454	.050	88	25	3.44	.031	707	46	17.0	107	100
C31311	8	10	W-229806	6.05	453	.100	80	24	3.36	.026	351	42	14.0	115	98
C31311	12	14	W-229807	6.33	471	.130	87	24	3.46	.020	319	44	9.1	110	99
C31311	16	18	W-229808	6.23	467	.120	87	24	3.37	.020	301	42	7.7	107	98
C31311	24	26	W-229809	6.17	465	.130	91	23	3.43	.020	319	47	7.3	110	98
C31311	28	30	W-229810	6.00	453	.130	91	23	3.29	.020	312	48	9.1	107	95

Table 7. - Chemical analyses of core samples subsectioned in 2 cm intervals. - Continued

Field no.	Top Dep (cm)	Bot Dep (cm)	Lab no.	Al (%)	Ba (ppm)	Cd (ppm)	Cr (ppm)	Cu (ppm)	Fe (%)	Hg (ppm)	Mn (ppm)	Ni (ppm)	Pb (ppm)	V (ppm)	Zn (ppm)
C41311	0	2	W-231769	5.63	412	.066	81	26	3.15	.032	783	40	20.0	92	100
C41331	2	4	W-231751	5.90	442	.066	78	25	3.28	.048	417	43	25.0	112	90
C41331	4	6	W-231752	6.00	437	.140	79	27	3.29	.040	355	45	22.0	124	91
C41331	6	8	W-231753	6.04	450	.120	81	26	3.23	.028	343	43	15.0	130	88
C41331	8	10	W-231754	6.07	444	.150	79	26	3.26	.020	343	43	11.0	121	88
C41331	10	12	W-231755	6.01	445	.160	78	23	3.22	.016	336	46	9.6	130	83
C41331	16	18	W-231756	5.93	434	.140	77	24	3.24	.021	341	40	9.6	121	85
C41331	22	24	W-231757	5.91	434	.120	77	24	3.26	.016	345	45	9.6	126	83
C41331	26	28	W-231758	5.96	476	.160	78	24	3.27	.012	363	45	9.6	130	85
C51311	0	2	W-233018	5.47	404	.075	79	20	3.12	.040	628	48	18.0	94	85
C51311	2	4	W-233755	6.26	428	.066	85	24	3.51	.050	358	60	12.0	151	83
C51311	4	6	W-233756	6.33	435	.140	81	25	3.48	.030	328	54	11.0	135	88
C51311	6	8	W-233757	6.29	437	.160	83	27	3.36	.040	342	56	11.0	129	91
C51311	8	10	W-233758	6.24	431	.150	81	23	3.31	.040	342	60	7.1	149	91
C51311	14	16	W-233759	6.23	433	.140	81	23	3.28	.040	333	60	8.0	139	91
C51311	22	24	W-233760	6.11	437	.170	82	23	3.33	.030	346	66	7.0	135	86
C51311	28	30	W-233761	6.02	416	.120	81	22	3.27	.030	338	60	6.6	129	80
C61311	0	2	W-234571	5.48	447	.055	76	20	3.06	.030	802	55	30.0	115	81
C61311	2	4	W-234572	6.12	436	.046	84	22	3.48	.040	1297	62	31.0	120	100
C61311	4	6	W-234573	6.22	443	.038	86	22	3.50	.040	464	60	20.0	130	85
C61311	6	8	W-234574	6.28	452	.055	86	24	3.38	.030	356	60	20.0	125	96
C61311	10	8	W-234575	6.21	453	.083	84	24	3.37	.020	348	61	16.0	125	85
C61311	16	18	W-234576	6.10	441	.083	84	23	3.33	.020	349	60	15.0	125	83
C61311	22	24	W-234577	6.07	434	.140	86	20	3.26	.010	341	60	12.0	120	80
C61311	28	30	W-234578	5.99	432	.120	86	21	3.37	.010	354	62	9.2	120	80
C11411	0	2	W-230725	5.91	406	.061	76	23	3.31	.040	766	42	23.0	97	83
C11411	2	4	W-230726	5.94	397	.055	75	22	3.34	.021	565	39	16.0	106	83
C11411	4	6	W-230727	6.00	410	.100	74	24	3.20	.021	334	40	15.0	106	85
C11411	6	8	W-230728	6.03	417	.140	78	23	3.16	.016	328	40	13.0	101	83
C11411	12	14	W-230729	5.84	400	.120	68	22	3.09	.012	319	40	11.0	93	80
C11411	18	20	W-230730	5.84	405	.100	73	22	3.21	.012	327	42	12.0	106	78
C11411	24	26	W-230731	5.86	408	.100	75	19	3.24	.012	324	40	8.3	101	78
C11411	28	30	W-230732	5.87	408	.120	73	21	3.24	.005L	335	42	7.8	101	81
C11411	32	34	W-230733	5.97	411	.180	76	23	3.32	.006	338	42	11.0	106	81
C41421	0	2	W-231773	5.59	411	.055	79	21	3.15	.040	832	42	18.0	82	88
C41421	2	4	W-231759	5.93	428	.083	77	25	3.21	.021	386	40	15.0	124	83
C41421	4	6	W-231760	6.00	443	.150	78	24	3.20	.024	350	40	13.0	126	83
C41421	6	8	W-231761	6.00	438	.140	78	23	3.18	.021	345	42	11.0	130	83
C41421	8	10	W-231762	5.95	444	.150	78	28	3.14	.020	346	42	10.0	130	85
C41421	10	12	W-231763	5.96	457	.150	77	30	3.14	.026	344	42	12.0	126	83
C41421	16	18	W-231764	6.00	446	.150	78	25	3.18	.015	345	42	9.7	125	83
C41421	22	24	W-231765	6.07	450	.190	76	23	3.23	.012	339	40	8.1	124	83
C51411	0	2	W-233019	5.20	381	.090	77	20	2.89	.040	641	44	19.0	78	85
C51411	2	4	W-233037	5.70	412	.091	84	25	3.20	.050	721	51	25.0	103	90
C51411	4	6	W-233038	5.86	434	.075	85	23	3.29	.045	728	52	19.0	96	88
C51411	6	8	W-233039	6.03	437	.042	86	21	3.36	.030	486	53	7.2	96	88
C51411	10	12	W-233040	5.97	418	.088	85	23	3.27	.015	357	52	14.0	98	87
C51411	16	18	W-233043	5.91	420	.120	82	22	3.20	.025	347	53	11.0	99	85
C51411	22	24	W-233042	5.82	422	.100	83	24	3.15	.020	336	52	8.1	103	85
C61411	0	2	W-234579	5.37	414	.055	74	19	2.92	.040	706	50	26.0	110	75
C61411	2	4	W-234580	5.89	411	.025	80	21	3.27	.040	698	55	22.0	115	80
C61411	4	6	W-234581	5.99	420	.042	82	23	3.32	.040	344	52	17.0	120	81
C61411	6	8	W-234582	6.08	428	.100	82	22	3.22	.020	327	58	12.0	140	80
C61411	8	10	W-234583	6.07	434	.190	78	23	3.17	.020	323	58	13.0	140	81
C61411	14	16	W-234584	6.01	413	.130	80	22	3.25	.020	326	58	11.0	135	78
C61411	18	20	W-234585	6.02	409	.110	80	22	3.26	.030	329	55	8.6	130	80
C61411	24	26	W-234586	6.38	415	.110	80	22	3.36	.010	349	59	14.0	135	78

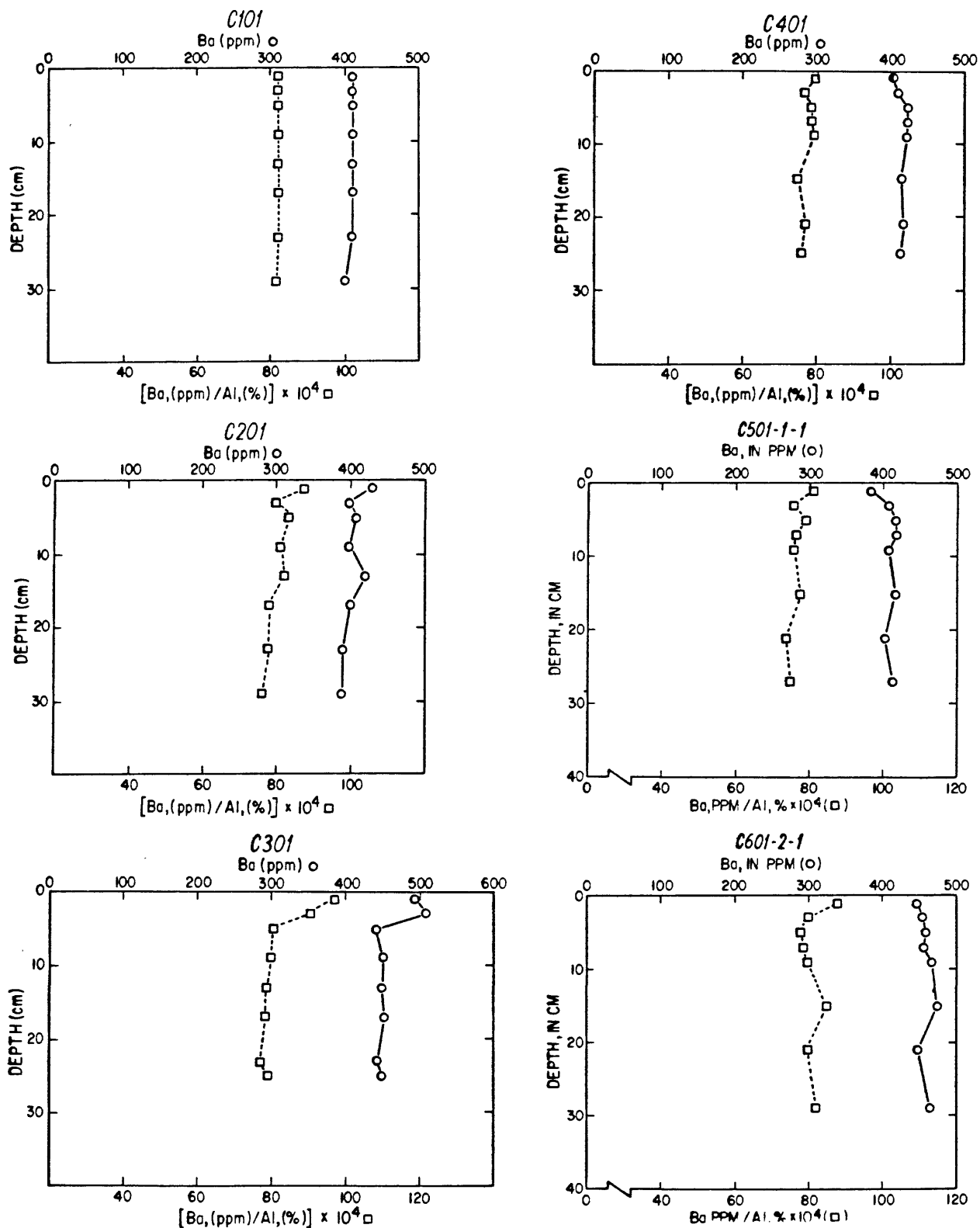


Figure 3. Distribution of barium and barium to aluminum ratio with sediment depth; Cruises 1-6, Station 1. (C101 = Cruise 1, Station 1).

ratio within 4 cm of the sediment surface were 13 and 25 percent higher, respectively, than in samples deeper in the sediment. These trends support the conclusion that a small increase in drilling-related Ba can be measured at Station 1.

Station 6 is located about 83 km from the drilling in Block 372. At this station the distributions of Ba and the Ba-to-Al ratio with depth showed no consistent patterns (Fig. 4). Small increases in the Ba-to-Al ratio were measured in the surface sediments in cores from Cruises 2 and 6, but no increases in Ba concentrations.

Similarly, cores from Station 13 showed no enrichment in the concentration of Ba and the Ba-to-Al ratio was slightly higher in only two of the five postdrilling samples (Fig. 5). This station is located about 1.4 km southwest of the drilling site in Block 93. Drilling began on July 14, 1984 about four weeks before Cruise 2 and was completed November 4, 1984 just before Cruise 3.

Samples from Station 14 (drill site in Block 93) were collected only on Cruises 1, 4, 5, and 6 (Fig. 6). The profiles of Ba and Ba-to-Al ratio are essentially the same for both the predrilling and postdrilling samples.

In cores collected on Cruise 1 at Stations 1, 6, 13, and 14, the concentration of Ba and the Ba-to-Al ratio in the surface sediments were not elevated in comparison with deeper sediments. This suggests that the drilling which occurred before Cruise 1 did not contribute Ba to the general area of this survey to a measurable degree.

The concentrations of Pb and Mn in the upper few centimeters of these cores were consistently higher than in the deeper sediments (Figs. 7-12). The profiles of these metals for all six cruises at a given station are very similar (Table 7, Figs. 7-12) confirming that the changes with depth are

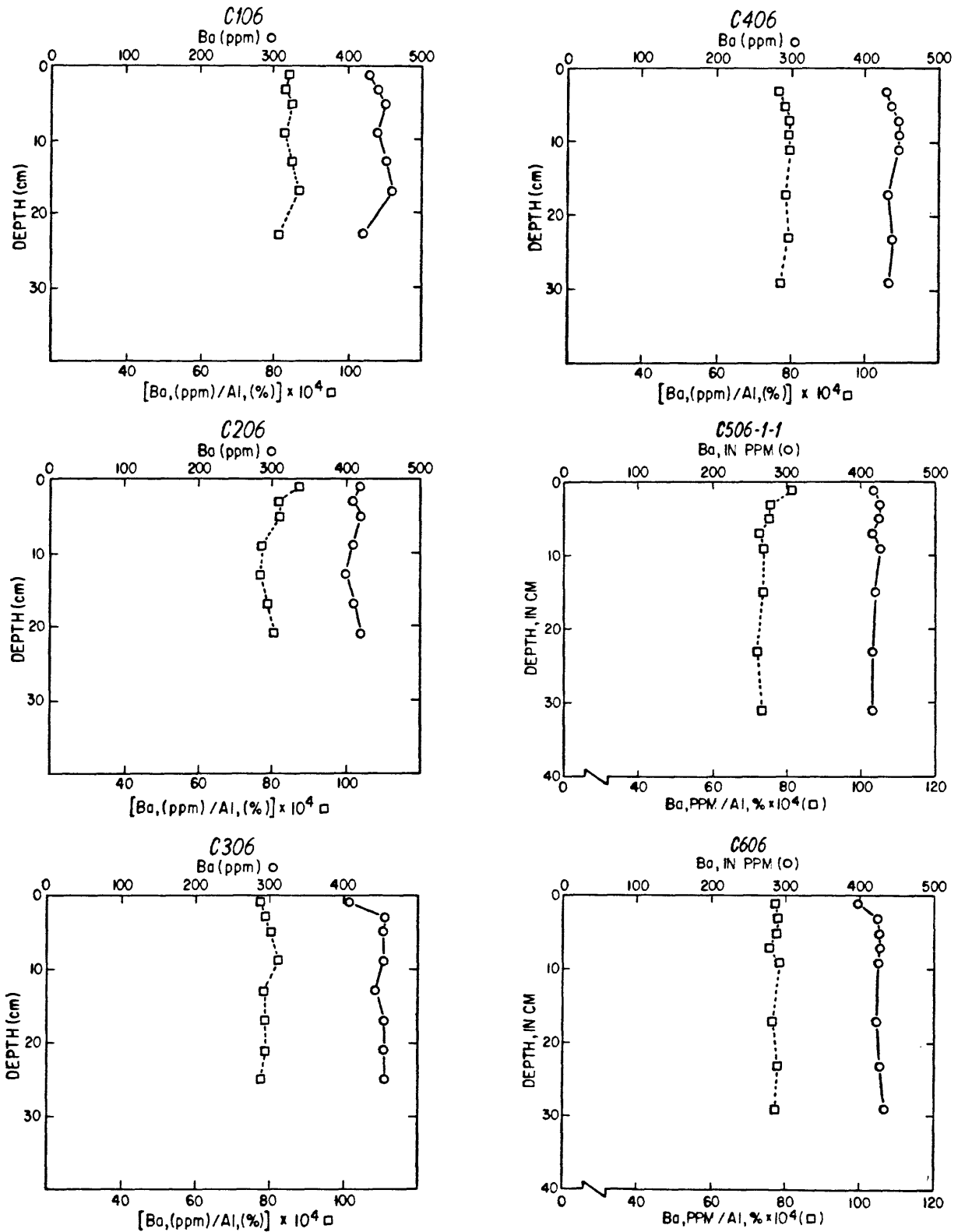


Figure 4. Distribution of barium and barium to aluminum ratio with sediment depth; Cruises 1-6, Station 6. (C106 = Cruise 1, Station 6).

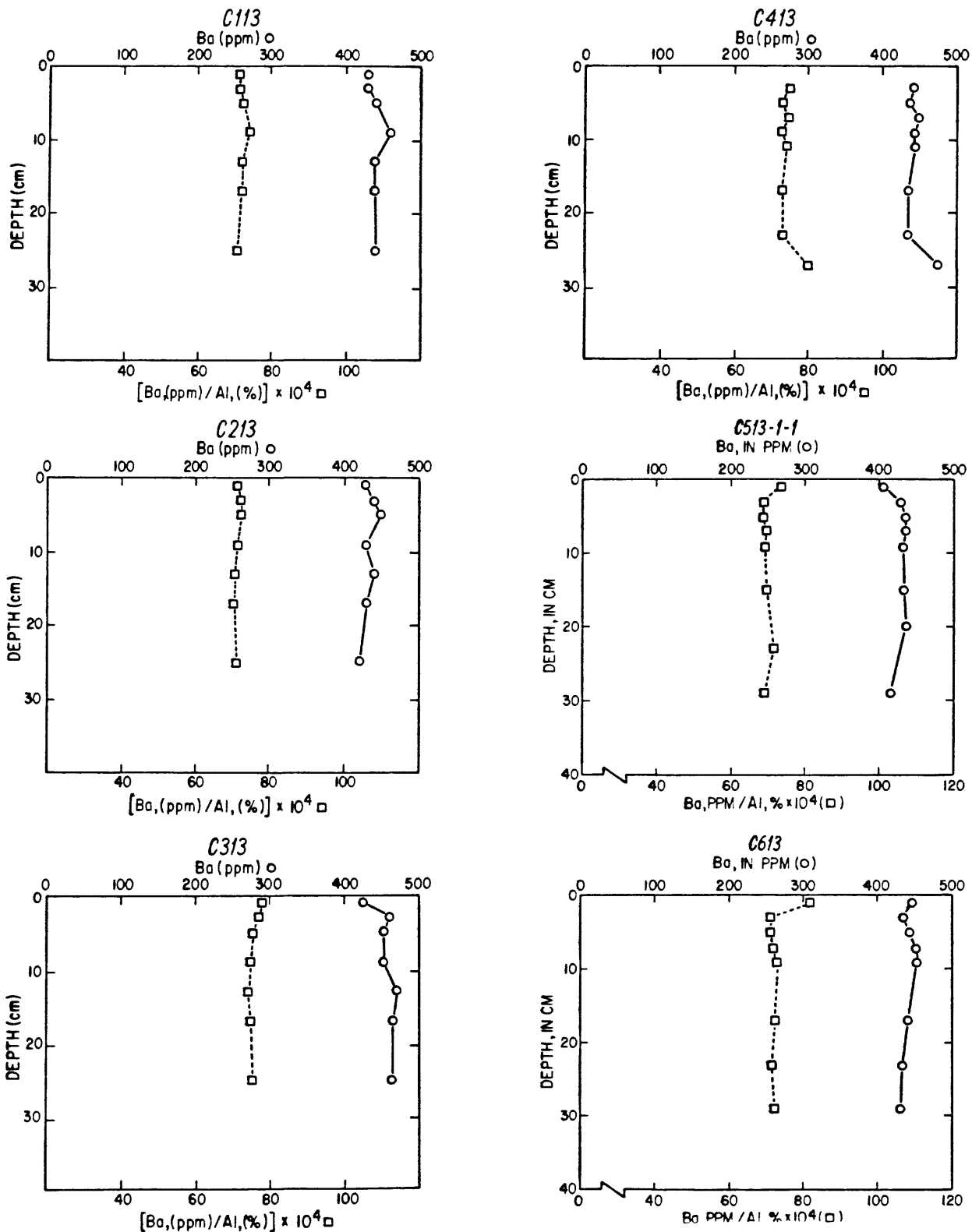


Figure 5. Distribution of barium and barium to aluminum ratio with sediment depth; Cruises 1-6, Station 13. (C113 = Cruise 1, Station 13).

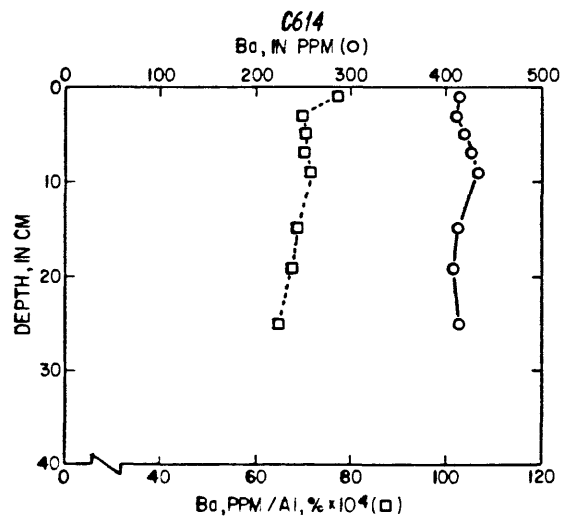
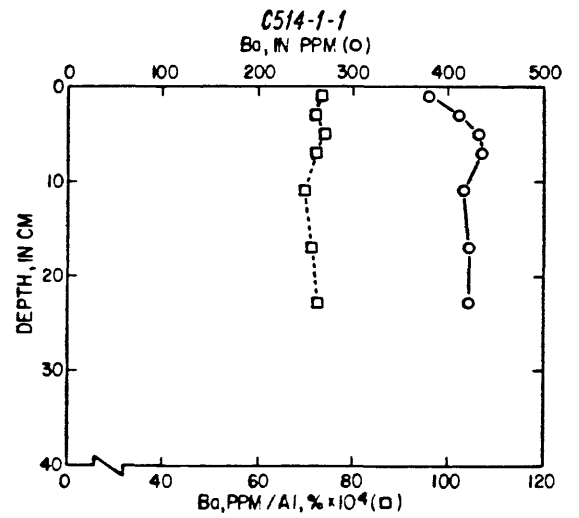
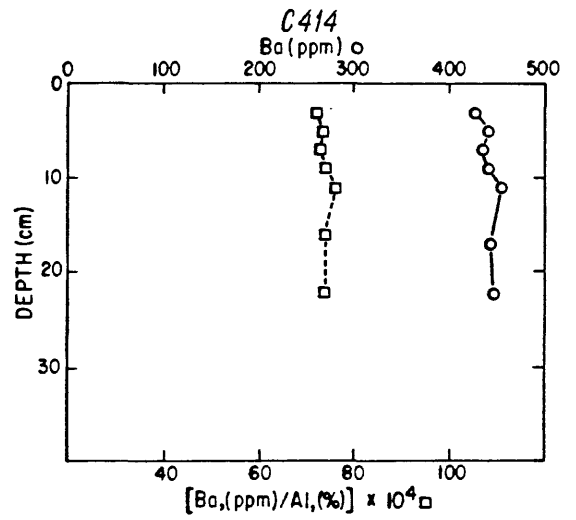
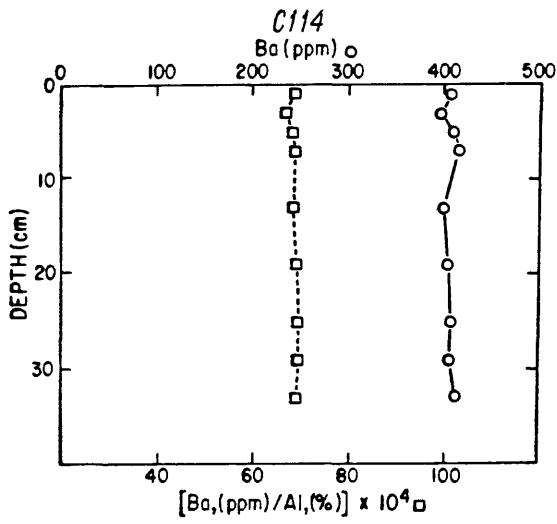


Figure 6. Distribution of barium and barium to aluminum ratio with sediment depth; Cruises 1, 4-6, Station 14. (C114 = Cruise 1, Station 14).

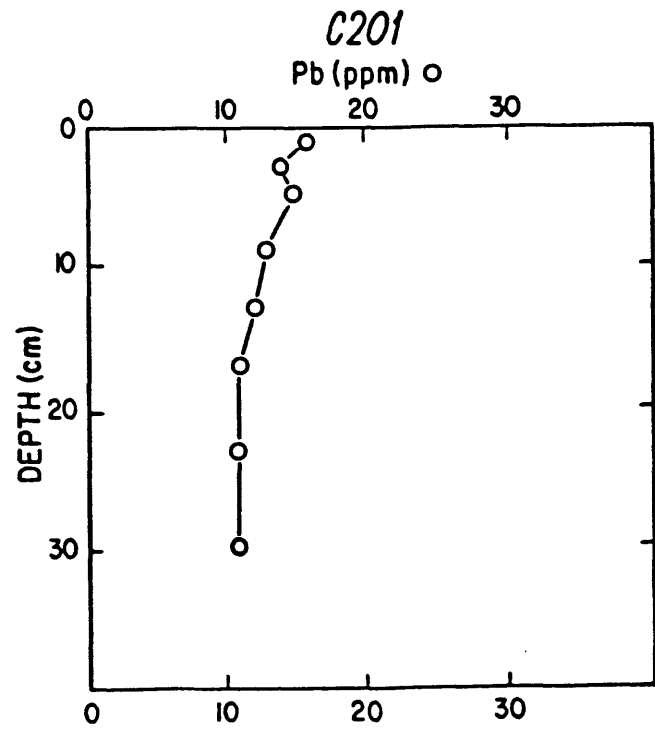
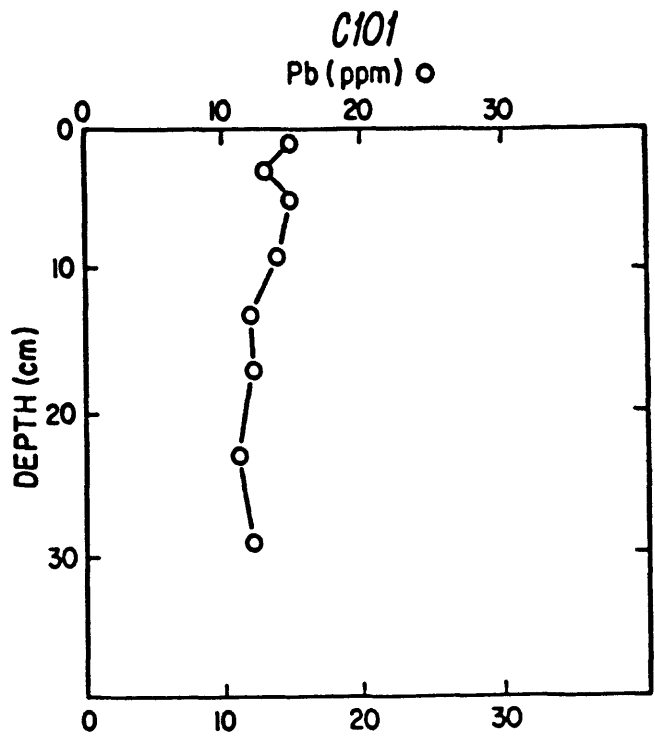


Figure 7. Distribution of lead with sediment depth; Cruises 1 and 2, Station 1. (C101 = Cruise 1, Station 1)

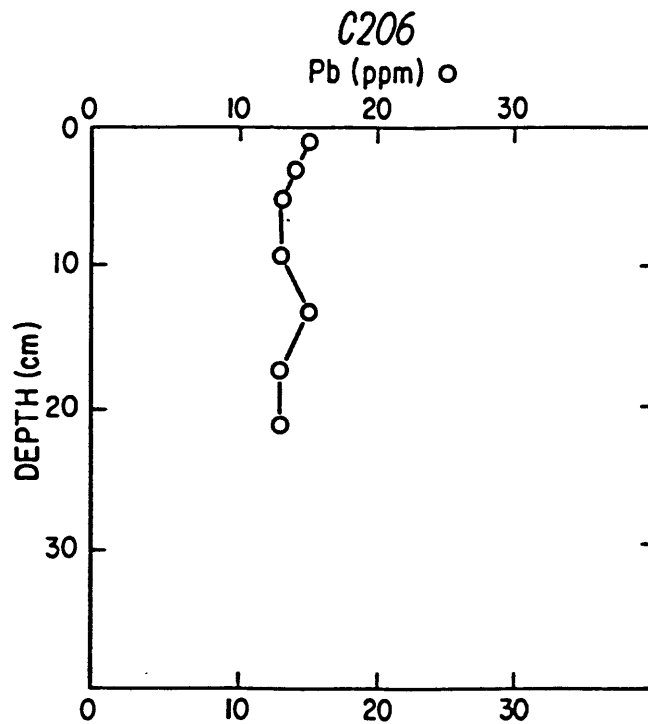
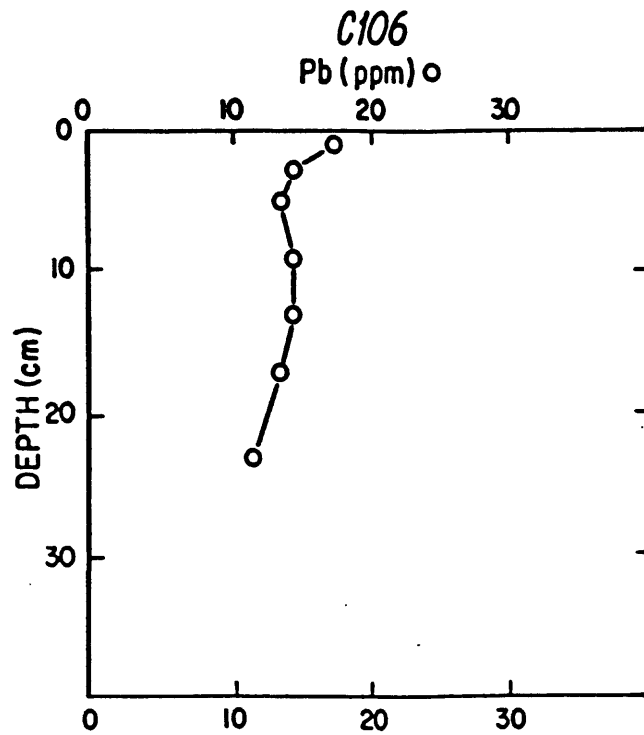


Figure 8. Distribution of lead with sediment depth; Cruises 1 and 2, Station 6. (C106 = Cruise 1, Station 6)

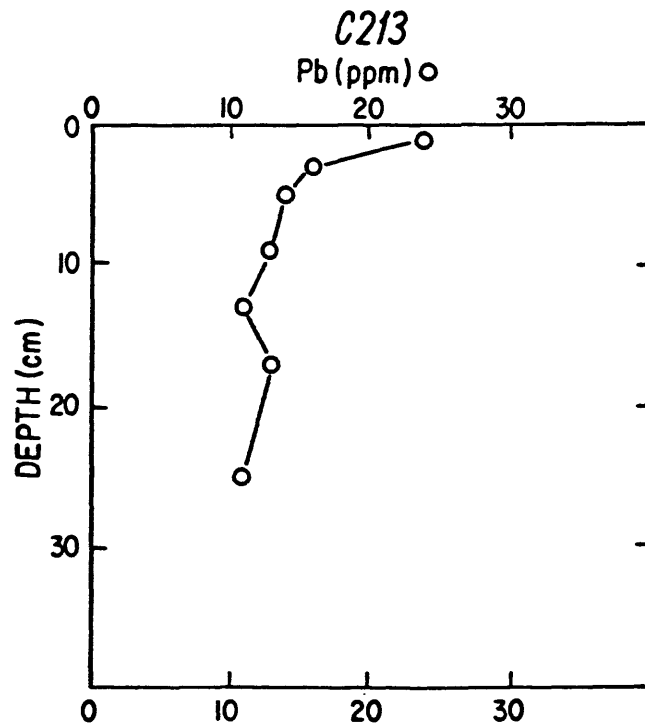
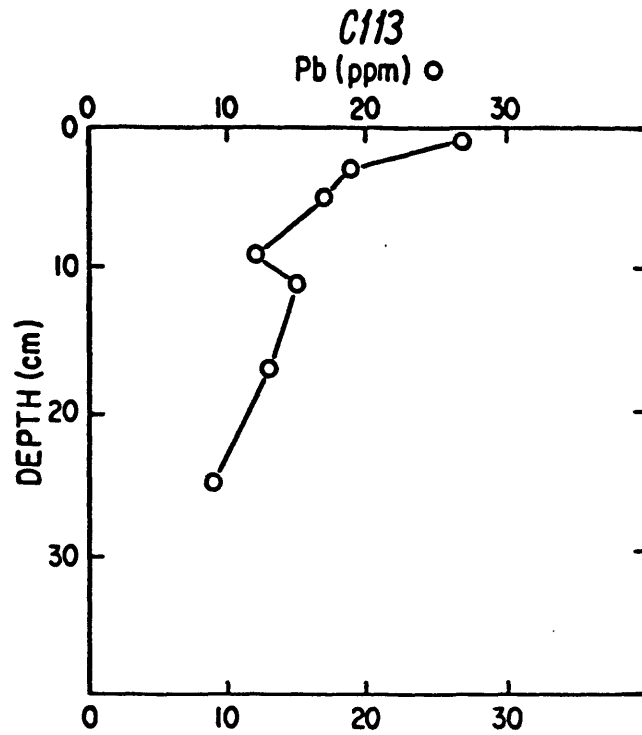


Figure 9. Distribution of lead with sediment depth; Cruises 1 and 2, Station 13. (C113 = Cruise 1, Station 13)

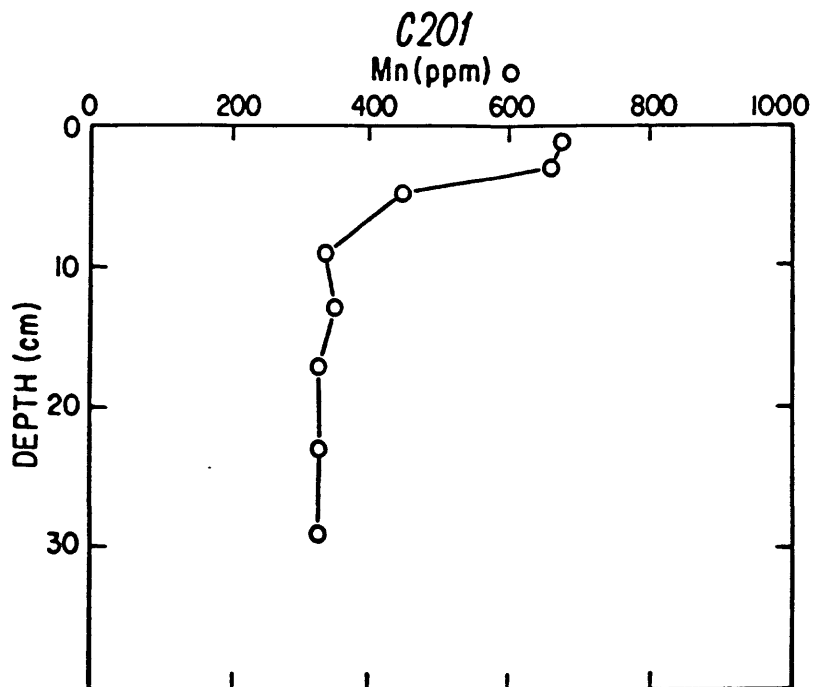
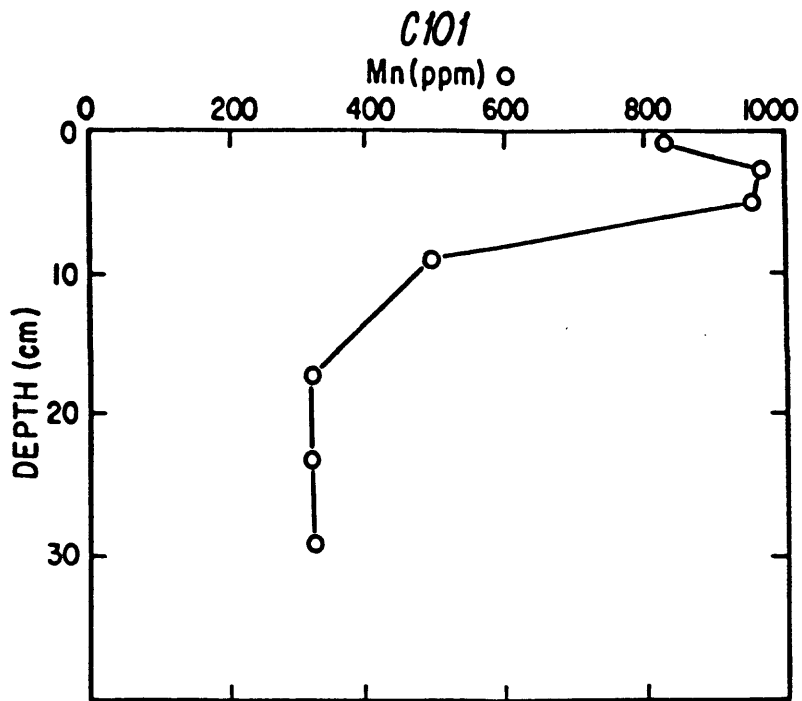


Figure 10. Distribution of manganese with sediment depth; Cruises 1 and 2, Station 1. (C101 = Cruise 1, Station 1)

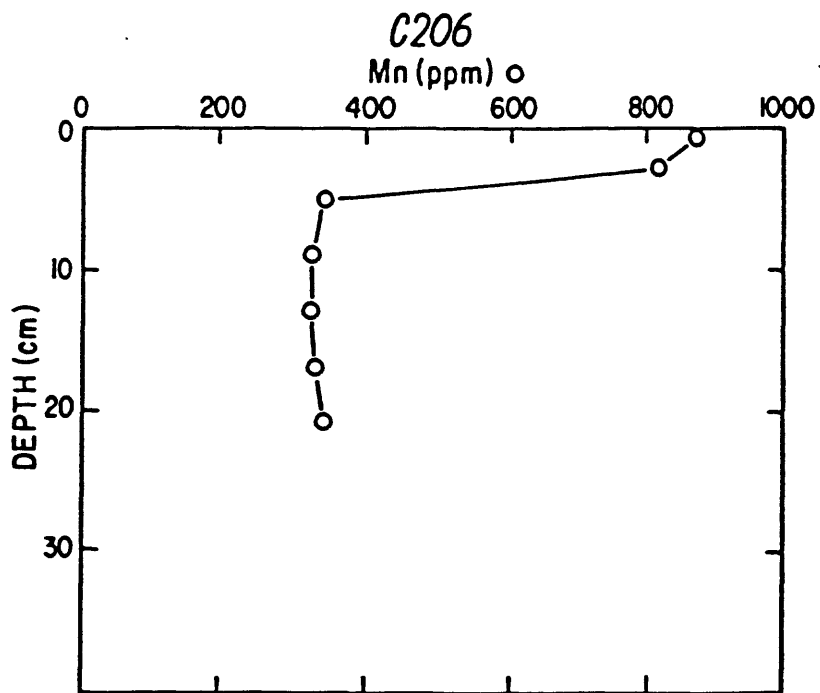
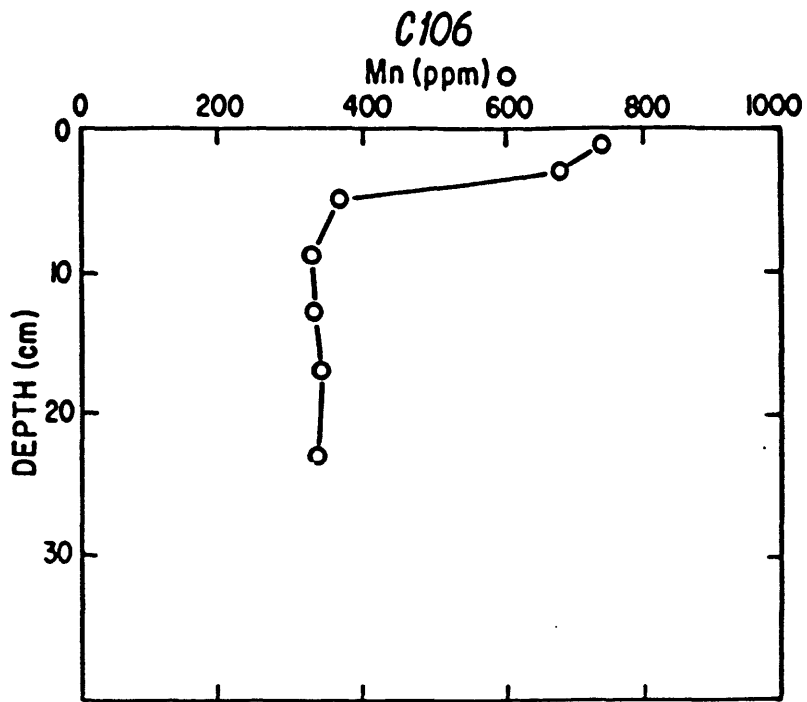


Figure 11. Distribution of manganese with sediment depth; Cruises 1 and 2, Station 6. (C106 = Cruise 1, Station 6)

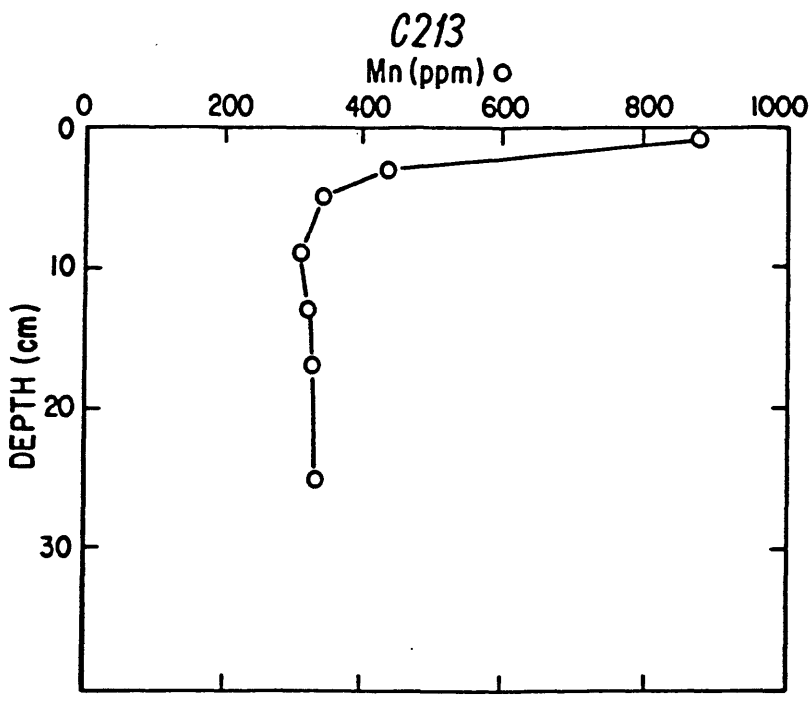
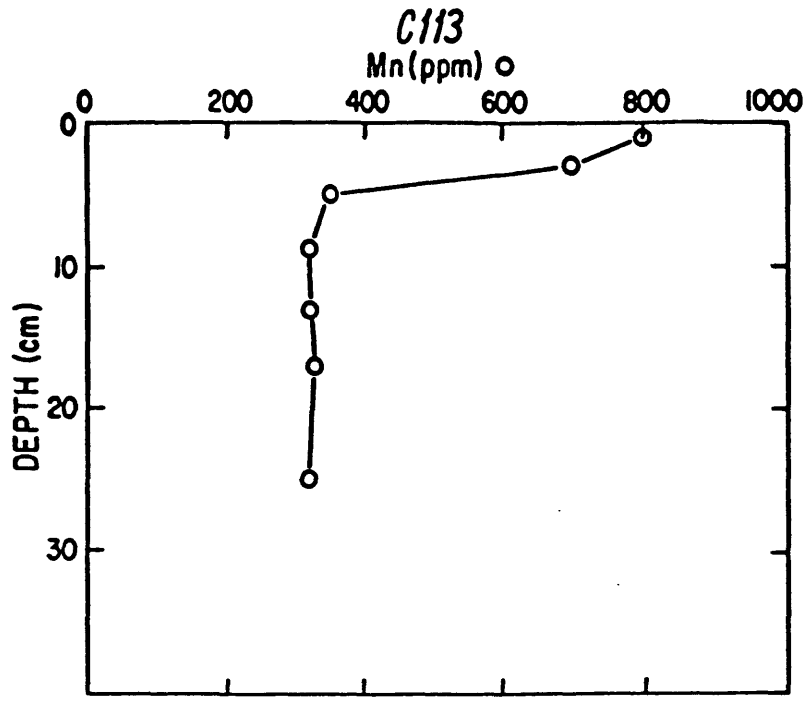


Figure 12. Distribution of manganese with sediment depth; Cruises 1 and 2, Station 13. (C113 = Cruise 1, Station 13)

unrelated to drilling. The Mn profile is typical for sediments that undergo a transition from oxidizing conditions near the water/sediment interface to reducing conditions in deeper sediments. The profile is a result of MnO₂ dissolving under reducing conditions, diffusing upward, and precipitating in the oxidizing conditions near the surface (Lynn and Bonati, 1965).

The absence of a gradient in the Ba profile in cores that have a strong gradient in Mn (for example, Stations 1 and 13 from Cruise 1) suggests that naturally occurring Ba is not migrating in the subsurface reducing conditions, at least not at a rate sufficient to measurably change the Ba concentrations of the sediments. Any increases we measure in the surface sediment relative to deeper sediment can thus be attributed to a recent addition of the metal, presumably from drilling activity, rather than to natural diagenetic processes.

The distribution of Pb with depth (Figs. 7-9 and Table 7) is a common feature in areas of fine sediment on the continental shelf and slope (Bothner and others, 1981; Bothner and others, 1985). The surficial sediments are typically as much as 2 to 3 times higher than sediments 25 to 30 cm below the water-sediment interface. The highest concentration measured in these cores is 31 ppm, slightly higher than the value in world average shales (20 ppm, Krauskopf, 1967).

The elevation in surficial sediments is thought to be related to an increased supply of lead to these sediments, probably from the burning of lead alkyls in gasoline in coastal metropolitan areas. The use of lead alkyls began in 1924 and has increased each year from 1940 until the recent switch to unleaded gasoline. The penetration of Pb to a depth of at least 10 cm is probably related to biological reworking of the sediment.

Lead inventories

From the profiles of lead with sediment depth, an inventory of the lead added to these sediments as a result of man's industrial use of lead can be estimated. For this calculation, we assumed that the enhanced concentrations of lead in the near surface sediments are from anthropogenic sources. This assumption seems justified because of the evidence against lead enrichment resulting from post-depositional mobility (Bruland and others, 1974). We also assumed that the background concentration of lead in a particular core was represented by the concentration in the lowest 5 to 10 cm, and remained constant throughout the core. In some cores, modern Pb may have penetrated to the bottom of the cores, which would make our estimate of background too high. The chosen background value was subtracted from the total value for each interval analyzed and the net values were summed to determine the anthropogenic contribution. Interpolated values were used for intervals not analyzed. Correcting for porosity (using water content) and assuming a constant grain density of 2.7 g/cc, the inventory of added lead in $\mu\text{g}/\text{cm}^2$ was calculated.

The atmospheric flux of lead to the Atlantic Ocean in the vicinity of Bermuda is estimated to have been about $1 \text{ mg}/\text{m}^2/\text{yr}$ during the early 1980's (Church and others, 1984, Jickells and others, 1984a,b; G. T. Shen, written communication, 10 April, 1986). Mr. G. T. Shen, Massachusetts Institute of Technology, has kindly provided data showing the variations in the Pb to Ca ratio in annual growth bands of a coral head (Diploria strigosa) over the last 100 years. Assuming that the record of lead incorporated into coral correlates with the atmospheric flux of lead to the ocean, it is possible to estimate and sum the total deposition of anthropogenic lead on an area basis. The value thus obtained is $6.2 \mu\text{g}/\text{cm}^2$.

The estimated inventories of lead at Stations 13 and 14 are $46 \pm 17 \mu\text{g}/\text{cm}^2$ and $44 \pm 22 \mu\text{g}/\text{cm}^2$ respectively (Fig.13). Somewhat lower values were measured at Stations 1 ($16 \pm 7 \mu\text{g}/\text{cm}^2$) and 6 ($25 \pm 17 \mu\text{g}/\text{cm}^2$). The high standard deviation, among as many as six cores at a single location, is due in part to our inability to accurately estimate background values of lead using these rather short cores.

The average lead inventories measured at these stations are higher than the estimated flux to the sea surface would predict, suggesting that there is preferential accumulation of anthropogenic lead in slope sediments. The magnitude of the lead inventories at these four Middle Atlantic slope stations are within the range measured in the South Atlantic study area ($4\text{-}68 \mu\text{g}/\text{cm}^2$, Bothner and others, 1987), but much lower than the inventories ($100\text{-}150 \mu\text{g}/\text{cm}^2$) calculated for the fine grained deposit on the continental shelf south of Martha's Vineyard (Bothner and others, 1981).

In the case of the deposit south of Martha's Vineyard, ^{210}Pb and ^{14}C radiochemical data have supported the interpretation that high lead inventories are a result of frequent sediment resuspension and a rapid rate of sediment accumulation (Bothner and others, 1981). Similar radiochemical analysis would be extremely useful for interpreting the high inventories of lead on the continental slope. It would also be valuable to determine if the excess lead inventory on the continental slope is accompanied by a deficiency in the inventory of lead in the sandy sediments on the adjacent continental shelf.

The impact of this excess Pb in slope sediments is unknown. Important questions are: How is the Pb bound in the sediments? What is the bioavailability of this Pb? What is the response of organisms at different life stages to long-term, low-level Pb contamination? Although a few studies

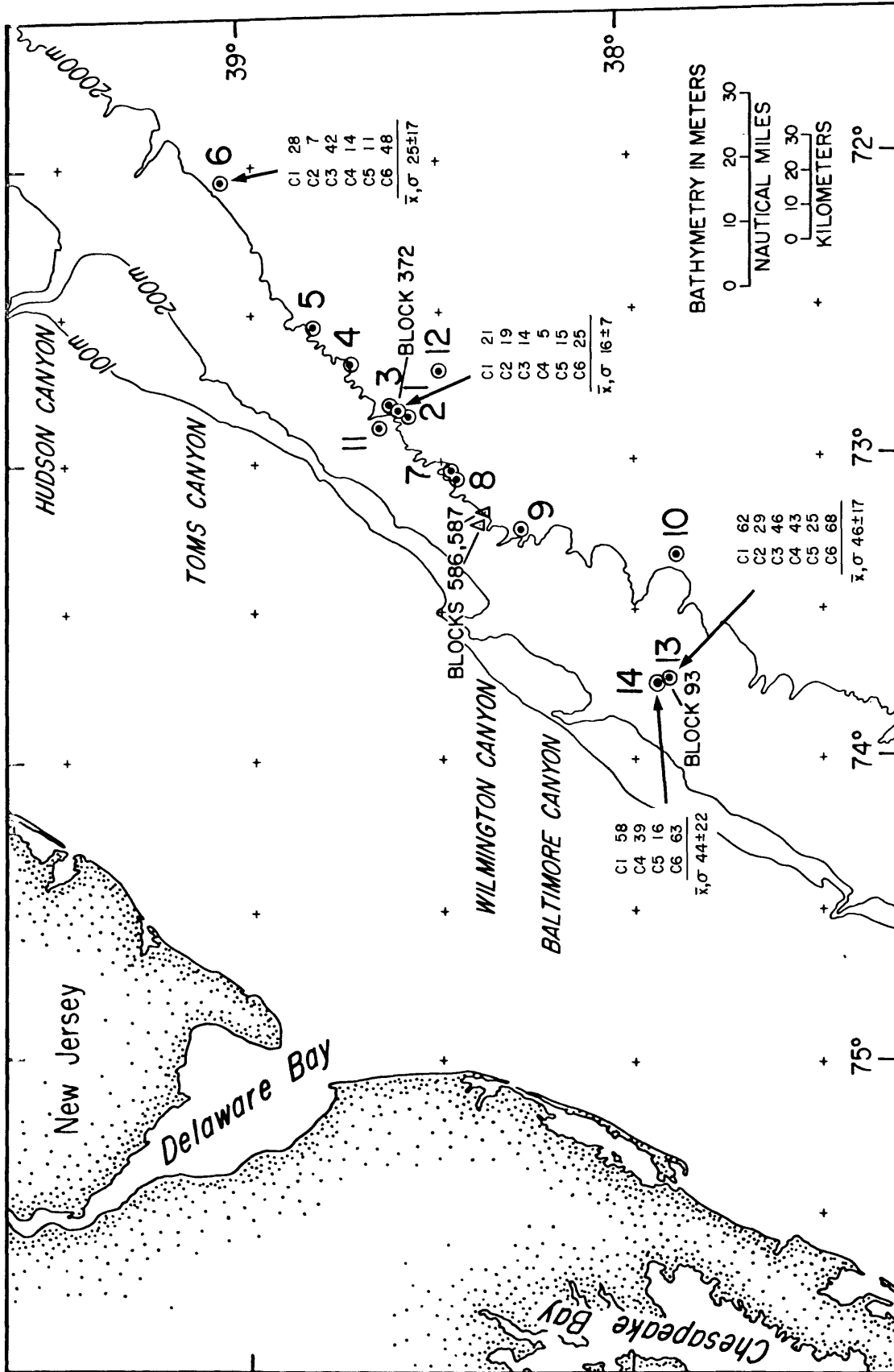


Figure 13. Pb inventory ($\mu\text{g}/\text{cm}^2$) at Stations 1, 6, 13 Cruises 1-6; and Station 14 Cruises 1, 4-6. \bar{x} = mean, σ = standard deviation.

show a relationship between the concentration of lead in the tissue of deposit feeding organisms and the lead concentration in acid leached sediment (Luoma and Bryan, 1978; Tessier and others, 1984), no guidelines for "safe" levels of lead in sediments have been established. Studies addressing this complex issue are presently funded by the Environmental Protection Agency.

Ba concentration in sediment trap samples

Thirteen sediment traps were deployed 2.8 km southwest of the Shell drilling site in Block 372 (Appendix Table 2) on June 21, 1984. The traps were placed at different elevations above the sea floor on a subsurface current-meter mooring set out by Science Applications, Inc. The traps were deployed for 99 days, which included the last 18 days of the drilling operations. The period near the end of drilling typically includes a final discharge of drilling fluid before the well is plugged and abandoned.

The Ba concentrations are highest in the sediment trap located nearest the surface and decrease with increasing trap depth throughout the upper half of the water column (Fig. 14). There is a small increase in Ba concentration from the middle of the water column to the bottom, but this apparent trend needs to be confirmed with additional analyses.

One subsample from trap 901 (220-m water depth) consisted of gray particles having relatively high density and containing at least 27,000 ppm Ba in the <1-mm size fraction (Table 8). This concentration is a lower limit because the acid decomposition method did not completely dissolve the particles. Examination by means of the scanning electron microscope (SEM) indicated that the particulate residue was barium sulfate.

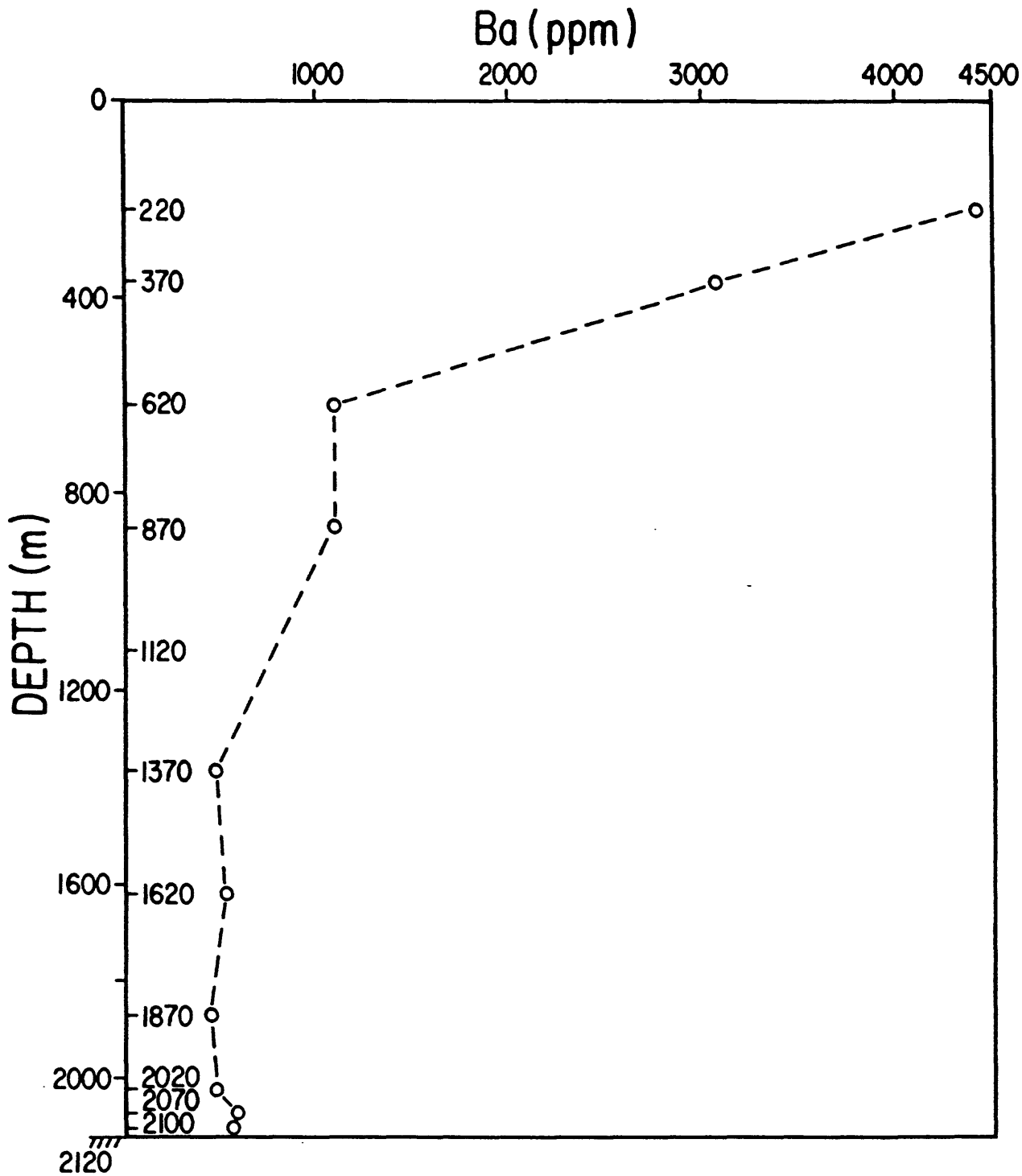


Figure 14. Average Ba concentration (ppm) in sediment trap samples (<1 mm size range) deployed at different depths near Block 93.

Table 8. Chemical analysis of sediment trap samples; mooring location: 38°35.1'N., 72°53.5'W., 2,120 m water depth.

[Missing data indicates insufficient sample size for analysis.]

Field no. 1	Top (cm)	Btm (cm)	Lab no.	Trap depth (m)	Al (%)	Ba (ppm)	Cd (ppm)	Cr (ppm)	Cu (ppm)	Fe (%)	Hg (ppm)	Mn (ppm)	Ni (ppm)	Pb (ppm)	V (ppm)	Zn (ppm)
ST901-W	0.5	2.5	W-231615	220	0.52	29	---	28	---	3.05	---	---	31	---	11	---
ST901-W	2.5	3	W-231613	220	.02	191	---	13	---	.08	---	---	2	---	7.6	---
ST901-W	3	5	W-231614	220	.70	5,890	---	77	---	.68	---	---	42	---	23	---
ST901-Z	0.5	2	W-231620	220	1.67	896	3,790	34	30	1.14	0.09	358	14	24	20	613
ST901-Z	2.5	3	W-231619	220	.85	1,460	5,670	31	34	.50	.12	240	15	15	6.3	609
ST901-Z	3	5	W-231621	220	1.75	8,090	3,810	45	34	.84	.15	217	14	58	20	775
ST901-Z	5	5.3	W-231622	220	4.93	27,600	1,540	130	45	1.86	---	292	18	14	49	974
ST901-Y2	5	5.3	W-231612	220	1.94	35,800	---	47	---	1.49	---	---	45	---	28	---
ST901-Z	5.3	6	W-231611	220	5.32	11,200	1,190	140	25	2.01	---	295	48	30	32	634
ST901-P	.5	2	W-231610	220	1.62	2,770	---	110	---	.33	---	---	74	---	36	---
ST901-P	2.5	3	W-231609	220	3.59	2,300	---	307	---	.72	---	---	178	---	159	---
ST901-P	3	5	W-231607	220	1.52	4,370	---	166	---	.30	---	---	63	---	65	---
ST901-P	5	5.3	W-231608	220	7.27	21,000	---	571	---	2.08	---	---	245	---	131	---
ST903-W			W-231618	620	.03	62	---	10	---	.06	---	---	<2	---	6	---
ST903-Z			W-231599	---	3.34	1,090	---	59	---	1.71	---	---	51	---	41	---
ST904-Z			W-231600	870	3.68	1,090	---	57	---	1.85	---	---	49	---	33	---
ST906-W			W-231617	1,370	5.29	958	---	285	---	.85	---	---	348	---	162	---
ST906-Z			W-231601	---	4.07	460	---	76	---	2.20	---	---	62	---	43	---
ST907-Z			W-231602	1,620	4.62	525	<.020	66	34	2.50	---	419	43	22	52	264
ST908-W			W-231616	1,870	6.45	725	---	509	---	2.81	---	---	285	---	151	---
ST908-Z			W-231603	---	4.54	447	.071	67	43	2.48	.18	456	46	17	56	146
ST909-Z			W-231604	2,020	5.18	476	.086	74	38	2.92	---	776	53	23	90	144
ST910-Z			W-231605	2,070	5.81	586	.110	77	44	3.22	---	681	58	16	106	182
ST911-Z			W-231606	2,100	5.64	559	.120	78	34	3.13	.37	633	48	19	85	171

1 Field number designation: P = supernatant from centrifugation;
W = >1 mm size fraction;
Y2 = panned concentrate;
Z = <1 mm size fraction.

Physical and chemical isolation of barite particles

We conducted a number of experiments to isolate barite particles that had settled through the water column to the bottom sediments. Our objectives were to determine if barite was present in bottom sediments near a drilling rig and to estimate the settling velocity of barite particles on the basis of particle dimensions. Analysis of particles was carried out using a SEM fitted with an energy-dispersive x-ray spectrometer.

The heavy liquid (bromoform) separation technique described by Carver (1971) was used on the 5-60 μm size fraction of bottom sediments. The density separation of particles in this size range was not efficient enough to concentrate barium and the procedure was abandoned.

The selective chemical leach technique of Church (1970) improved our ability to concentrate and find barite particles. Sediment traps 902, 905, and 912 and sediment samples from Station 1 (Cruises 1 and 3) were prepared for analysis by this method. To evaluate the effect of the selective leaching on barite, we spiked an aliquot of sediment from trap 912 with a small amount of barite ore finer than 30 μm . SEM analysis of the barite surfaces of the leached samples were very similar to those of the unleached particles.

We found that the leaching procedures removed silicate and organic material from all samples except trap 902 which had a high concentration of zooplankton and a resistant organic fraction. Barite was identified in an aliquot of this sample, however, after heavy particles were concentrated by gravity settling. The other trap samples yielded barite particles following the selective leach method. Maximum particle sizes of about 23 x 11 μm were found in each of these three traps (Fig. 15c). The thickness dimension is not easily estimated using the SEM.

In the samples of bottom sediment, 19 barite particles in the size range of 3 x 4 μm per 1,000 particles analyzed were observed in the post-drilling sample. Only 2 particles per 1,000 analyzed were found in the predrilling sample. These may have come from the earlier drilling activity on the continental slope and shelf.

The largest (60 x 90 μm) particles of barite were found in trap 901 by analyzing residues from the HNO_3 - HClO_4 - HF decomposition. Some of the particles appeared to have retained a basic outline (Fig. 15a) and the measured dimensions are assumed to approximate the original size of the particles entering the trap. Where leaching was extensive (Fig. 15b), the size measurements may underestimate the dimensions of the original particles. This particular sample consisted of a thin layer of grey material apparently highly enriched with drilling mud. A comparable layer was not observed in traps located deeper in the water column.

We estimated the fall velocity of the largest particles and calculated the current speed and direction necessary to account for these particles in the trap. The fall velocity calculations follow the model described by Baba and Komar (1981) and correct for changes in density, viscosity, and grain shape. Hydrographic data in the study area (Lyne and Csanady, 1984) were used to estimate viscosity from tables presented in Riley and Skirrow (1975). Assuming a nominal grain diameter of 60 μm and grain shape 60 x 60 x 90 μm , the fall velocity varies through the upper 200 meters of the water column between 0.589 and 0.467 cm/sec. The current necessary to carry the barite particle of the above specifications to the trap is 7.2 cm/s to the south-west (240°). The current-meter data collected at 380-m water depth on a mooring 2 km west of the trap mooring by Science Applications Inc. showed a current of about 7 cm/s flowing in a southerly direction over the last 18 days of the

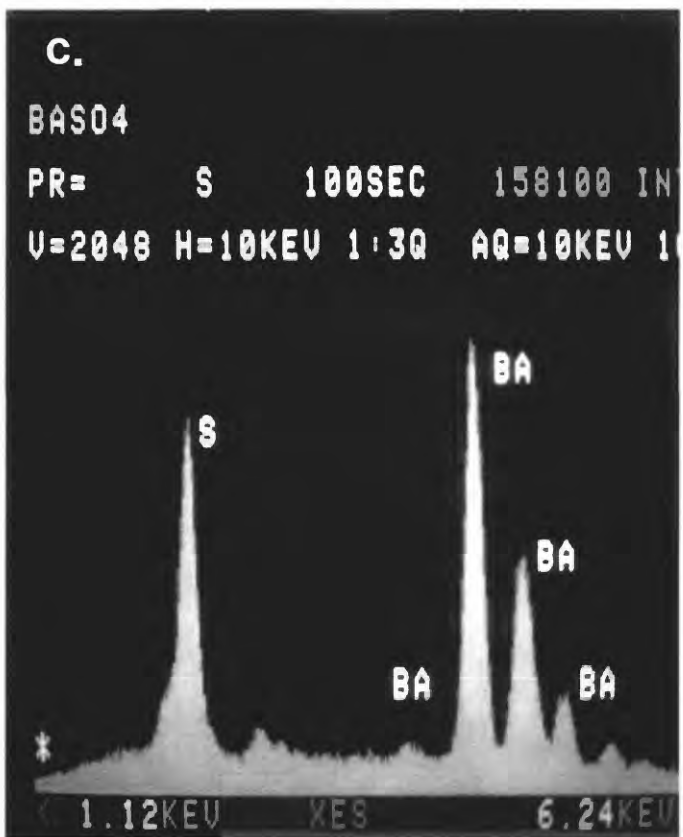
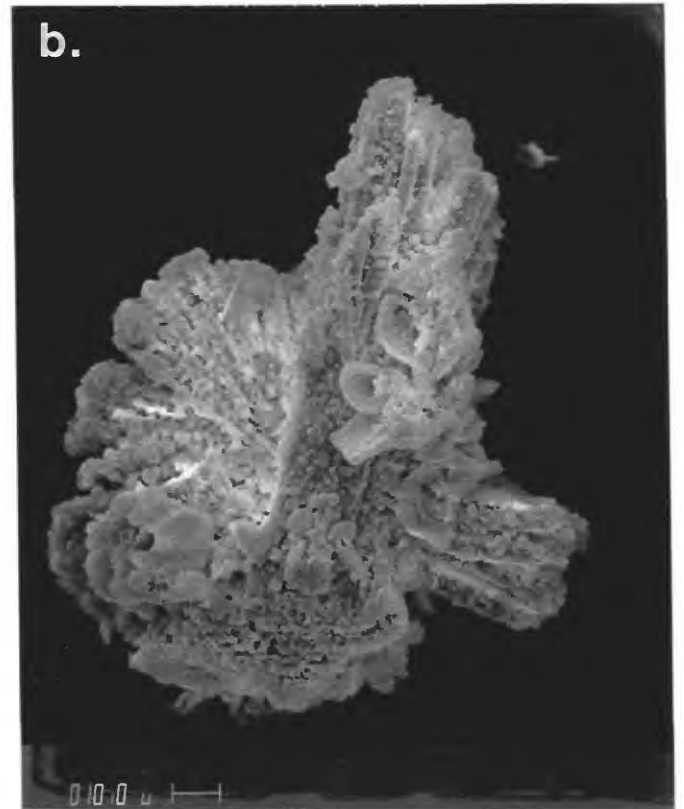
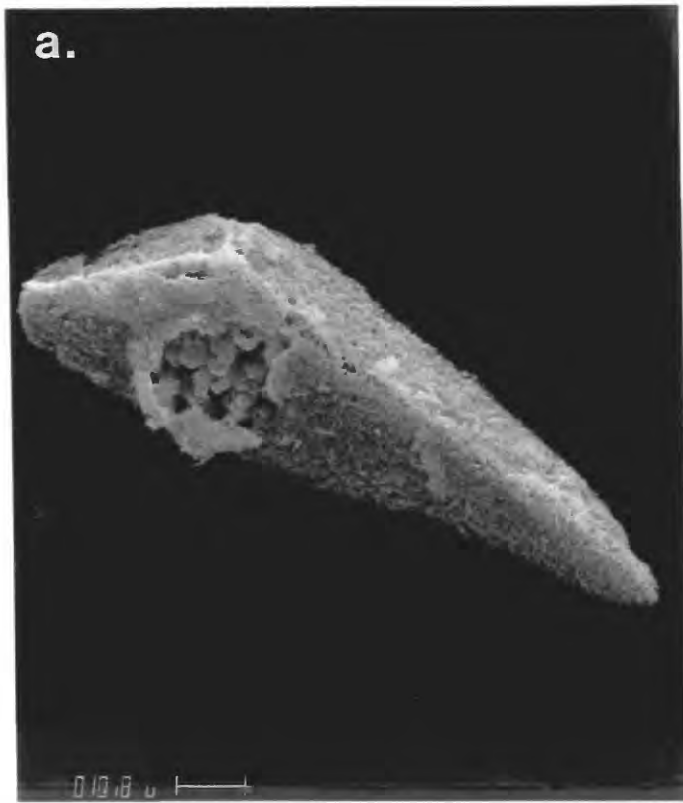


Figure 15. Scanning electron photomicrographs and a typical energy dispersive x-ray spectrum (c) of barite particles. Particles from trap 901 are moderately (a) and extensively (b) etched using $\text{HNO}_3\text{-HClO}_4\text{-HF}$ acids. Particle (d) from trap 912 was subjected to a milder leaching procedure (Church, 1970).

drilling period. Unfortunately, the current meter at 280-m water depth failed to operate during this deployment period.

If the calculated currents required to transport the largest particles of Ba from the drilling rig to the sediment trap agree with the measured currents, then an interesting question remains regarding the presence of the finer barite particles in the sediment traps. Deuser et al. (1981) found evidence for rapid transport of fine-grained particulates through the water column after incorporation in fecal pellets of zooplankton, and this may be a possible explanation for our observations.

Trace metals in sediments from recolonization trays

One objective of the biological studies within this program was to estimate settling and recruitment of organisms on the sea bed. To meet this objective, trays filled with mixed azoic sediment were deployed on the sea floor for a period of months using a device known as a free vehicle (Maciolek and others, 1987).

The free-vehicle samples were deployed at Stations 2 and 4 while drilling was underway at Station 1. Trace-metal concentrations were determined to identify accumulations of drilling mud in these trays. The results (Table 9) show no differences in metal concentrations within the trays compared to the range of values obtained at the slope stations from which the sediment was originally derived.

Trace metals in different size fractions of sediment

Using nylon sieves, we separated sediment samples into different size fractions and analyzed each fraction for trace metals. Barite used in drilling mud has a modal size range between 31 and 63 μm (coarse silt), and so

Table 9. - Chemical analyses of sediments from recolonization trays deployed at station 2 (2206 and 2209) and station 4 (2207 and 2210) between May 1984 and November 1984.

Free Vehicle	Top (cm)	Btm (cm)	Lab no.	Al (%)	Ba (ppm)	Cd (ppm)	Cr (ppm)	Cu (ppm)	Fe (%)	Hg (ppm)	Mn (ppm)	Ni (ppm)	Pb (ppm)	V (ppm)	Zn (ppm)
FV2206	0	2	W-233008	5.67	431	0.055	82	22	3.16	0.030	502	53	13	94	78
FV2207	0	2	W-233009	5.37	421	.075	80	21	2.97	.035	500	45	12	90	78
FV2209	0	2	W-233010	5.11	390	.058	73	19	2.83	.020	460	44	12	82	75
FV2210	0	2	W-233011	5.34	416	.083	82	21	2.93	.030	492	64	18	94	76

analysis of this fraction might specifically concentrate any barite deposited in slope sediments.

The samples analyzed in this detailed manner were collected before and after drilling at Station 14, and after drilling at Station 1 and Station 4 (about 20 km northeast of a drilling site). The results (Table 10) show no increase in Ba in postdrilling samples compared to predrilling samples. With very few exceptions, there is a steady increase in metal concentrations from the coarsest to the finest fraction of the sediment. This trend supports the strong correlation between metal concentration and the percentage of fine sediments that is demonstrated in Figure 2.

Sediment texture

Sediment texture within the upper 30 cm of the sea floor is quite uniform (Fig. 16 and Table 11). On the basis of mean grain size, the sediments are classified as silty clays or clayey silts. The sand component varies between about 1 percent and 15 percent and is composed mostly of foraminifera and diatom tests and minor amounts of rock fragments.

The sand content at Station 1 is higher in samples taken on Cruise 2 than on Cruise 1. This difference is probably not related to the drilling. Although a few large particles, thought to be drill cuttings, were observed in other replicate surface samples from Station 1, Cruise 2 (Battelle and others, 1985), we found no unusual particles in the sand fraction of the subcores we analyzed. Natural variability at this station is a more likely explanation of the apparent difference in texture between samples collected on these two cruises.

Although small differences in the silt and clay content were observed between predrilling and postdrilling cores, the differences are generally

Table 10. - Chemical analyses of the following size fractions of bottom sediment: S0, undifferentiated; S1, >1,000 µm; S2, 1,000-5,000 µm; S3, 500-210 µm; S4, 210-105 µm; S5, 105-60 µm; S6, 60-30 µm; S7, 30-10 µm; S8, 10-1 µm; S9, <1 µm.

Field no.	Top (cm)	Btm (cm)	Lab no.	Al (%)	Ba (ppm)	Cd (ppm)	Cr (ppm)	Cu (ppm)	Fe (%)	Hg (ppm)	Mn (ppm)	Ni (ppm)	Pb (ppm)	V (ppm)	Zn (ppm)
C20410S0	0	2	W-231641	4.89	381	.058	72	20	2.66	.028	617	31	11.0	82	65
C20410S1	0	2	W-231642	1.32	161	-	38	-	.74	-	-	7	-	14	-
C20410S2	0	2	W-231643	1.37	132	.063	16	4.5	.71	.042	128	4	3.8	11	17
C20410S3	0	2	W-231644	1.13	125	.081	22	13	.73	-	324	6	4.2	17	23
C20410S4	0	2	W-231645	3.34	279	.170	48	14	1.75	.068	505	15	5.8	56	45
C20410S5	0	2	W-231646	3.69	298	.055	47	12	1.72	.032	512	12	8.0	58	42
C20410S6	0	2	W-231647	4.26	327	.058	56	15	1.86	.032	554	18	9.1	68	45
C20410S7	0	2	W-231648	5.76	423	.075	81	24	3.11	.088	754	43	14.0	112	80
C20410S8	0	2	W-231649	5.99	537	.130	85	33	3.30	.010	897	55	16.0	124	95
C20410S9	0	2	W-231650	7.04	537	.156	98	39	4.10	.125	783	60	15.6	156	117
C11400S0	0	2	W-231651	5.48	396	.066	86	24	3.09	.061	703	40	18.0	112	88
C11400S1	0	2	W-231652	3.94	312	.100	61	24	2.45	.072	567	27	14.0	86	73
C11400S5	0	2	W-231653	3.64	293	.042	41	12	1.45	.072	322	12	8.3	56	45
C11400S6	0	2	W-231654	4.57	353	.030	49	12	1.90	.056	465	18	15.0	56	50
C11400S7	0	2	W-231655	5.47	377	.110	73	23	2.79	.072	699	38	20.0	106	76
C11400S8	0	2	W-231656	5.98	407	.120	84	27	3.29	.076	819	49	25.0	124	98
C11400S9	0	2	W-231657	6.80	490	.157	100	39	4.22	.096	887	65	28.2	163	130
C41400S0	0	2	W-235351	5.45	387	.075	68	23	3.07	.060	699	43	23.0	100	79
C41400S1-4*	0	2	W-235352	3.46	291	.079	47	19	2.05	.090	562	24	19.0	80	61
C41400S5	0	2	W-235353	3.87	304	.061	59	15	1.84	.120	509	29	18.0	61	51
C41400S6	0	2	W-235354	4.90	364	.068	100	17	2.37	.070	609	37	20.0	79	56
C41400S7	0	2	W-235355	5.64	385	.084	62	21	2.86	.090	732	38	22.0	110	68
C41400S8	0	2	W-235356	5.00	453	.120	100	35	3.94	.170	943	60	35.0	140	110
C41400S9	0	2	W-235357	5.68	486	.114	90	40	3.88	.160	805	62	24.0	145	104
C40100S0	0	2	W-235344	5.23	404	.082	57	22	2.95	.040	358	39	15.0	100	73
C40100S1-4*	0	2	W-235345	2.48	248	.077	40	11	1.64	.040	456	22	9.9	48	44
C40100S5	0	2	W-235346	3.62	291	.032	80	20	1.78	.050	533	38	12.0	52	41
C40100S6	0	2	W-235347	4.24	329	.046	42	12	1.79	.060	553	27	12.0	62	42
C40100S7	0	2	W-235348	5.07	346	.059	54	16	2.37	.050	790	33	16.0	88	57
C40100S8	0	2	W-235349	5.92	430	.059	73	21	3.05	.150	855	43	14.0	120	79
C40100S9	0	2	W-235350	6.78	517	.098	83	37	3.86	.070	861	58	18.0	144	101

* Size fractions 1-4 combined because of small sample size.

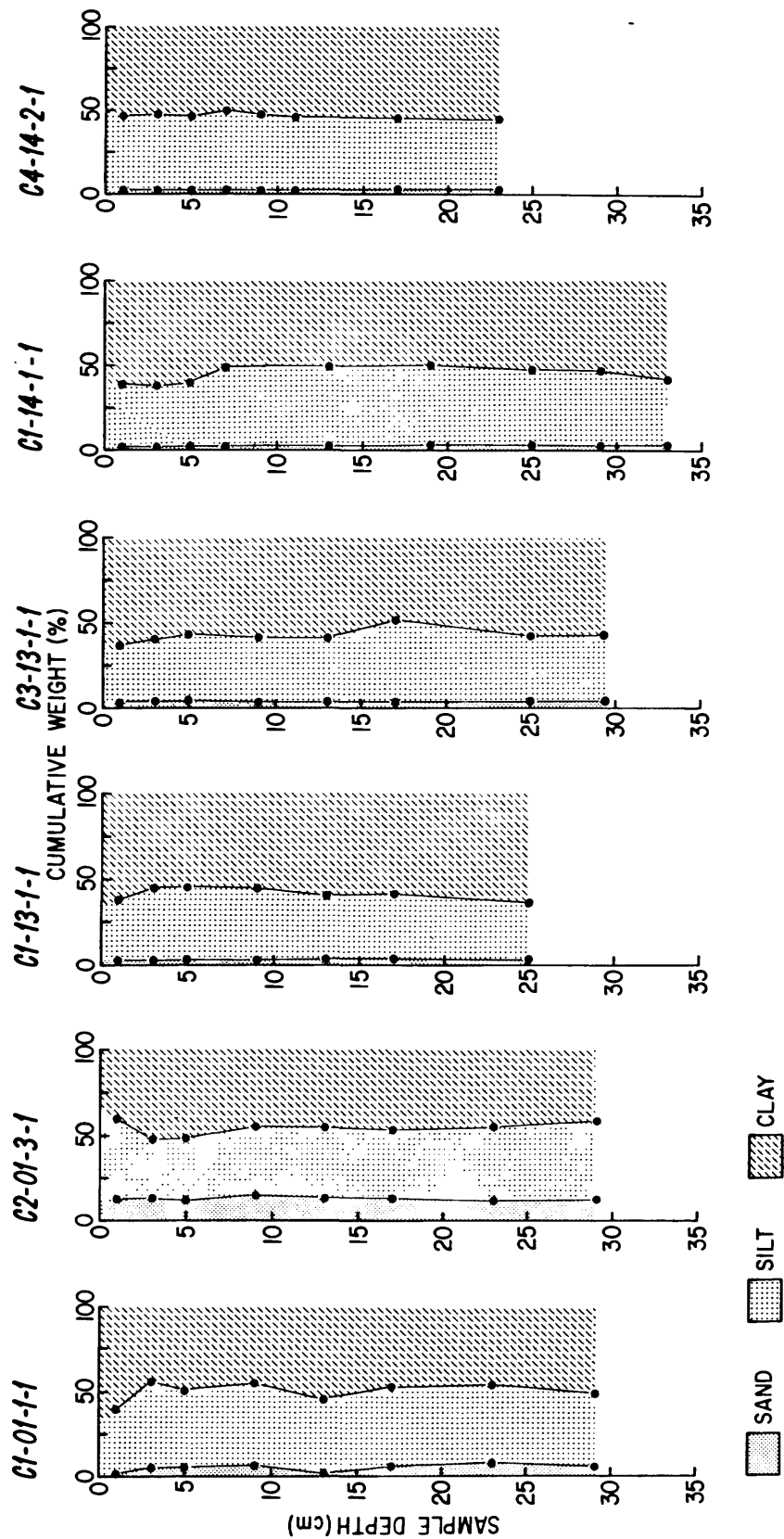


Figure 16 . Grain-size analysis of sediment cores before drilling (Cruise 1) and after drilling (Cruises 2-4).

Table 11. - Textural analysis of select cores from the Mid-Atlantic Slope and Rise. [Values accurate to two significant figures]

Field no.	Depth (cm)	Gravel (%)	Sand (%)	Silt (%)	Clay (%)	Mean (φ)	Median (φ)	St.dev. (φ)	Very coarse sand (%)	Coarse sand (%)	Medium sand (%)	Fine sand (%)	Very fine sand (%)	Silt				Clay		
														5 phi	6 phi	7 phi	8 phi	9 phi	10 phi	>10 phi
C10121*	0-2	0.00	1.52	35.66	62.81	8.62	10.06	2.29	0.00	0.00	0.00	0.00	1.52	10.19	8.05	8.43	8.99	5.47	4.26	53.08
C10111	2-4	.00	6.37	49.86	43.77	7.48	6.95	2.61	.00	.00	.00	.00	6.37	20.02	12.44	11.79	5.62	5.41	.70	37.66
C10111	4-6	.00	6.05	44.49	49.46	7.82	7.94	2.53	.00	.00	.00	.00	6.05	14.20	11.67	9.63	8.99	7.59	1.03	40.84
C10111	8-10	.00	7.00	50.47	42.52	7.51	7.36	2.48	.00	.00	.00	.00	7.00	16.25	10.80	11.68	11.74	5.58	5.54	31.40
C10111	12-14	.00	.71	47.52	51.77	8.13	8.35	2.40	.00	.00	.00	.00	.71	14.56	11.28	12.52	9.16	5.05	.37	46.35
C10111	16-18	.00	6.71	45.91	47.38	7.71	7.67	2.51	.00	.00	.00	.00	6.71	12.91	13.38	11.70	7.92	6.55	3.82	37.01
C10111	22-24	.00	7.04	49.09	43.88	7.44	7.23	2.51	.00	.00	.00	.00	7.04	17.87	11.71	11.55	7.96	7.74	4.95	31.19
C10111	28-30	.00	6.47	42.70	50.83	7.87	8.16	2.56	.00	.00	.00	.00	6.47	14.30	10.32	10.44	7.64	5.12	4.95	40.76
C11311	0-2	.00	1.62	36.46	61.91	8.74	10.10	2.13	.00	.00	.00	.00	1.62	1.25	14.91	9.88	10.42	6.11	.09	55.71
C11311	2-4	.00	1.39	45.32	53.29	8.17	9.06	2.27	.00	.00	.00	.00	1.39	10.95	13.36	7.88	13.13	2.41	14.60	36.28
C11311	4-6	.00	1.55	43.60	54.87	8.32	8.84	2.28	.00	.00	.00	.00	1.55	8.71	11.92	11.69	11.27	5.78	3.28	45.81
C11311	8-10	.00	1.26	43.14	55.60	8.32	8.93	2.26	.00	.00	.00	.00	1.26	8.90	11.69	12.06	10.49	6.00	5.34	44.26
C11311	12-14	.00	1.43	40.44	58.13	8.13	8.62	2.35	.00	.00	.00	.00	1.43	13.92	11.05	11.59	3.88	13.03	4.54	40.56
C11311	16-18	.00	1.76	40.02	58.22	8.43	8.98	2.25	.00	.00	.00	.00	1.76	7.46	9.85	15.26	7.45	8.35	.96	48.91
C11311	24-26	.00	2.06	34.13	63.82	8.66	10.05	2.18	.00	.00	.00	.00	2.06	8.00	4.80	10.93	10.40	11.14	.27	52.41
C11411	0-2	.00	1.98	38.91	59.12	8.42	9.42	2.28	.00	.00	.00	.00	1.98	7.45	13.53	9.36	8.56	7.00	5.03	47.09
C11411	2-4	.00	1.60	37.01	61.40	8.55	10.02	2.24	.00	.00	.00	.00	1.60	7.45	9.77	12.34	7.45	7.77	2.59	51.04
C11411	4-6	.00	1.46	39.61	58.83	8.53	10.02	2.26	.00	.00	.00	.00	1.46	7.59	10.96	11.37	9.69	3.77	4.08	50.98
C11411	6-8	.00	1.96	48.11	49.92	7.96	7.99	2.28	.00	.00	.00	.00	1.96	10.92	13.02	14.20	9.97	9.52	4.07	36.33
C11411	12-14	.00	2.76	47.58	49.67	7.96	7.97	2.25	.00	.00	.00	.00	2.76	7.94	15.81	11.73	12.10	10.54	3.64	35.49
C11411	18-20	.00	2.76	48.93	48.32	7.90	7.85	2.33	.00	.00	.00	.00	2.76	12.74	10.96	13.60	11.63	8.27	3.66	36.39
C11411	24-26	.00	2.80	45.10	52.10	7.93	8.16	2.31	.00	.00	.00	.00	2.80	12.90	11.02	11.16	10.02	13.06	3.66	35.38
C11411	28-30	.00	2.72	45.72	51.57	8.05	8.15	2.29	.00	.00	.00	.00	2.72	9.72	11.40	14.88	9.72	10.32	1.69	39.56
C11411	32-34	.00	2.40	39.50	58.11	8.32	8.78	2.28	.00	.00	.00	.00	2.40	7.96	12.42	10.48	8.64	10.41	2.52	45.18
C20131	0-2	.00	12.75	45.90	41.35	7.33	7.17	2.64	.00	.00	.00	.00	12.75	16.27	7.94	11.24	10.45	6.22	1.98	33.15
C20131	2-4	.00	11.85	35.21	52.93	7.93	8.64	2.68	.00	.00	.00	.00	11.85	10.12	9.28	6.81	9.00	4.56	3.94	44.43
C20131	4-6	.00	11.92	37.39	50.70	7.82	8.15	2.66	.00	.00	.00	.00	11.92	9.52	11.76	6.41	9.70	4.73	4.61	41.36
C20131	8-10	.00	14.83	40.36	44.80	7.36	7.21	2.67	.00	.00	.00	.00	14.83	8.46	20.39	4.90	6.61	5.46	6.82	32.52
C20131	12-14	.00	14.03	40.66	45.30	7.46	7.25	2.63	.00	.00	.00	.00	14.03	8.52	14.10	11.81	6.24	7.16	4.00	34.14
C20131	16-18	.00	13.29	40.15	46.56	7.56	7.64	2.55	.00	.00	.00	.00	13.29	8.69	9.20	12.79	9.48	8.19	6.54	31.83
C20131	22-24	.00	12.66	43.77	43.57	7.44	7.20	2.60	.00	.00	.00	.00	12.66	12.28	9.01	14.48	8.00	7.81	1.27	34.50
C20131	28-30	.00	13.23	44.70	42.07	7.37	7.28	2.60	.00	.00	.00	.00	13.23	10.80	14.48	8.35	11.08	7.45	1.75	32.87
C31311	0-2	.00	2.32	34.33	63.34	8.61	10.06	2.29	.00	.00	.00	.00	2.32	8.81	6.00	15.19	4.34	6.51	3.59	53.24
C31311	2-4	.00	2.26	38.87	58.88	8.38	9.15	2.29	.00	.00	.00	.00	2.26	9.40	9.63	10.78	9.06	8.17	4.75	45.96
C31311	4-6	.00	2.58	43.62	53.80	8.22	8.91	2.31	.00	.00	.00	.00	2.58	8.52	13.67	10.18	11.26	4.17	7.46	42.17
C31311	8-10	.00	2.43	39.80	57.77	8.29	9.08	2.29	.00	.00	.00	.00	2.43	8.26	14.46	7.51	9.57	6.95	9.91	40.91
C31311	12-14	.00	2.23	37.48	60.28	8.39	9.16	2.23	.00	.00	.00	.00	2.23	8.58	9.81	10.08	9.02	8.55	10.48	41.25
C31311	16-18	.00	2.77	51.27	45.96	7.96	7.74	2.21	.00	.00	.00	.00	2.77	8.69	11.52	15.40	15.66	1.73	12.90	31.33
C31311	24-26	.00	3.13	38.54	58.33	8.32	9.12	2.22	.00	.00	.00	.00	3.13	7.48	9.50	11.45	10.12	6.74	13.61	37.98
C31311	28-30	.00	2.90	41.17	55.94	8.12	9.00	2.31	.00	.00	.00	.00	2.90	13.03	7.84	10.94	9.36	5.95	16.65	33.34
C41421	0-2	.00	3.11	44.18	52.72	8.07	8.89	2.32	.00	.00	.00	.00	3.11	9.10	14.58	11.70	8.80	3.03	14.89	34.80
C41421	2-4	.00	2.16	46.86	50.99	8.07	8.17	2.31	.00	.00	.00	.00	2.16	10.49	13.12	12.09	11.15	5.80	6.00	39.19
C41421	4-6	.00	2.09	44.70	53.21	8.10	8.46	2.36	.00	.00	.00	.00	2.09	12.75	10.41	13.04	8.49	7.00	4.72	41.49
C41421	6-8	.00	2.17	48.48	49.36	8.11	7.96	2.26	.00	.00	.00	.00	2.17	9.29	12.60	10.33	16.25	3.93	6.94	38.49
C41421	8-10	.00	2.19	45.83	51.99	8.04	8.23	2.37	.00	.00	.00	.00	2.19	12.04	11.60	15.91	6.28	8.50	1.15	42.34
C41421	10-12	.00	2.32	46.87	50.81	8.09	8.14	2.28	.00	.00	.00	.00	2.32	9.58	12.82	10.94	13.53	5.69	7.12	38.00
C41421	16-18	.00	2.32	44.46	53.23	7.98	8.48	2.48	.00	.00	.00	.00	2.32	17.11	11.44	10.05	5.85	6.76	4.63	41.84
C41421	22-24	.00	2.21	41.95	55.85	8.26	8.70	2.33	.00	.00	.00	.00	2.21	9.79	11.51	11.75	8.90	8.31	1.67	45.87

*Replicate 2 used because insufficient sample from replicate 1.

within the 10-percent resolution of the analysis method and therefore not attributable to accumulation of drilling muds or cuttings.

SUMMARY OF IMPORTANT FINDINGS

1. At Station 1, adjacent to the drilling in Block 372, there are indications of small and localized additions of drilling mud to the bottom sediments. In one replicate core from Cruise 3, the top 4 cm of sediment had Ba concentrations as much as 13 percent higher than deeper sediments. In one replicate from Cruise 6 the top sample was 20 percent higher than deeper sediment. Ba to Al ratios in the same interval were 25 percent higher. The fact that this increase was measured in only one of three subcores from the same replicate box core indicates that the elevations of Ba from drilling are patchy on a very small scale, possibly due to the random addition of relatively large particles of barite. There is no systematic temporal change in the average Ba concentration at any of the stations sampled.

The small increase in Ba is probably not deleterious to benthic marine organisms. This opinion is based on its patchy occurrence and on the data generated during the Georges Bank Monitoring Program which showed no environmental effects to benthic organisms attributable to drilling at stations where Ba increased as much as 5.9 times background levels (Battelle-WHOI, 1985). Barium in the form of barium sulfate is also known to be of low toxicity from its wide use in the field of medicine. However, because of a lack of scientific data, there is some uncertainty in predicting the response of marine organisms to long term, low level contamination.

2. The strongest signal from drilling mud was observed in sediment trap

samples collected within the upper 850 m of the water column at a mooring 2.8 km southwest of the drilling rig in Block 372. Discrete particles of barite as large as 60 x 60? x 90 μm were identified by means of a scanning electron microscope. Their occurrence in sediment traps suggests that these large particles fall individually through the water column at speeds predicted by a comprehensive model based on Stokes Law.

3. There are no changes in Ba concentration at Station 14 and 13, .65 km and 1.4 km, respectively, from the drill site in Block 93.
4. In cores collected on Cruise 1 at Stations 1, 6, 13, and 14, the concentration of Ba and the Ba-to-Al ratio in the surface sediments were not elevated with respect to deeper sediments. This suggests that the drilling mud from exploratory wells, which were active on the continental slope and shelf before Cruise 1, either was not deposited in the general area of this survey or was diluted to levels below detection by natural sediments.
5. Within the surface sediments sampled in this program, the analyzed metals are the same or lower in concentration than they are in average shales from around the world, an indication of uncontaminated sediments. For example, the highest concentration of Ba in sediments collected at the drill site in Block 372 after the completion of drilling was 555 ppm, less than the published value of 580 ppm for average shales (Krauskopf, 1967).
6. Pb concentrations are as much as three times higher in the upper 5 to 10 cm than they are in deeper sediments of the cores collected. The highest concentration measured in this study area is 31 ppm, slightly higher than the value in world average shales (20 ppm). Similar Pb profiles have been previously described in sediments from other locations

off the U.S. East Coast. The enrichment is thought to be related to the burning of gasoline containing lead additives and its subsequent atmospheric transport to offshore marine areas. Too little data are available in the literature to evaluate the potential impact of this increase in Pb. Data are lacking on the speciation and bioavailability of lead in sediments and on the effects of small increases (compared to the increases in some estuaries) of Pb on organisms inhabiting this deep environment.

7. The inventories of anthropogenic lead in sediments of the continental slope off the Middle Atlantic states appear to be higher by a factor of 2 to 7 than would be predicted from estimates of the long-term atmospheric flux of lead. This implies a preferential focusing of lead disposition (and of other sediment-reactive pollutants) in slope sediments, perhaps by increased scavenging of lead from the water column. We recommend analysis of ^{210}Pb , ^{137}Cs , and Pu isotopes on selected cores from the same area to test this hypothesis and to help describe the processes.
8. The analysis of sediment texture in sediment cores revealed no differences in predrilling and postdrilling samples at stations adjacent to drilling operations. This suggests that measurable amounts of drill cuttings are not accumulating at the locations sampled.

REFERENCES

- Baba, Jumpei, and Komar, P. D., 1981, Settling velocities of irregular grains at low Reynolds numbers: *Journal of Sedimentary Petrology*, v. 51, no. 1, p. 121-128.
- Battelle New England Marine Research Laboratory and Woods Hole Oceanographic Institution, 1985, The Georges Bank Monitoring Program: Final report for the third year of monitoring, v. 1, prepared for the USDOI Minerals Management Service under Contract 14-12-0001-29192, 38 p.
- Beardsley, R. C., Chapman, D. C., Brink, K. H., Ramp, S. R., and Schlitz, R., 1985, The Nantucket Shoals flux experiment (NSFE79) Part 1, A basic description of the current and temperature variability: *Journal of Physical Oceanography*, in press.
- Bothner, M. H., Spiker, E. C., Johnson, P. P., Rendigs, R. R., and Aruscavage P. J., 1981, Geochemical evidence for modern sediment accumulation on the Continental Shelf off southern New England: *Journal of Sedimentary Petrology*, v. 51, no. 1, p. 281-292.
- Bothner, M. H., Butman, B., and Parmenter, C. M., 1987, A field comparison of four sediment traps: changes in collection with trap geometry and size; in Butman, B., ed., *North Atlantic Slope and Canyon Study: A field report to the U.S. Minerals Management Service, MMS 86-0086, Volume 2, Appendix 1.*
- Bothner, M. H., Rendigs, R. R., Campbell, E., Doughten, M. W., Aruscavage, P. J., Dorrzapf, A. F., Jr., Johnson, R. G., Parmenter, C. M., Pickering, M. J., Brewster, D. C., and Brown, F. W., 1982, The Georges Bank monitoring program: Analysis of trace metals in bottom sediments: Final Report submitted to the U.S. Bureau of Land Management under Interagency Agreement AA851-IA2-18, 62 p. (published in 1984 as U.S. Geological Survey Circular 915, 36 p.)

- Bothner, M. H., Rendigs, R. R., Campbell, Esma, Doughten, M. W., Parmenter, C. M., Pickering, M. J., Johnson, R. G., and Gillison, J. R., 1983, The Georges Bank monitoring program: Analysis of trace metals in bottom sediments during the second year of monitoring: Final report submitted to the U.S. Minerals Management Service under Interagency Agreement No. 14-12-0001-30025, 88 p. (published in 1984 as U.S. Geological Survey Circular 936, 54 p.)
- Bothner, M. H., Rendigs, R. R., Campbell, Esma, Doughten, M. W., Parmenter, C. M., O'Dell, C. H., DiLisio, G. P., Johnson, R. G., Gillison, J. R., and Rait, Norma, 1985, The Georges Bank monitoring program: Analysis of trace metals in bottom sediments during the third year of monitoring: Final report submitted to the U.S. Minerals Management Service under Interagency Agreement No. 14-12-0001-30153, 99 p.
- Bothner, M. H., Campbell, E. Y., DiLisio, G. P., Parmenter, C. M., Rendigs, R. R., and Gillison, J. R., 1986, Analysis of trace metals in support of deepwater biological processes on the U.S. South Atlantic Continental Slope and Rise: Draft final report submitted to the U.S. Minerals Management Service under Interagency Agreement No. 14-12-00010-30197, 42 p.
- Bruland, K. W., Bertine, Kathe, Koide, Minoru, and Goldberg, E. D., 1974, History of metal pollution in southern California coastal zone: Environmental Science and Technology, v. 8, p. 425-432.
- Butman, B., 1985, Physical processes causing surficial sediment movement: in Backus, R. H., ed., Georges Bank and Its Surroundings: Cambridge, Mass., M.I.T. Press, in press.
- Carver, R. E., 1971, Procedures in sedimentary petrology: New York, Wiley Interscience, 653 p.

- Church, T. M., 1970, Marine barite: Ph.D. Dissertation, University of California, San Diego, 100 p.
- Church, T. M., Tramontano, J. M., Scudlark, J. R., Jickells, T. D., Tokos, J. J., Jr., and Knap, A. H., 1984, The wet deposition of trace metals to the western Atlantic Ocean at the Mid-Atlantic coast and on Bermuda: Atmospheric Environment, v. 18, p. 2657-2664.
- Jickells, T. D., Deuser, W. G., and Knap, A. H., 1984, The sedimentation rates of trace elements in the Sargasso Sea measured by sediment trap: Deep-Sea Research, v. 31, p. 1169-1178.
- Jickells T. D., Knap, A. H., and Church, T. M., 1984, Trace metals in Bermuda rainwater: Journal of Geophysical Research, v. 89, p. 1423-1428.
- Folk, R. L., 1974, Petrology of sedimentary rocks: Austin, TX, Hemphill Publishing Company, 182 p.
- Krauskopf, K. B., 1967, Introduction to geochemistry: New York, McGraw-Hill Book Co., 721 p.
- Luoma, S. N., and Bryan, G. W., 1978, Factors controlling the availability of sediment-bound lead to the estuarine bivalve Scrobicularia plana: Journal of Marine Biological Association, v. 58, p. 793-802.
- Lyons, W. B. and Fitzgerald, W. F., 1983, Trace metal speciation in nearshore anoxic and suboxic pore waters; in Wong, C. S., Boyle, E., Brulard, K. W., Burton, J. D., and Goldberg, E. D., eds., Trace Metals in Sea Water: New York, Plenum Press, p. 621-641.
- Lyne, V. D., and Csanady, G. T., 1984, A compilation and description of hydrographic transects of the Mid-Atlantic Bight Shelf-Break Front: Woods Hole Oceanographic Institution Technical Report, WHOI-84-19.
- Lynn, D. C., and Bonati, E., 1965, Mobility of manganese in diagenesis of deep-sea sediments: Marine Geology, v. 3, p. 457-474.

- Maciolek, N., Grassle, J. F., Hecker, B., Boehm, P. D., Brown, B., Dade, B., Steinhauer, W. G., Baptiste, E., Ruff, R. E., and Petrecca, R., 1987, Study of biological processes on the U.S. Mid-Atlantic Slope and Rise: Final report submitted to the U.S. Minerals Management Service under Contract No. 14-12-0001-30064.
- McCullough, J. R., Irwin, B. J., and Bowles, R. M., 1982, LORAN-C latitude-longitude conversion at sea: programming considerations: The Wild Goose Association, Annual Technical Symposium, 11th, Proceedings, p. 42-75.
- McCullough, J. R., Irwin, B. J., Hayward, R. C., and Bowles, R. M., 1983, A first look at LORAN-C calibration data in the Gulf of Mexico: The Wild Goose Association, Annual Technical Symposium, 12th, Proceedings, p. 25-67.
- Riley, J. P., and Skirrow, G., 1975, Chemical Oceanography, v. 2, 2nd ed.: London, Academic Press, Appendix Tables 25, 26.
- Tessier, A., Campbell, P. G. C., Auclair, J. C., and Bisson, M., 1984, Relationships between the partitioning of trace metals in sediments and their accumulation in the tissues of the freshwater mollusc elliptio complanata in a mining area: Canadian Journal of Fisheries and Aquatic Science, v. 41, p. 1463-1472.

Appendix Table 1. - Navigation data for samples analyzed for trace metals.

[Time delay X (Nantucket Island, Mass.) and
time delay Y (Carolina Beach, N.C.) are Loran-C
time delay values for the 9960 Loran-C chain]

Field no.	Sta.	Yr	Mo	Dy	Water depth (m)	TDX (μ s)	TDY (μ s)	Latitude Deg. Min.	Longitude Deg. Min.
<u>Core profiles</u>									
C10111	01	1984	3	31	2195	26365.60	42588.70	38 35.9085	-72 52.8983
C20131	01	1984	8	3	2194	26365.20	42589.00	38 35.9357	-72 52.8284
C30111	01	1984	12	2	2165	26366.00	42588.10	38 35.8499	-72 52.9697
C40121	01	1985	5	17	2180	26365.80	42588.40	38 35.8791	-72 52.9340
C50111	01	1985	8	5	2185	26365.70	42588.70	38 35.9094	-72 52.9154
C60100	01	1985	11	13	2195	26365.90	42588.60	38 35.9010	-72 52.9501
C10611	06	1984	5	3	2090	26062.80	42877.70	39 05.5429	-72 02.9310
C20611	06	1984	3	1	2084	26062.70	42878.10	39 05.5880	-72 02.9186
C30631	06	1984	11	28	2085	26063.30	42878.40	39 05.6229	-72 03.0197
C40600	06	1985	5	15	2087	26063.30	42878.20	39 05.6003	-72 03.0177
C50611	06	1985	8	2	2080	26063.10	42878.20	39 05.6000	-72 02.9850
C60611	06	1985	11	10	2089	26064.00	42878.40	39 05.6241	-72 03.1341
C11311	13	1984	4	2	1603	26628.40	42121.00	37 53.2693	-73 45.0185
C21311	13	1984	8	7	1614	26628.00	42121.20	37 53.2794	-73 44.9400
C31311	13	1984	11	30	1615	26628.50	42120.90	37 53.2620	-73 45.0390
C51311	13	1985	8	9	1490	26626.40	42126.70	37 53.7745	-73 44.5521
C61311	13	1985	11	15	1609	26628.50	42121.20	37 53.2910	-73 45.0342
C11411	14	1984	4	2	1503	26627.20	42125.90	37 53.7156	-73 44.7153
C41421	14	1985	5	19	1492	26626.30	42127.10	37 53.8110	-73 44.5270
C51411	14	1985	8	10	1490	26626.40	42126.70	37 53.7745	-73 44.5521
C61411	14	1985	11	15	1515	26625.80	42125.80	37 53.6735	-73 44.4533
<u>Station blends</u>									
C10100	01	1984	3	31	2177	26365.20	42589.30	38 35.9671	-72 52.8269
C10200	02	1984	4	1	2021	26369.60	42586.00	38 35.6672	-72 53.5960
C10300	03	1984	5	5	2057	26356.20	42598.20	38 36.8079	-72 51.2469
C10400	04	1984	5	8	2108	26296.70	42674.80	38 44.3716	-72 40.9176
C10500	05	1984	5	8	2067	26249.90	42734.40	38 50.4352	-72 33.0450
C10600	06	1984	5	3	2089	26062.90	42877.70	39 05.5431	-72 02.9474
C10700	07	1984	5	6	2107	26423.00	42498.80	38 27.2520	-73 03.3668
C10800	08	1984	5	8	2149	26431.40	42498.20	38 27.2964	-73 04.8347
C10900	09	1984	5	6	2106	26480.70	42391.80	38 17.1690	-73 14.4620
C11000	10	1984	5	7	2095	26496.30	42137.00	37 51.7331	-73 19.8003
C11100	11	1984	5	7	1518	26386.40	42627.50	38 40.1426	-72 56.2076
C11200	01	1984	5	8	2501	26302.30	42532.20	38 29.2604	-72 42.1044
C11300	13	1984	4	3	1613	26628.40	42121.20	37 53.2887	-73 45.0154
C11400	14	1984	4	2	1500	26626.80	42126.70	37 53.7838	-73 44.6274

Appendix Table 1. - Navigation data for samples analyzed for trace metals.
Continued.

[Time delay X (Nantucket Island, Mass.) and
time delay Y (Carolina Beach, N.C.) are Loran-C
time delay values for the 9960 Loran-C chain]

Field no.	Sta.	Yr	Mo	Dy	Water depth (m)	TDX (μ s)	TDY (μ s)	Latitude Deg. Min.	Longitude Deg. Min.
<u>Station blends - Continued</u>									
C20100	01	1984	8	3	2194	26365.70	42590.10	38 36.0556	-72 52.9083
C20200	02	1984	8	3	2014	26369.90	42586.30	38 35.7015	-72 53.6458
C20300	03	1984	8	3	2055	26357.10	42597.90	38 36.7853	-72 51.4019
C20400	04	1984	8	1	2114	26296.80	42675.60	38 44.4574	-72 40.9328
C20500	05	1984	8	1	2084	26249.40	42734.00	38 50.3892	-72 32.9619
C20600	06	1984	8	1	2077	26062.70	42878.30	39 05.6106	-72 02.9206
C20700	07	1984	8	5	2102	26422.80	42499.20	38 27.2906	-73 03.3290
C20800	08	1984	8	6	2159	26430.80	42497.00	38 27.1659	-73 04.7396
C20900	09	1984	8	6	2112	26480.60	42391.90	38 17.1775	-73 14.4432
C21000	10	1984	8	7	2100	26495.80	42137.20	37 51.7414	-73 19.7030
C21100	11	1984	8	5	1509	26386.80	42627.40	38 40.1358	-72 56.2756
C21200	12	1984	8	5	2509	26301.50	42532.10	38 29.2402	-72 41.9639
C21300	13	1984	8	8	1617	26628.70	42120.40	37 53.2183	-73 45.0845
C30100	01	1984	12	2	2175	26366.00	42588.40	38 35.8812	-72 52.9682
C30200	02	1984	12	2	2013	26369.70	42585.80	38 35.6474	-72 53.6142
C30300	03	1984	12	3	2050	26357.50	43597.90	40 24.3556	-72 41.2359
C30400	04	1984	12	5	2107	26297.50	42674.30	38 44.3245	-72 41.0531
C30500	05	1984	12	5	2082	26249.80	42733.80	38 50.3700	-72 33.0283
C30600	06	1984	11	28	2088	26062.30	42877.70	39 05.5421	-72 02.8492
C30700	07	1984	12	2	2110	26423.00	42498.50	38 27.2212	-73 03.3690
C30800	08	1984	12	1	2153	26430.90	42497.00	38 27.1671	-73 04.7570
C30900	09	1984	12	1	2107	26480.30	42392.00	38 17.1829	-73 14.3887
C31000	10	1984	11	30	2100	26496.40	42136.90	37 51.7254	-73 19.8203
C31100	11	1984	12	4	1527	26386.40	42626.90	38 40.0804	-72 56.2114
C31200	12	1984	12	4	2507	26301.90	42531.70	38 29.2024	-72 42.0347
C31300	13	1984	11	30	1614	26628.30	42120.90	37 53.2573	-73 45.0013
C40100	01	1985	5	17	2192	26365.90	42588.40	38 35.8802	-72 52.9511
C40200	02	1985	5	17	2011	26369.70	42586.10	38 35.6786	-72 53.6126
C40300	03	1985	5	16	2051	26357.10	42597.80	38 36.7749	-72 51.4024
C40400	04	1985	5	16	2097	26297.50	42675.00	38 44.3989	-72 41.0517
C40500	05	1985	5	16	2078	26249.60	42734.30	38 50.4227	-72 32.9952
C40600	06	1985	5	15	2087	26063.30	42878.20	39 05.6003	-72 03.0177
C40700	07	1985	5	18	2102	26480.60	42392.20	38 17.2078	-73 14.4403
C40900	09	1985	5	18	2102	26480.60	42392.20	38 17.2078	-73 14.4403
C41000	10	1985	5	19	2095	26496.10	42136.90	37 51.7182	-73 19.7631
C41100	11	1985	5	17	1510	26386.70	42627.20	38 40.1142	-72 56.2600
C41200	12	1985	5	18	2505	26301.70	42531.90	38 29.2213	-72 41.9993
C41300	13	1985	5	19	1609	26628.50	42120.90	37 53.2620	-73 45.0389
C41400	14	1985	5	19	1491	26626.40	42127.00	37 53.8036	-73 44.5474

Appendix Table 1. - Navigation data for samples analyzed for trace metals.
Continued.

[Time delay X (Nantucket Island, Mass.) and
time delay Y (Carolina Beach, N.C.) are Loran-C
time delay values for the 9960 Loran-C chain]

Field no.	Sta.	Yr	Mo	Dy	Water depth (m)	TDX (μ s)	TDY (μ s)	Latitude Deg. Min.	Longitude Deg. Min.
<u>Station blends - Continued</u>									
C50100	01	1985	8	5	2185	26365.70	42588.70	38 35.9095	-72 52.9154
C50200	02	1985	8	5	2008	26369.50	42586.30	38 35.6975	-72 53.5774
C50300	03	1985	8	5	2053	26356.70	42598.00	38 36.7919	-72 51.3332
C50400	04	1985	8	3	2095	26297.30	42675.00	38 44.3974	-72 41.0180
C50500	05	1985	8	3	2079	26249.60	42734.00	38 50.3904	-72 32.9951
C50600	06	1985	8	2	2080	26063.20	42878.20	39 05.6001	-72 03.0014
C50700	07	1985	8	7	2089	26063.40	42878.00	39 05.5779	-72 03.0321
C50900	09	1985	8	8	2100	26480.80	42392.30	38 17.2211	-73 14.4750
C51000	10	1985	8	10	2094	26496.40	42137.10	37 51.7456	-73 19.8183
C51100	11	1985	8	6	1503	26386.80	42627.30	38 40.1254	-72 56.2762
C51200	12	1985	8	7	2495	26301.80	42532.00	38 29.2332	-72 42.0167
C51300	13	1985	8	9	1607	26628.40	42120.90	37 53.2597	-73 45.0201
C51400	14	1985	8	10	1490	26626.40	42126.70	37 53.7745	-73 44.5521
C60100	01	1985	11	13	2195	26365.90	42588.60	38 35.9010	-72 52.9501
C60200	02	1985	11	13	2014	26369.50	42586.50	38 35.7183	-72 53.5763
C60300	03	1985	11	13	2061	26357.30	42598.30	38 36.8291	-72 51.4342
C60400	04	1985	11	11	2108	26297.40	42674.60	38 44.3556	-72 41.0357
C60500	05	1985	11	11	2084	26249.40	42734.40	38 50.4323	-72 32.9620
C60600	06	1985	11	10	2091	26063.40	42877.80	39 05.5553	-72 03.0301
C60700	07	1985	11	10	2067	26423.00	42499.00	38 27.2726	-73 03.3653
C60900	09	1985	11	17	2107	26481.60	42391.90	38 17.1932	-73 14.6216
C61000	10	1985	11	16	2107	26494.30	42139.00	37 51.8876	-73 19.4001
C61100	11	1985	11	13	1514	26386.80	42627.00	38 40.0943	-72 56.2781
C61200	12	1985	11	14	2503	26302.20	42531.80	38 29.2167	-72 42.0873
C61300	13	1985	11	16	1609	26628.50	42120.80	37 53.2523	-73 45.0405
C61400	14	1985	11	15	1503	26626.20	42126.40	37 53.7409	-73 44.5192

Appendix Table 1. - Navigation data for samples analyzed for trace metals.
Continued.

[Time delay X (Nantucket Island, Mass.) and
time delay Y (Carolina Beach, N.C.) are Loran-C
time delay values for the 9960 Loran-C chain]

Field no.	Sta.	Yr	Mo	Dy	Water depth (m)	TDX (μ s)	TDY (μ s)	Latitude Deg. Min.	Longitude Deg. Min.
<u>Replicate box core and within-box core comparisons</u>									
C10111	01	1984	3	31	2195	26365.60	42588.70	38 35.9084	-72 52.8983
C10121	01	1984	3	31	2195	26365.60	42589.00	38 35.9398	-72 52.8968
C10122	01	1984	3	31	2195	26365.60	42589.00	38 35.9398	-72 52.8968
C10123	01	1984	3	31	2195	26365.60	42589.00	38 35.9398	-72 52.8968
C10131	01	1984	3	31	2143	26364.30	42590.20	38 36.0520	-72 52.6686
C10511	05	1984	5	8	2055	26250.10	42734.90	38 50.4903	-72 33.0782
C10521	05	1984	5	4	2065	26249.90	42734.30	38 50.4245	-72 33.0450
C10531	05	1984	5	8	2080	26249.70	42734.00	38 50.3910	-72 33.0117
C11311	13	1984	4	2	1613	26628.40	42121.00	37 53.2693	-73 45.0185
C11321	13	1984	4	2	1613	26628.40	42121.30	37 53.2984	-73 45.0138
C11331	13	1984	4	3	1613	26628.40	42121.20	37 53.2887	-73 45.0154
C20111	01	1984	8	3	2209	26366.30	42590.10	38 36.0616	-72 53.0108
C20112	01	1984	8	3	2209	26366.30	42590.10	38 36.0616	-72 53.0108
C20113	01	1984	8	3	2209	26366.30	42590.10	38 36.0616	-72 53.0108
C20121	01	1984	8	3	2179	26365.70	42591.10	38 36.1599	-72 52.9033
C20131	01	1984	8	3	2194	26365.20	42589.00	38 35.9357	-72 52.8284
C20211	02	1984	8	3	2019	26369.30	42586.50	38 35.7163	-72 53.5421
C20221	02	1984	8	3	2014	26369.70	42586.10	38 35.6786	-72 53.6126
C20231	02	1984	8	3	2004	26370.60	42586.20	38 35.6982	-72 53.7660
C20411	04	1984	8	1	2124	26297.20	42675.30	38 44.4286	-72 41.0006
C20421	04	1984	8	1	2114	26298.30	42675.60	38 44.4688	-72 41.1848
C20431	04	1984	8	2	2099	26296.80	42675.90	38 44.4893	-72 40.9322
C20611	06	1984	3	1	2084	26062.70	42878.10	39 05.5880	-72 02.9186
C20621	06	1984	8	1	2084	26062.70	42878.30	39 05.6106	-72 02.9206
C20631	06	1984	8	1	2084	26062.80	42878.50	39 05.6334	-72 02.9389
C21311	13	1984	8	7	1614	26628.00	42121.20	37 53.2794	-73 44.9406
C21321	13	1984	8	8	1619	26629.30	42120.20	37 53.2129	-73 45.2008
C21331	13	1984	8	8	1619	26628.80	42119.70	37 53.1529	-73 45.1145
C30111	1	1984	12	2	2165	26366.00	42588.10	38 35.8499	-72 52.9697
C30112	01	1984	12	2	2165	26366.00	42588.10	38 35.8499	-72 52.9697
C30113	01	1984	12	2	2165	26366.00	42588.10	38 35.8499	-72 52.9697
C30121	01	1984	12	2	2175	26366.10	42588.40	38 35.8822	-72 52.9853
C30131	01	1984	12	3	2185	26366.00	42588.70	38 35.9125	-72 52.9666

Appendix Table 1. - Navigation data for samples analyzed for trace metals.
Continued.

[Time delay X (Nantucket Island, Mass.) and
time delay Y (Carolina Beach, N.C.) are Loran-C
time delay values for the 9960 Loran-C chain]

Field no.	Sta.	Yr	Mo	Dy	Water depth (m)	TDX (μ s)	TDY (μ s)	Latitude Deg. Min.	Longitude Deg. Min.
<u>Replicate box core and within-box core comparisons - Continued</u>									
C30611	06	1984	11	28	2090	26061.70	42877.40	39 05.5071	-72 02.7480
C30621	06	1984	11	28	2090	26061.90	42877.30	39 05.4961	-72 02.7798
C30631	06	1984	11	28	2085	26063.30	42878.40	39 05.6229	-72 03.0197
C31311	13	1984	11	30	1615	26628.50	42120.90	37 53.2620	-73 45.0390
C31321	13	1984	11	30	1615	26628.10	42121.30	37 53.2914	-73 44.9573
C31331	13	1984	11	30	1612	26628.50	42120.40	37 53.2136	-73 45.0469
C40111	01	1985	5	17	2200	26366.10	42588.40	38 35.8822	-72 52.9853
C40121	01	1985	5	17	2180	26365.80	42588.40	38 35.8792	-72 52.9340
C40131	01	1985	5	17	2195	26365.80	42588.50	38 35.8896	-72 52.9335
C41311	13	1985	5	19	1615	26628.40	42120.80	37 53.2500	-73 45.0217
C41321	13	1985	5	19	1607	26628.70	42121.00	37 53.2763	-73 45.0751
C41331	13	1985	5	19	1605	26628.50	42120.80	37 53.2523	-73 45.0405
C41411	14	1985	5	19	1490	26626.50	42126.90	37 53.7962	-73 44.5678
C41412	14	1985	5	19	1490	26626.50	42126.90	37 53.7962	-73 44.5678
C41413	14	1985	5	19	1490	26626.50	42126.90	37 53.7962	-73 44.5678
C41421	14	1985	5	19	1492	26626.30	42127.10	37 53.8109	-73 44.5270
C41431	14	1985	5	19	1490	26626.30	42127.00	37 53.8013	-73 44.5286
C51411	14	1985	8	10	1490	26626.40	42126.70	37 53.7745	-73 44.5521
C51421	14	1985	8	10	1490	26626.40	42126.70	37 53.7745	-73 44.5521
C51431	14	1985	8	10	1484	26625.90	42127.90	37 53.8792	-73 44.4392
C51412	14	1985	8	10	1490	26626.40	42126.70	37 53.7745	-73 44.5521
C51413	14	1985	8	10	1490	26626.40	42126.70	37 53.7745	-73 44.5521
C60111	01	1985	11	13	2194	26365.80	42588.20	38 35.8583	-72 52.9350
C60112	01	1985	11	13	2194	26365.80	42588.20	38 35.8583	-72 52.9350
C60113	01	1985	11	13	2194	26365.80	42588.20	38 35.8583	-72 52.9350
C60121	01	1985	11	13	2199	26365.80	42588.60	38 35.9000	-72 52.9330
C60131	01	1985	11	13	2194	26366.20	42588.90	38 35.9354	-72 52.9999
C60611	06	1985	11	10	2089	26064.00	42878.40	39 05.6241	-72 03.1341
C60621	06	1985	11	10	2191	26063.30	42878.10	39 05.5890	-72 03.0167
C60631	06	1985	11	10	2192	26062.80	42877.00	39 05.4637	-72 02.9241
C61311	13	1985	11	15	1609	26628.50	42121.20	37 53.2910	-73 45.0342
C61321	13	1985	11	16	1611	26628.60	42120.80	37 53.2547	-73 45.0594
C61331	13	1985	11	16	1607	26628.50	42120.80	37 53.2523	-73 45.0405

Appendix Table 1. - Navigation data for samples analyzed for trace metals.
Continued.

[Time delay X (Nantucket Island, Mass.) and
time delay Y (Carolina Beach, N.C.) are Loran-C
time delay values for the 9960 Loran-C chain]

Field no.	Sta.	Yr	Mo	Dy	Water depth (m)	TDX (μ s)	TDY (μ s)	Latitude Deg. Min.	Longitude Deg. Min.
<u>Replicate box core and within-box core comparisons - Continued</u>									
C61411	14	1985	11	15	1515	26625.80	42125.80	37 53.6735	-73 44.4533
C61421	14	1985	11	15	1499	26626.40	42126.80	37 53.7842	-73 44.5505
C61431	14	1985	11	15	1489	26626.40	42126.60	37 53.7648	-73 44.5537
C10111	01	1984	3	31	2195	26365.60	42588.70	38 35.9085	-72 52.8983
<u>Fine fraction analyses Fine fraction samples</u>									
C10100X	01	1984	3	31	2177	26365.20	42589.30	38 35.9670	-72 52.8269
C20100X	01	1984	8	3	2194	26365.70	42590.10	38 36.0556	-72 52.9083
C30100X	01	1984	12	2	2175	26366.00	42588.40	38 35.8812	-72 52.9682
C40100X	01	1985	5	17	2192	26365.90	42588.40	38 35.8802	-72 52.9511
C50100X	01	1985	8	5	2185	26365.70	42588.70	38 35.9094	-72 52.9154
C60100X	01	1985	11	13	2195	26365.90	42588.60	38 35.9010	-72 52.9501
C10200X	02	1984	4	1	2021	26369.60	42586.00	38 35.6672	-72 53.5960
C20200X	02	1984	8	3	2014	26369.90	42586.30	38 35.7015	-72 53.6458
C30200X	02	1984	12	2	2013	26369.70	42585.80	38 35.6474	-72 53.6142
C60200X	02	1985	11	13	2014	26369.50	42586.50	38 35.7183	-72 53.5763
C10300X	03	1984	5	5	2057	26356.20	42598.20	38 36.8079	-72 51.2469
C20300X	03	1984	8	3	2055	26357.10	42597.90	38 36.7853	-72 51.4019
C10400X	04	1984	5	8	2108	26296.70	42674.80	38 44.3716	-72 40.9176
C20400X	04	1984	8	1	2117	26296.80	42675.60	38 44.4574	-72 40.9328
C30400X	04	1984	12	5	2107	26297.50	42674.30	38 44.3245	-72 41.0531
C40400X	04	1985	5	16	2097	26297.50	42675.00	38 44.3989	-72 41.0517
C60400X	04	1985	11	11	2108	26297.40	42674.60	38 44.3556	-72 41.0357
C50600X	06	1985	8	2	2080	26063.20	42878.20	39 05.6001	-72 03.0014
C11300X	13	1984	4	3	1613	26628.40	42121.20	37 53.2887	-73 45.0154
C21300X	13	1984	8	8	1617	26628.70	42120.40	37 53.2183	-73 45.0846
C31300X	13	1984	11	30	1614	26628.30	42120.90	37 53.2573	-73 45.0013
C41300X	13	1985	5	19	1609	26628.50	42120.90	37 53.2620	-73 45.0390
C51300X	13	1985	8	9	1607	26628.40	42120.90	37 53.2597	-73 45.0201
C61300X	13	1985	11	16	1609	26628.50	42120.80	37 53.2523	-73 45.0405

Appendix Table 1. - Navigation data for samples analyzed for trace metals.
Continued.

[Time delay X (Nantucket Island, Mass.) and
time delay Y (Carolina Beach, N.C.) are Loran-C
time delay values for the 9960 Loran-C chain]

Field no.	Sta.	Yr	Mo	Dy	Water depth (m)	TDX (μ s)	TDY (μ s)	Latitude Deg. Min.	Longitude Deg. Min.
<u>Fine fraction analyses</u>					<u>Fine fraction samples</u>				
C41400X	14	1985	5	19	1491	26626.40	42127.00	37 53.8036	-73 44.5474
C51400X	14	1985	8	10	1490	26626.40	42126.70	37 53.7745	-73 44.5521
C61400X	14	1985	11	15	1503	26626.20	42126.40	37 53.7409	-73 44.5192
Block 372 - Drill rig position								38 36.0197	-72 52.2304
Block 93 - Drill rig position								37 53.5767	-73 44.1668

Appendix Table 2. - Sediment Trap Mooring J

Trap No.	Deployed	Recovered	Water Meters		TDX	TDY	Latitude		Longitude	
			Depth (m)	Above Bottom			Deg.	Min.	Deg.	Min.
ST901	6/21/1984	9/26/1984	2120	1900	26371.4	42582.4	38	35.310	72	53.923
ST902	6/21/1984	9/26/1984	2120	1750	26371.4	42582.4	38	35.310	72	53.923
ST903	6/21/1984	9/26/1984	2120	1500	26371.4	42582.4	38	35.310	72	53.923
ST904	6/21/1984	9/26/1984	2120	1250	26371.4	42582.4	38	35.310	72	53.923
ST905	6/21/1984	9/26/1984	2120	1000	26371.4	42582.4	38	35.310	72	53.923
ST906	6/21/1984	9/26/1984	2120	750	26371.4	42582.4	38	35.310	72	53.923
ST907	6/21/1984	9/26/1984	2120	500	26371.4	42582.4	38	35.310	72	53.923
ST908	6/21/1984	9/26/1984	2120	250	26371.4	42582.4	38	35.310	72	53.923
ST909	6/21/1984	9/26/1984	2120	100	26371.4	42582.4	38	35.310	72	53.923
ST910	6/21/1984	9/26/1984	2120	50	26371.4	42582.4	38	35.310	72	53.923
ST911	6/21/1984	9/26/1984	2120	20	26371.4	42582.4	38	35.310	72	53.923
ST912	6/21/1984	9/26/1984	2120	10	26371.4	42582.4	38	35.310	72	53.923
ST913	6/21/1984	9/26/1984	2120	4	26371.4	42582.4	38	35.310	72	53.923